Final Report

Contract BDV24 962-01

Real Time Monitoring and Prediction of Reduced Visibility Events on Florida's Highways

UNIVERSITY OF CENTRAL FLORIDA

Mohamed A. Abdel-Aty, Ph.D., P.E.
Amr Oloufa, Ph.D., P.E.
Yichuan Peng, Ph.D.
Tsung-Sei Shen, Ph.D.
XiaoBao Yang Ph.D
Jaeyoung Lee, Ph.D.

PRAXSOFT

Rhonda Copley
Amin Ismail, Ph.D.
Fred Eady
Ronnie Lalchan
Brian Jarvis

November 2014

DISCLAIMER

"The opinions, findings, and conclusions expressed in this publication are those of the authors and not necessarily those of the State of Florida Department of Transportation."

UNITS CONVERSION

APPROXIMATE CONVERSIONS TO SI UNITS

SYMBOL	WHEN YOU KNOW	MULTIPLY BY	TO FIND	SYMBOL
LENGTH				
in	inches	25.4	millimeters	mm
ft	feet	0.305	meters	m
yd	yards	0.914	meters	m
mi	miles	1.61	kilometers	km
SYMBOL	**WHEN YOU KNOW**	**MULTIPLY BY**	**TO FIND**	**SYMBOL**
AREA				
in^2	squareinches	645.2	square millimeters	mm^2
ft^2	squarefeet	0.093	square meters	m^2
yd^2	square yard	0.836	square meters	m^2
ac	acres	0.405	hectares	ha
mi^2	square miles	2.59	square kilometers	km^2
SYMBOL	**WHEN YOU KNOW**	**MULTIPLY BY**	**TO FIND**	**SYMBOL**
VOLUME				
fl oz	fluid ounces	29.57	milliliters	mL
gal	gallons	3.785	liters	L
ft^3	cubic feet	0.028	cubic meters	m^3
yd^3	cubic yards	0.765	cubic meters	m^3

NOTE: volumes greater than 1000 L shall be shown in m^3				
SYMBOL	**WHEN YOU KNOW**	**MULTIPLY BY**	**TO FIND**	**SYMBOL**
MASS				
oz	ounces	28.35	grams	g
lb	pounds	0.454	kilograms	kg
T	short tons (2000 lb)	0.907	megagrams (or "metric ton")	Mg (or "t")
SYMBOL	**WHEN YOU KNOW**	**MULTIPLY BY**	**TO FIND**	**SYMBOL**
TEMPERATURE (exact degrees)				
^oF	Fahrenheit	5 (F-32)/9 or (F-32)/1.8	Celsius	^oC
SYMBOL	**WHEN YOU KNOW**	**MULTIPLY BY**	**TO FIND**	**SYMBOL**
ILLUMINATION				
fc	foot-candles	10.76	lux	lx
fl	foot-Lamberts	3.426	candela/m^2	cd/m^2
SYMBOL	**WHEN YOU KNOW**	**MULTIPLY BY**	**TO FIND**	**SYMBOL**
FORCE and PRESSURE or STRESS				
lbf	poundforce	4.45	newtons	N
lbf/in^2	poundforce per square inch	6.89	kilopascals	kPa
SYMBOL	**WHEN YOU KNOW**	**MULTIPLY BY**	**TO FIND**	**SYMBOL**
LENGTH				
mm	millimeters	0.039	inches	in

m	meters	3.28	feet	ft
m	meters	1.09	yards	yd
km	kilometers	0.621	miles	mi
SYMBOL	**WHEN YOU KNOW**	**MULTIPLY BY**	**TO FIND**	**SYMBOL**
		AREA		
mm^2	square millimeters	0.0016	square inches	in^2
m^2	square meters	10.764	square feet	ft^2
m^2	square meters	1.195	square yards	yd^2
ha	hectares	2.47	acres	ac
km^2	square kilometers	0.386	square miles	mi^2
SYMBOL	**WHEN YOU KNOW**	**MULTIPLY BY**	**TO FIND**	**SYMBOL**
		VOLUME		
mL	milliliters	0.034	fluid ounces	fl oz
L	liters	0.264	gallons	gal
m^3	cubic meters	35.314	cubic feet	ft^3
m^3	cubic meters	1.307	cubic yards	yd^3
SYMBOL	**WHEN YOU KNOW**	**MULTIPLY BY**	**TO FIND**	**SYMBOL**
		MASS		
g	grams	0.035	ounces	oz
kg	kilograms	2.202	pounds	lb
Mg (or "t")	megagrams (or "metric ton")	1.103	short tons (2000 lb)	T

SYMBOL	WHEN YOU KNOW	MULTIPLY BY	TO FIND	SYMBOL
TEMPERATURE (exact degrees)				
ºC	Celsius	1.8C+32	Fahrenheit	ºF
SYMBOL	**WHEN YOU KNOW**	**MULTIPLY BY**	**TO FIND**	**SYMBOL**
ILLUMINATION				
lx	lux	0.0929	foot-candles	fc
cd/m^2	candela/m^2	0.2919	foot-Lamberts	fl
SYMBOL	**WHEN YOU KNOW**	**MULTIPLY BY**	**TO FIND**	**SYMBOL**
FORCE and PRESSURE or STRESS				
N	newtons	0.225	poundforce	lbf
kPa	kilopascals	0.145	poundforce per square inch	lbf/in^2

1. Report No. BDV24 962-01	2. Government Accession No.	3. Recipient's Catalog No.
4. Title and Subtitle Real Time Monitoring and Prediction of Reduced Visibility Events on Florida's Highways		5. Report Date November 10, 2014
		6. Performing Organization Code
7. Author(s) Mohamed A. Abdel-Aty, PhD, PE; Amr Oloufa, PhD, PE; Yichuan Peng, PhD; Tsung-Sei Shen, PhD; XiaoBao Yang, PhD; Jaeyoung Lee, Ph.D.		8. Performing Organization Report No.
9. Performing Organization Name and Address Center for Advanced Transportation and Systems Simulation, University of Central Florida, P.O. Box 162450, Orlando, FL 32816-2450		10. Work Unit No. (TRAIS)
		11. Contract or Grant No.
12. Sponsoring Agency Name and Address Florida Department of Transportation		13. Type of Report and Period Covered **Final Report**
		14. Sponsoring Agency Code
15. Supplementary Note		

16. Abstract

Visibility is one of the most important weather factors on road systems; weather-related visibility reduction is most often due to fog. The reduced visibility also has a negative impact on traffic flow. This research attempted to identify the effect of reduced visibility on traffic flow as well as predict the reduced visibility events by using weather parameters including air temperature, wind speed, surface moisture etc. In order to achieve the objective, the following tasks were conducted in this research:

- Development of fog detection algorithm and the corresponding software by using an array of low-cost environmental sensors;
- Analysis of the effect of weather parameters on reduced visibility;
- Analysis of the impact of reduced visibility on traffic flow characteristics;
- Analysis of the distribution and influencing factors of fog duration;
- Evaluation of the performance of the fog detection algorithm; and
- Exploring the relationship between reduced visibility and traffic flow characteristics.

A series of statistical results showed that several traffic parameters significantly change by visibility/weather conditions. Also, it was found that the fog detection algorithm is efficient to detect fog. Lastly, the matched case control logistic models revealed that higher variance of speed, headway, variance of headway, occupancy, and lower speed can be key precursors of reduced visibility conditions.

17. Key Word Real time monitoring, Reduced visibility, Fog detection algorithm, Hazard based duration model, Matched case control logistic model	18. Distribution Statement		
19. Security Classif. (of this report)	20. Security Classif. (of this page) Unclassified	21. No. of Pages 180	22. Price

EXECUTIVE SUMMARY

Visibility is one of the most important impacts weather can have on road systems; weather-related visibility reduction is most often due to fog. Florida is among the top-rated states in the United States with regards to traffic safety problems resulting from adverse visibility conditions caused by fog/smoke (FS). The reduced visibility also has a negative impact on traffic flow. This research attempted to identify the effect of reduced visibility on traffic flow as well as predict the reduced visibility events by using weather parameters including air temperature, wind speed, surface moisture etc. In detail, the following tasks were completed in this research:

- Development of fog detection algorithm and the corresponding software by using an array of low-cost environmental sensors
- Analysis of the effect of weather parameters on reduced visibility
- Analysis of the impact of reduced visibility on traffic flow characteristics
- Analysis of the distribution and influencing factors of fog duration
- Evaluation of the performance of the fog detection algorithm developed by PraxSoft
- Exploring the relationship between reduced visibility and traffic flow characteristics

In summary, there are several major conclusions from the research:

- An array of low-cost environmental sensors, arranged at varying levels above the ground surface, could effectively detect the onset of fog and meet or exceed existing performance of traditional and much more expensive technologies.

- The fog is most likely to form when the values of humidity and subsurface moisture are higher. It is also more likely to form fog when the wind speed is lower and the air temperature is more close to the dew point.
- The mean headway and headway variation are significantly higher while the mean speed and volume are significantly lower in fog cases compared to clear cases. There isn't significant difference in speed variation based on the comparison of a single case.

Overall, the impact of reduced visibility on passenger cars is more significant compared to trucks. The mean headway, variation of headway and speed are significantly higher while the mean speed is significantly lower in the fog case compared to the clear case for the cars. In comparison, there isn't significant difference in the standard deviation of speed for the trucks and the difference of mean speed, headway and standard deviation of headway between fog cases and clear cases for passenger cars are all larger than trucks.

The differences of mean of headway, speed and standard deviation of headway are all significant under different visibility levels. The mean of headway increases when the visibility drops. The mean speed decreases when the visibility drops. The mean of standard deviation of headway increases when the visibility drops.

The effect of reduced visibility on both directions is similar. The effects of reduced visibility on different lanes are different. For the outer lane, the mean speeds under good visibility and moderate visibility levels are both significantly higher than mean speed under low visibility level. The difference of mean speed under good and moderate visibility levels is not significant. The mean headway under good visibility level is significantly higher than both mean headways under low and moderate visibility levels. The difference of mean headway under low and moderate visibility levels is not significant. For the middle lane, the mean speeds increases as the visibility increases. The mean headway increases as the visibility drops and the mean headway under good visibility level are significantly higher than both mean headways under low and moderate visibility levels. The difference of mean headway under low and moderate visibility levels is not significant. For the inner lane, the mean speeds under good and moderate visibility levels are both significantly higher than the mean speed under low visibility level. The difference of mean speed under good and moderate visibility levels is not significant. The mean headway decreases as the visibility increases.

Hazard-based duration model is appropriate to model fog duration time and its influencing factors. The lognormal distribution model gives the best description of fog duration without covariates. The log-logistic model gives the best description of fog duration with covariates. The increase of “humidity”, “barometric_pressure” and “subsurface_moisture” would increase the fog duration time. Meanwhile, the increase of “wind_speed” and “solar_radiation” would decrease the fog duration time.

Praxsoft developed the fog detection algorithm and the updated algorithm is efficient to detect the fog days but it is still likely to make false positive alarms when the day is actually clear.

The results of matched control case logistic regression model indicated that higher mean of headway, variance of speed and headway and higher occupancy were related to the increase of the likelihood of reduced visibility while lower mean speed was related to the increase of the likelihood of reduced visibility.

TABLE OF CONTENTS

LIST OF FIGURE

LIST OF TABLES

1. INTRODUCTION

Visibility is one of the most important impacts weather can have on road systems; weather-related visibility reduction is most often due to fog. At least 18 states have installed visibility detection systems in the US. Florida is among the top-rated states in the United States with regards to traffic safety problems resulting from adverse visibility conditions caused by fog/smoke (FS) and heavy rain. The reduced visibility also has a great impact on traffic flow. It is necessary to figure out the effect of reduced visibility on traffic flow and it will be very beneficial if we can accurately predict the reduced visibility events using to provide accurate warning messages to drivers in advance. Therefore, the major objectives of this research are as follows:

- To develop the fog detection algorithm and the corresponding software by using an array of low-cost environmental sensors
- To analyze the effect of some important weather parameters on reduced visibility
- To analyze the impact of reduced visibility on traffic flow characteristics
- To analyze the distribution and influencing factors of fog duration
- To evaluate the performance of the fog detection algorithm developed by PraxSoft company
- To further explore the relationship between reduced visibility and traffic flow characteristics

This report is divided into ten chapters. A review of existing research related to reduced visibility and its impact on traffic flow is provided in Chapter 2. The development of fog detection algorithm and the corresponding software are introduced in Chapter 3. Data collection and preparation are presented in Chapter 4. Chapter 5 mainly analyzes the effect of weather parameters on reduced visibility. Analysis of the impact of reduced visibility on traffic flow characteristics are presented in Chapters 6. Chapter 7 provides analysis about the distribution and influencing factors of fog duration. The evaluation of the performance of the fog detection algorithm developed by PraxSoft Company is provided in Chapter 8 and Chapter 9 further explores the relationship between reduced visibility and traffic parameters. Finally, conclusions and further research are provided in Chapter 10.

2 .LITERATURE REVIEW

2.1 State-of-the-art and Practice Visibility Systems in the US and around the World

Recently, two comprehensive reports were published regarding Visibility/Fog Detection Systems. Abdel-Aty et al. (2012a) offers a synthesis of the various visibility systems and traffic control techniques currently being deployed and implemented in the US and around the world. The second chapter of that report reviews all developed fog detection systems currently in use in the US. By examining the configurations and management strategies of these fog detection systems, the report indicates that some of these systems can detect reduction in visibility below certain acceptable levels, and respond accordingly in real time to convey specific and effective warning messages to drivers. These systems are also able to report this information to the appropriate Traffic Management Centers (TMCs). Finally, the report also mentioned that the increased severity levels of vision obstruction related to crashes derive from the inadequacy of traffic control techniques available to provide guidance to drivers, and the unpredictability of locations and times of reduced visibility on highways.

Visibility is also a critical factor for the departure and landing processes of aircraft. Three major types of visibility detection systems are used in aviation: Automated Weather Observing System (AWOS), Automated Surface Observing System (ASOS), and Automated Weather Sensor System (AWSS). Automated airport weather stations are prevalent in the United States and Canada. They are automated sensor suites designed to serve aviation and meteorological observation organizations' needs for safe and efficient aviation and weather forecasting operations.

Chapters three and four of the above-mentioned report provide an analysis of fog/smoke-related crashes in Florida, and an analysis of fog hotspot identification, respectively. All crashes on the examined roads were extracted from the Crash Analysis and Reporting (CAR) system database maintained by the FDOT. Crash data collected from all roadways in Florida from the years 2005 to 2010 were investigated. There were 1,492,446 crashes that occurred without any vision obstructions. Among them, 2,078 crashes were fog related and 278 crashes were smoke related. In terms of temporal distribution, it was found from the crash data records that the morning hours from December to February were the deadliest for FS crashes.

This information suggests an increased use of the new visibility detection systems that are being derived from existing affordable technologies such as roadway-side cameras. One can also conclude that the utilization of airport visibility detection information might be a promising way of increasing the coverage of road visibility detection systems.

Shahabi et al. (2012) also provide a complete description of the fog detection and warning system currently active across the US. First, this system determines favorable fog conditions in terms of the different meteorological components. In addition, it introduces various forecasting tools which are utilized by different agencies in their fog detection processes (a detailed description of these forecasting tools will be provided in the Fog/Visibility Detection and Prediction Method section of this report). The system also identified the critical fog-prone areas across West Virginia, based on the amount of foggy days recorded each year, by using the West Virginia weather observation stations that reported foggy days to show the fog levels and heaviest fog days for the five stations. These stations are located at airports, and mainly are used in forecasting for aviation purposes. In the final section of the report, a benefit cost analysis is provided to justify the implementation of fog systems. Table 2.1 shows the cost estimation for an active fog warning system. Determining the exact quantity of benefits is not easy. The reduction in the number of crashes comprised the major part of benefits for the fog detection system.

Table 2.1 Cost Estimation Table for An Active Fog Detection System (Shahabi et al. 2012)

Cost Estimation			
Item	**Number**	**Unit Price**	**Cost**
Roadway Weather Information System	4	11,000	44,000
Variable Message Signs	4	50,000	200,000
Fiber Optic Cable Installation	-	40,000 (per Mile)	200,000
Closed Circuit Television (CCTV)	4	20,000	80,000
Inductive Loop Surveillance	6	12,000	72,000
Environmental Sensor Station	4	40,000	160,000
Highway Advisory Radio	3	25,000	75,000
Conduit Design and Installation	-	40,000 (per Mile)	200,000
		Total Cost	1,031,000

With the advancements that have been made in data collection and real-time communication, it is plausible to detect and predict low visibility areas in real time. Real-time measurements of visibility may help in warning drivers when visibility has fallen below certain acceptable levels. The credibility of visibility detection and warning systems is essential to ensure drivers' compliance with these systems. Furthermore, how drivers react to a "reduced visibility" message is crucial to the effectiveness of fog warning systems. The goal of this research is to provide a cost-effective approach that provides early detection of the onset fog by installing innovative, low-cost sensors, and augmenting them with algorithms that can predict the probability of fog formation. The following two sections summarize the update on state-of-the-practice visibility systems and state-of-the-art studies.

2.2 State of the Practice of Visibility Detection Systems

Fog detection and warning systems have been installed across the US. Several systems were installed more than a decade ago, such as the systems used for I-75 in southeastern Tennessee, state route 99 near the San Joaquin Valley in California, and I-10 in Alabama. With the introduction of new technologies, some existing systems have been upgraded and several new types of systems have been proposed. Abdel-Aty et al. (2012a) and Shahabi et al. (2012) provide a comprehensive survey of the fog detection and warning systems used in the US. Here, we summarize the new systems and any findings that have not been included in the above-mentioned reports regarding systems used in the US and around the world.

Virginia Fog Detection and Warning System (Murphy et al., 2012)

An advanced Fog Detection and Warning System (FDWS) has been proposed by the Virginia Department of Transportation (VDOT) for use on a 14-mile corridor of I-77 that runs between the North Carolina state line and US 58/221. Four elements are included in this system: detection (visibility and traffic), communication, data processing, and an advisory information system.

New forward-scatter visibility sensors are currently being used to improve the accuracy of fog/limited visibility detection systems. Along with these sensors, upgraded millimeter wave traffic detectors are equipped to monitor traffic speed, volume, and occupancy data. Traffic detectors can be placed upstream and downstream from the visibility sensors. Traffic sensors detect unusual changes in travel speeds or occupancy rates to alert upstream drivers that the speed of traffic ahead is slower due to fog or incident.

Tennessee DOT Low Visibility Warning System (Shahabi et al., 2012) (Murphy et al., 2012)

Tennessee DOT (TDOT) and the Tennessee Department of Safety implemented a low visibility warning system on I-75 in Tennessee. The system covers 19 miles (30.6 kilometers) and consists of two Environmental Sensor Stations (ESS), eight forward-scatter visibility sensors, 44 vehicle detectors, 10 DMS, 10 VSL signs, and two highway advisory radio transmitters. Traffic and environmental data are transmitted from the sensors to an on-site computer for processing through underground fiber optic cables. Then the data are submitted to the central computer in the Highway Patrol office in Tiftonia via a microwave communication system.

From October 1st of 2011 through March 31st of 2012, the system issued twelve speed reductions for fog conditions. Of these events, two were evaluated to require closure of the Interstate section. During the same period, the system was also manually activated to provide 34 alerts to drivers for non-fog related incidents.

Fog Warning System in Venice Region, Italy (Leviäkangas et al., 2010) (Lindqvist et al., 2009)

This fog warning system, called Fog Pilot, is one of the pilot programs of the ROADIDEA project organized under 7th Framework Program of the European Union.

Fog is a relatively frequent phenomenon in the Po Valley and has caused major issues for road traffic.

The idea behind Fog Pilot was to develop an aerial monitoring system of the fog presence in the territory comprising the Venice Region, combining in a novel way all ground-based observations and satellite imagery, in an effort to develop suitable products for disseminating the information to end users. This process can yield drivers several options:

- Change of route in view of thick fog. For professional end users this can mean taking a detour, but also saving travel time and lowering the risk of incurring an accident.
- Break the trip until visibility conditions improve. For professional truck drivers who are subject to systematic rests, this option could optimize their planning.
- Private users could decide to modify their route, take a train instead of a car, or simply postpone their trip.

This system includes information obtained from a variety of data sources such as satellite direct visibility measurements, standard meteorological measurements, web cams, and visibility meters. In this pilot system, 10 visibility meters were built (see Figure 2.1). The following list highlights these parameters:

- Visibilimeters: very high reliability response close to the measurement site, decreasing with increases in distance. The choice of this decreasing rate should take into account two important aspects: one concerning the average distance among the visibilimeters, and the other regarding the importance of the contribution (that is, how smooth this contribution should be; too rapid a decrease would imply only local information with a consequent loss of large scale information, and too slow a decrease would result in the smearing out of the information with a loss of variability).

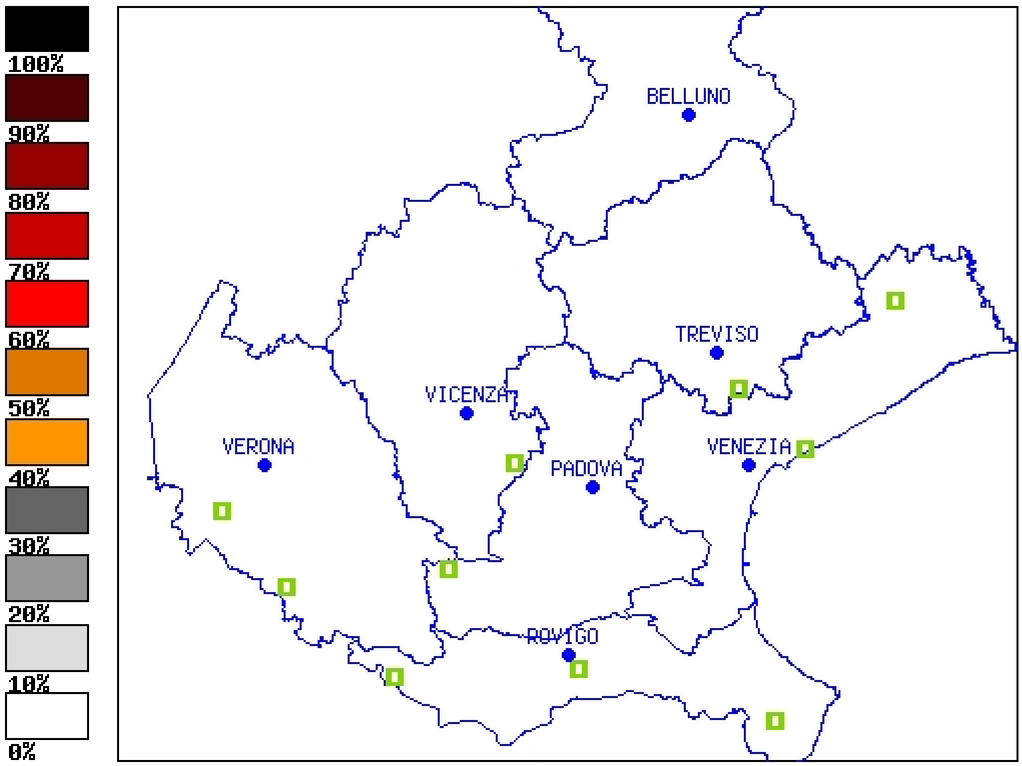

Figure 2.1 Locations of Visibilimeters in the Veneto Region (Lindqvist et al., 2009)

• Satellite: Attribution of probability of fog (POF) and probability of severe fog (POSF) could, in principle, be derived by a statistical analysis of data archives; for the time being, the sample size is too small and all such probabilities are subjectively attributed.

• Meteorological stations: The relationship between the standard meteorological observations and visibility, or fog, is done by statistical analysis; since fog is a strongly non-linear phenomenon (in terms of meteorological observations), a nonparametric approach has been chosen (cf. AMANOVA). The high level of dimensionality (12 variables) makes a direct evaluation of the probability density description very difficult, so that the Classification and Regression Tree (CART) form of analysis was chosen. The output of a well-tuned tree is the probability distribution for the defined visibility classes which have to be translated to a weight (peaked/flat distributions give high/low weights). The decrease with distance can be performed as it was for the visibilimeters, but with a different length scale (the network is denser).

• Meteorological stations via CALMET: Besides the use of meteorological station sites for the calculation of fog probability distributions, the fog risk model is able to take advantage of the CALMET meteorological model. CALMET can be used to generate a grid of the meteorological parameters where the corresponding weights assigned to each grid point depend upon the distance to the station locations since interpolation of the humidity field could induce error and lead to erroneous estimations.

The principle structure of Fog Pilot is shown in Figure 2.2.

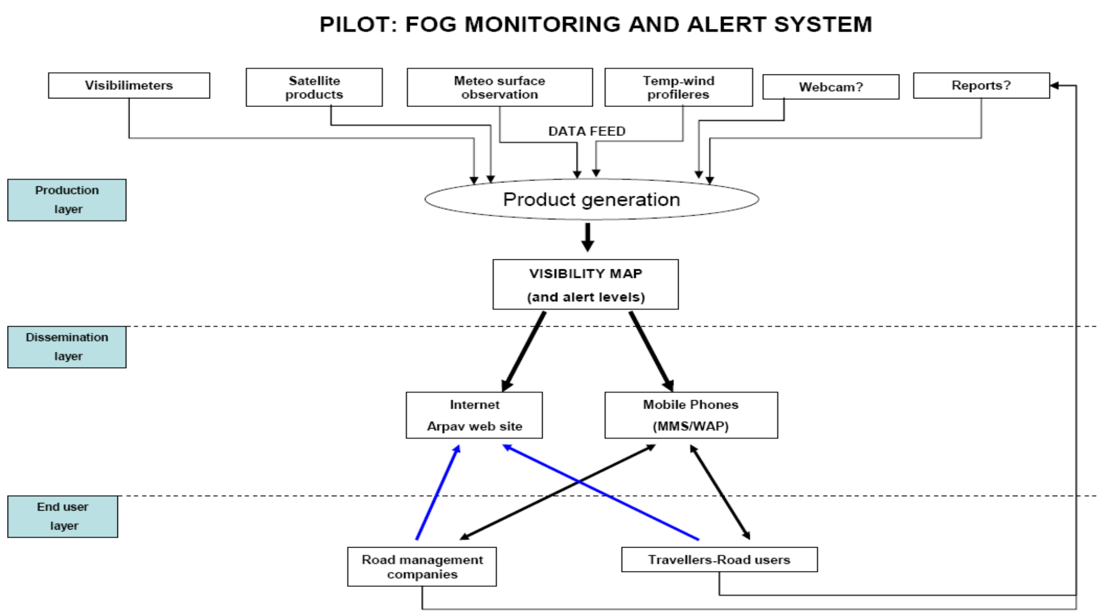

Figure 2.2 Fog Pilot Principle Structure (Leviäkangas et al., 2010)

A real-time probability map (see Figure 2.3) has been generated based on the above data sources. The probability of reduced visibility under 500 meters is presented in this map as colors referring to ten different probability ranges between 0% and 100%. These maps can be produced every hour, with a delay of about 30 minutes. In the beginning, the maps were available only as .jpgs. The system plans to include the information yielded from the merging system in geographical database such as GoogleMaps, or an equivalent.

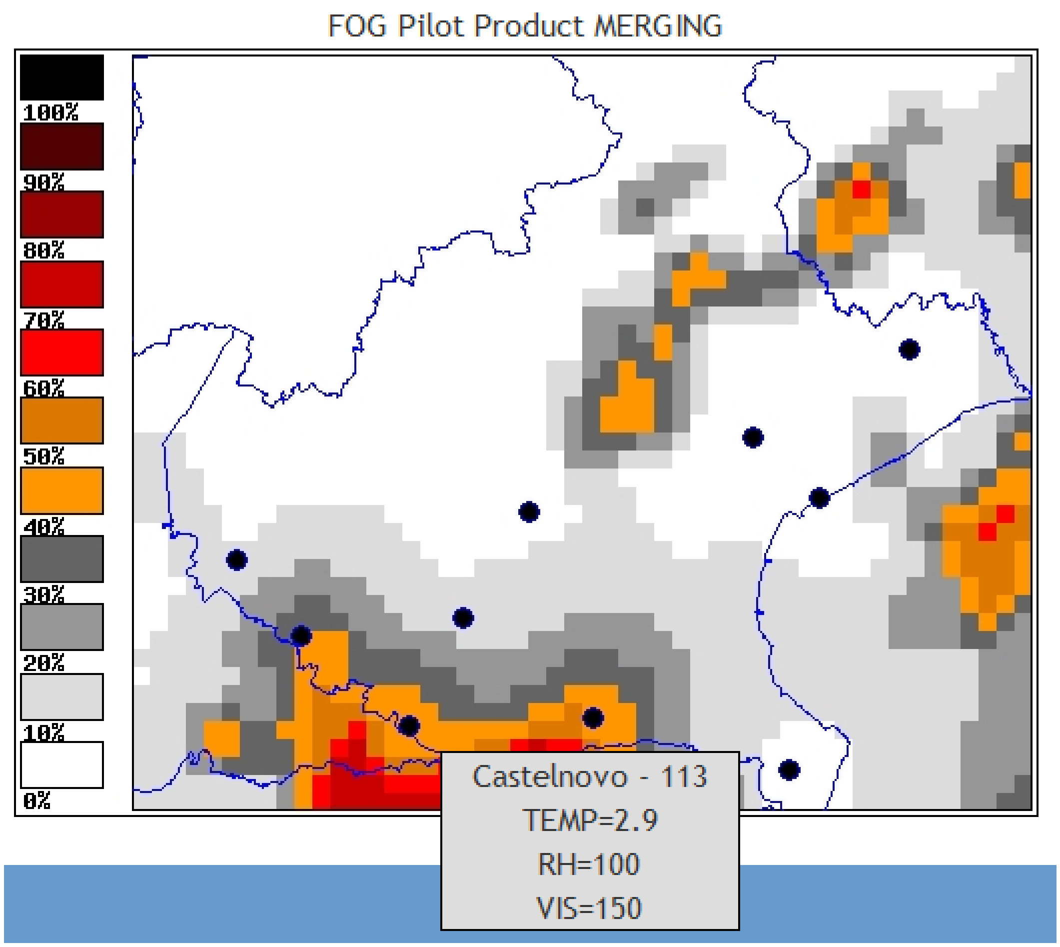

Figure 2.3 Map of Probability of Visibility Reduction under 500 meters over Veneto Plain (Leviäkangas et al., 2010)

Fog Pilot aims to test the usefulness of such a product by involving end user testing. The plan is to evaluate the best threshold of visibility for a “Dense Fog Presence” alert; possible choices to be evaluated could include 100, 150 and 200 meters.

Fog Warning System in Abu Dhabi Emirate (UAE) (Ali et al., 2013)

A real-time fog detection and warning system was proposed in Abu Dhabi. It has three main components: a fog sensing (detection) component, a fog density data collection and analysis component, and a driver fog notification component. Fog sensors were installed on light poles, radar stations, and cell phone towers along the highway. In addition, the detection of slow traffic movement due to poor visibility by the wireless device inside vehicles will also pass to the fog analysis component. Data collected from the fog sensors and traffic movement will be used to conduct the appropriate analyses necessary to determine the geographical boundaries of the poor visibility sectors of the highway. Furthermore, the patrol officer would approach the boundaries of the fog zone and send a signal to the fog analysis component to improve the accuracy of the virtual zone. The fog density data collection and analysis component conducts the analysis to decide the boundaries of poor visibility zones, and it can also identify which area is affected frequently by fog. In driver fog notification component, there are three possible methods of disseminating the information to drivers: Changeable Message Signs (CMS), radio weather channels, and Short Message Service (SMS) submissions through cell phones. By using these techniques, this system is able to define, efficiently and accurately, the boundaries of the fog zones in the coverage area.

2.3 Studies of Visibility Systems

In addition to the fog detection programs used in the US and in other countries around the world, there are several new procedures, more advanced with respect to visibility-related studies. This section of the literature review discusses the impact of these types of systems on broad inclement weather.

Traffic Flow in Inclement Weather

Weather causes a variety of impacts on the characteristics of traffic flow. Day-to-day weather events such as rain, snow, and fog can seriously affect the mobility and safety of road users. Billot et al. (2010) developed weather-responsive traffic state estimation tools that apply Sequential Monte Carlo methods. Such methods are used to detect in space the occurrence of rain events, and to adjust the parameter estimations for traffic analysis. Compared to the impact of rain, there is very limited research on the impact of low visibility on traffic flow. Hou et al. (2013) developed systematic procedures for calibrating weather effects on traffic flow models. They found that visibility and precipitation intensity significantly impact both free flow speed and maximum flow rate. Maze et al. (2006) showed that reduced visibility decreased traffic speed by 12% on freeways in the Minneapolis/St. Paul metropolitan area. In the old study of Jones & Goolsby (1970), it was shown that rain results in a 12-19% reduction of capacity of the freeway. Lamm et al. (1990) looked into the impact of the reduced visibility due to rain on the vehicle speeds. The authors found that speeds are not influenced by wet pavement due to light rain so long as visibility is not affected significantly by heavy rain. In the same way, Ibrahim and Hall (1994) found that there was no considerable reduction in maximum observed traffic flows and operating speeds in light rain; however, the capacity in heavy rain is reduced by 14-15%.

Moreover, Kockelman (1998) found that the binary dummy variable indicating a rainy condition has a significant effect in traffic flow models. Edwards (1999) compared traffic parameters by weather conditions such as clear, rain, and fog. The author found that the average peak hour traffic flow decrease in heavy rain and fog by 2.9% and 9.2%, respectively. Speeds were also investigated in each weather condition and it was found that the 85 percentile speeds in clear, rain, and fog are 71.38, 68.10, and 62.11 mph, respectively.

Smith et al. (2004) examined the impact of rain at various levels of intensity on the capacity and operating speeds to figure out the impact of weather conditions on traffic parameters. The authors used a maximum observed throughput approach to estimate freeway link capacity; the mean of the highest 5% flow rates was used to determine the percentage changes in capacity due to rain. It was found that the capacity was reduced statistically significant as rainfall intensity becomes greater. Light rain reduces the freeway link capacity by 4-10%, whereas heavy rain lowers it by 25-30%. Akin et al. (2011) found that rain reduces the average vehicle speed and capacity by 8-12% and 7-8%, respectively. The authors also revealed that light rain results in 65-66% traffic volume reduction. Meanwhile, few studies have focused on the direct relationship between the reduced visibility and traffic flow. Kyte et al. (2001) investigated the effectiveness of the low visibility due to rain on speeds. The authors found that a 0.77 kph (kilometer per hour) reduction in speed for every 0.01 km.

Effect of reduced visibility on driving behavior

Not many researchers have concentrated on the reduced visibility due to fog since they are less frequent compared to rain. Thus, researchers have conducted driving simulator based study in order to find out the effect of fog. Broughton et al. (2007) studied the car following behavior using driver simulator data and found that the average headway distances were reduced in reduced visibility conditions. Mean distances in clear, light fog, and dense fog are 42.7m, 34.6m, and 26.0m, respectively. The authors asserted the headway distances decrease because drivers seek visible cues when in foggy conditions that obscures scenery and roadway visibility.

In recent, Yan et al. (2014) examined the influence of foggy conditions on the speed behavior using driving simulator data. The authors compared the average speed in different geometric alignments such as straight, uphill, downhill, and S type curve in various weather conditions like clear, light fog, and heavy fog. It was shown that driving speeds are significantly reduced by the existence of fog in the straight segments. However, no significant difference was found between speeds in light fog and heavy fog in the straight segments. In case of downhill and uphill segments, there was no meaningful difference in speeds between clear and light fog. It is interesting that in S-curve segments, speeds in light fog are significantly higher than that in clear conditions. One of important findings of the authors is that the effect of fog is not consistent in different geometric alignments.

Ni et al. (2010) examined age-related difference in car following behavior in foggy conditions. The authors used driving simulator data and found that the largest reduction in the car following performance occurs at moderate speeds under the highest fog density condition, with older drivers keeping a much closer headway distance (21%) compared to young drivers. The result implies that older drivers are at higher risk especially under high fog density. Muller and Trick (2012) investigated the influence of driving experience on driving speeds in simulated foggy conditions. The authors found that both novice and experience drivers reduce their speeds in foggy conditions but experience drivers reduce their speed more than novice drivers in the same situation.

As stated previously, many researchers agreed that drivers reduce their speeds in adverse weather conditions but some researchers found opposite results. Snowden et al. (1998) asserted that drivers unintentionally increase their speed in foggy weather from their simulation experiment. The authors found that drivers think that they are driving far more slowly than they actually are in foggy conditions and therefore they increase their speed. Similarly, Brooks et al. (2011) also claimed that drivers keep their high speeds while driving in fog since fog does not appear to limit drivers' ability to keep their lane positions.

Previous research studies have shown that low visibility conditions due to the adverse weather considerably affect to traffic flow and driving behavior. It was shown that the rainy condition reduces the speed, traffic volume (or flow rate), and capacity. Nevertheless, it is still controversial that the effect of fog on traffic and driving behavior.

Most studies found that the fog reduce driving speeds while other claimed the opposite (Snowden et al. 1998; Brooks et al., 2011). One of the common limitations of these fog studies is that they only relied on simulation results. Therefore, it is needs further investigation that can clearly describe the driving behavior and traffic flow changes in foggy conditions using real traffic and weather data.

Weather Responsive Traffic Management Strategies (WRTM)

Three types of road weather management strategies may be employed in response to inclement weather; these include advisory, control, and treatment. Advisory and control strategies are the main measures for low visibility conditions. Advisory strategies provide prevailing or predicted weather information to road users. Control strategies range from the voluntary compliance of speed management to compulsory strategies such as route and vehicle restrictions.

Alfelor et al. (2013) described the state-of-the practice in weather-responsive traffic management (WRTM) used in the US and Europe. This system generally includes weather and traffic data collection, traffic analysis and modeling, human factors analysis, and performance evaluation. This research also discussed the gaps in current practices, as well as research related to weather-responsive traffic management. Recommendations on how these gaps could be filled are also described. First, real-time and location-specific information for road users at adverse weather is limited for most existing practice. Recent advances in mobile sensing and data collection technologies for adverse weather have great potential to provide the weather information more accurately and timely. Second, the concepts of advanced WRTM systems and strategies were developed but need to be implemented and evaluated to demonstrate the benefits and provide guidance to agencies on how they can be successfully implemented. Third, there are several new researches such as Advanced Driver Assistance Systems (ADAS) and Adaptive Cruise Control (ACC) that could have significant impact on traffic management especially under the inclement weather.

Visibility-related Crash Prediction

Recently, researchers have been trying to understand the relationship between real-time traffic flow characteristics and crashes that occur during reduced-visibility conditions. Abdel-Aty et al. (2012b) examined the relationship between real-time traffic data and the risk of crashes during reduced visibility related (VR) conditions by using Bayesian matched case-control logistic regression with the available loop/radar detectors (LDs) and automatic vehicle identification (AVI) data. It was found that 73% of VR crashes could be identified. Hassan and Abdel-Aty (2013) used Random Forests and matched case-control logistic regression models to examine how real-time traffic flow data could predict crash occurrence during reduced visibility conditions. The results also indicated that traffic flow variables leading to visibility-related crashes were slightly different from variables leading to clear visibility crashes.

Evaluation of Traffic Management Tools

The evaluation of traffic management tools can be divided into two categories. From the perspective of engineering economics, a benefit and cost analysis is needed in order to decide whether to purchase and/or deploy system components. The other issue is the evaluation of the effects of the tool on driver behavior. There are a large number of studies that have tested the effectiveness of reducing vehicle speed. Few studies have focused on expected driver responses to different messages in reduced visibility conditions, or their preferences with regards to the forms of these messages.

Mueller and Trick (2012) compared speed and hazard avoidance rates during fog between experienced drivers and novice drivers. Novice drivers exhibited higher speeds and less hazard avoidance in foggy weather. Jomaa et al. (2013) evaluated the effectiveness of vehicle-activated signs on driver behavior and the trigger parameters used in each study. This research suggests that the newly-developed dynamic activation threshold values should be considered in future studies. Ni et al. (2013) found that under reduced visibility conditions, older drivers face an increased risk of accident due to their decreased ability to successfully steer the vehicle. Hassan and Abdel-Aty (2011) adopted Explanatory Factor Analysis (EFA) and Structural Equation Modeling (SEM) to examine drivers' compliance and satisfaction with VSL/CMS under low visibility.

Fog/Visibility Detection and Prediction Method

Most fog forecasting is used for aviation purposes, using sensors located at airports. The sensors used at airports are called Automated Surface Observing Stations (ASOS). ASOS constantly collect and stream data and help the National Weather Service (NWS) to monitor and forecast the formation of fog. One limitation of ASOS is its inability to see weather not encountered by the sensors.

With regards to visibility detection for airports, Chan (2013) proposed a new algorithm that combines Light Detection and Ranging's (LiDAR) backscattered power data and measurements from the forward scatter sensors to generate visibility maps for the Hong

Kong International Airport. The LiDAR is a monostatic, heterodyne system operating at a wavelength of about 2 μm. The forward scatter sensor has a transmitter and a receiver at an angle of 33º with respect to each other. This new algorithm is able to generate a visibility map without using the empirical relationship for a specific weather type. This research has shown that the LiDAR-based visibility estimates are generally of satisfactory quality, particularly for visibility of 1500 m or above.

Shahabi et al. (2012) introduced various fog detection tools which are currently being utilized by different agencies' fog forecasting processes. Sounding profiles can be a valuable method of diagnosing and forecasting fog. However, this tool has three limitations. First, it is unreliable for predicting local events because the observations are sparse. Second, the intervals between sounding observations can be quite large, which makes it difficult to identify timely any changes in conditions. Third, the resolution of the sounding instrument affects the accuracy of the detection of fog formation and dissipation.

Another data source used for fog detection is satellite imagery. Satellite imagery is useful for showing fog events if they are spreading out at a synoptic scale. In addition, satellite imagery can also be used to monitor mid and high level clouds to predict their effects on underlying fog. However, it is hard to differentiate between low-lying stratus cloud and fog.

Fog prediction generally combines data obtained from sources such as sensing techniques, supplemental meteorological information, and core algorithms or forecasting models. Using models to forecast fog at a local scale, however, remains a difficult task. Higher levels of forecast accuracy have been achieved by developing very sophisticated parameterization schemes, especially for the simulation of subgrid-scale atmospheric processes. However, improving the accuracy of fog prediction remains a challenge.

Using existing highway cameras to monitor/forecast fog is of great interest to researchers, as these uses might already be deployed for other purposes. There are two general approaches to measuring meteorological visibility with a camera. The first is to detect the contrast between the most distant targets. The second general approach is based on machine learning and requires a calibration phase, with meteorological data collected with a visibility meter. Babari et al. (2012) used existing highway cameras and a technique based on the gradient magnitude to estimate visibility. The module of the Sobel gradient indicates the value of the largest change from bright to dark at each pixel. Researchers established a link between visibility and the gradient in the image. The visibility estimates were obtained with an average error of 30%.

In summary, fog detection and warning systems have been widely implemented across the US and other countries. With the advancements being made in detection and communication techniques, road users can now be advised through variable message signs and highway advisory radios. An analysis of the existing literature indicates that most systems use traditional visibility sensors and cameras; these implementations are, however, very expensive.

More important, the majority of systems can only detect existing fog and lack the ability to provide predictive guidance. The prediction of visibility obstructions could help drivers avoid crashes and possibly guide traffic to alternative routes, or help save money via a more advanced deployment of law enforcement services.

The real time fog probability map in Italy and the visibility map used at the Hong Kong International Airport are the only two applications that try to provide uniform geospatial coverage. The fog probability map can provide predictions regarding fog for an entire area, rather than just several fixed points or segments, by the construction of several sensors. However, it should be noted that these two systems provide fog nowcasting rather than fog forecasting.

This project attempts a much more cost-effective approach by mounting lower cost sensor arrays at different levels above the ground. These sensor arrays are combined with adaptive learning modules to provide more accurate local predictions and, to the best of our knowledge, no other existing systems or studies use this technology.

2.4 Chapter Summary

This chapter first introduced the state-of-the-art and practice visibility systems in the US and around the world. After that previous researches related to the effect of reduced visibility on traffic flow and driver behavior as well as fog detection and prediction methods were generalized. One of the common limitations of those fog studies is that they only relied on simulation results. Therefore, it needs further investigation that can clearly describe the driving behavior and traffic flow changes in foggy conditions using real traffic and weather data. In addition, most fog detection systems can only detect existing fog and lack the ability to provide predictive guidance. It is meaningful to develop fog prediction algorithm to help drivers avoid crashes and possibly guide traffic to alternative routes, or help save money via a more advanced deployment of law enforcement.

3. INTRODUCTION OF METEOROLOGICAL THEORY AND DEVELOPMENT OF FOG ALGORITHM

3.1 Introduction

The presence of fog, smoke, and heavy rain contribute to an increase in the potential for traffic crashes. Improved detection and prediction of visibility obstructions can help avoid crashes, improve traffic management from reduced congestion, save money and most importantly save lives via more efficient advance deployment of law enforcement or other crews necessary to monitor deteriorating visibility conditions. The purpose of this chapter was to validate that an array of alternative low-cost environmental sensors combined with decision support logic specifically designed to detect the onset of fog, can meet or exceed existing performance of traditional technologies to identify fog and also provide the potential for short-term fog prediction.

An analysis of existing technologies indicates that most states have achieved some degree of improvement in safety via the deployment of visibility sensors and cameras along select sections of highways that can send information to dynamic message signs and traffic management centers. These traditional implementations are however expensive, purely reactive in nature, and typically limited to only very few locations due to budget constraints. These traditional approaches do not provide the necessary spatial coverage nor do they provide predictive guidance that is desired for optimum safety.

During this project PraxSoft worked to refine current low-cost environmental sensor array, interfaced it with an innovative communications system for real-time data collection, determined necessary supplemental data, developed initial decision support software algorithms to process and analyze the data, and deployed a prototype system at a test site on I-4 in Polk County, FL. A traditional visibility sensor and camera were used as a baseline "ground truth" to determine the presence of restricted visibility. Initial results confirmed the ability of the PraxSoft system to identify the presence of fog with promising potential for at least short term prediction of fog formation.

3.2 Meteorological Theory

The foundation of the initial PraxSoft fog algorithm was based on correlations between observed fog events and other meteorological parameters (e.g. temperature, dew point, relative humidity, wind speed, visibility, etc.) derived from a historical data set of high-quality hourly weather observation records which included 179 airport, land and marine based stations with a core of 76 sites that are from airports and report the necessary parameters for fog in Florida. This analysis of historical meteorological observation data indicated a positive relationship between the occurrences of low visibility (less than 0.1 mile) and certain measured atmospheric conditions. Specifically, most fog events were reported (or inferred from low visibility measurements) when relative humidity measurements exceeded certain thresholds. In some cases there was also a correlation of fog formation with clear skies in the evening and early morning hours, though the sample set for this was limited due to fewer available observation points with reliable reporting of sky conditions than expected. It was further determined that the occurrence of recent precipitation events and associated increased levels of soil moisture could also potentially increase the onset of low visibility during the following 12-24 hour period.

The findings were consistent with meteorological phenomena known as radiation fog, a type of fog that typically forms at night under clear skies with calm winds when heat absorbed by the earth's surface during the day is radiated into space. As the earth's surface continues to cool, provided a deep enough layer of moist air is present near the ground, the humidity will reach at or near 100% and fog will form. Radiation fog occurs close to the ground, near the level of an automobile windshield, can reduce visibility to near zero at times, and has the potential to make driving extremely hazardous.

For any type of fog to form the Temperature/Dew Point (T/Td) spread must be small enough or a RH of 100% will never be reached. Also, an abundance of condensation nuclei must to be present for dense fog to form (why smoke-related fog events produce denser fog). PraxSoft originated the concept of a "Fog Index", designed to provide an objective prediction of the formation of radiation fog, the most common type of fog in Florida. Radiation fog has several characteristics:

- forms over land only
- occurs most often with high air pressure under clear skies
- requires relatively high humidity and a stable atmosphere
- requires very light winds
- disappears some period of time after sunrise with an increase in winds

Please note that persistent light winds are typically necessary for dense radiation fog formation helping ensure that cool surface air will mix with the layers above and within the layer where water droplets are present. If there is too much wind, fog will not form, but low stratus cloud cover that is detached from the surface is likely and will not cause traffic impediments.

It should also be noted that fog dissipation typically occurs after sunrise with an increase in winds when the sun starts to heat up the friction layer at the top of the fog bank and mixing of the air begins. Fog will dissipate even more as the droplets at the top of the bank start to evaporate demanding more latent heat. This physics phenomenon sometimes creates a brief intensification of fog immediately prior to dissipation, all usually occurring within about the first hour after sunrise.

Usually within about an hour of sunrise, the heat of the sun has a chance to warm up the ground, the fog bank will detach and will start to lift off in a few places and sometimes a low stratus and/or stratocumulus cloud will be formed. In the absence of sunshine (with high altitude clouds) this fog can persist for hours. Sometimes this type of fog can be very persistent, especially near water bodies or in lower areas such as valleys where katabatic winds will help the formation. (Radiation Fog Formation, 2014)

As mentioned earlier, radiation fog usually forms during the nighttime hour when clear skies and light to calm winds are present and when air temperatures are close to saturation near the ground surface. As the air cools to saturation due to heat escaping to space and lack of wind, the moisture condenses out to form fog as illustrated below (Radiation Fog, 2014):

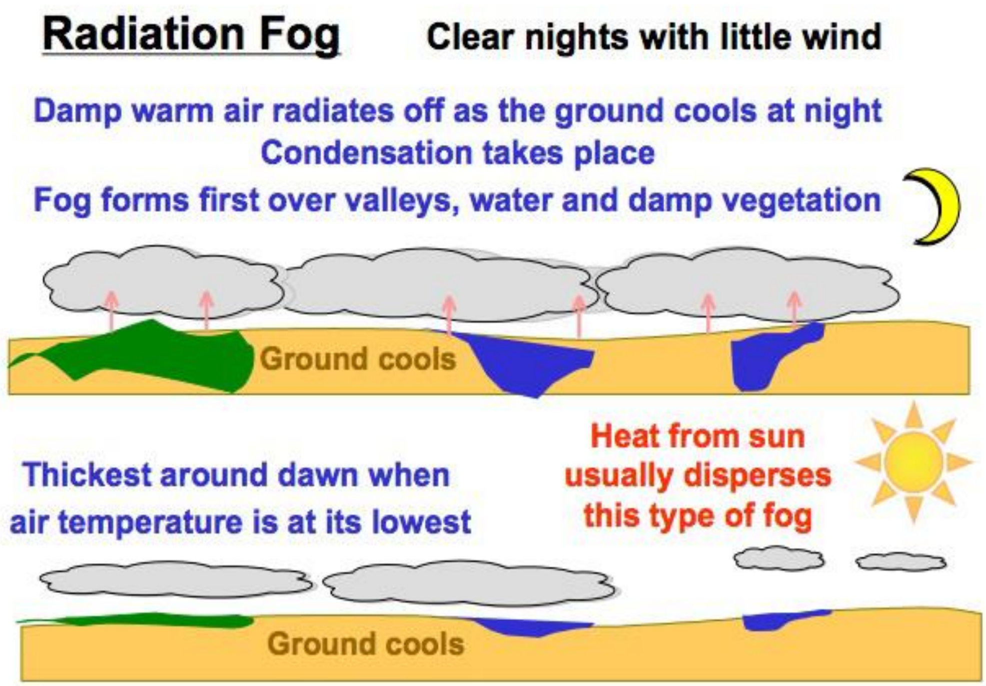

Figure 3.1 Formation of Radiation Fog

As the sun rises it increases the temperature, the air becomes less saturated and winds increase. The fog then dissipates. A more technical explanation of the physics of fog droplet formation is offered below (Knupp, 2014):

Conservation equations for water vapor mixing ratio (q), temperature (T) and saturation (δ, think of this in terms of relative humidity)

The mass of water vapor per unit volume can be obtained from the equation of state for water vapor:

$$\rho_v = e_s/R_v T$$

Differentiation of this equation yields

$$d\rho_v = \frac{de_s}{R_v T} - \left(\frac{e_s}{R_v T^2}\right) dT \approx \frac{de_s}{R_v T}$$

(This approximation is accurate to within ~5%; which can be shown with the C-C eq. or even with a more simplistic scale analysis.)

As cooling produces condensation in the fog, the differential amount of condensate (mass per unit volume) can be found using

$$dM = \frac{-de_s}{R_v T} = -\left(\frac{L_{vl} e_s}{R_v^2 T^3}\right) dT$$

Example:

find the cooling required to form a fog liquid water content of 1 g m^{-3} (a vary large value) if the air is saturated at 10 °C.

$\Delta T = -\Delta M[R_v^2 T^3 / L_{vl} e_s(T)]$

$= -10^{-3}$ kg m^{-3} [(461 J K^{-1} kg^{-1})^2(283 K)^3/(2.5x10^6 J kg^{-1})(1227 Pa)

= -1.57 K temperature

Figure 3.2 Explanation of the Physics of Fog Droplet Formation

3.3 Sensor Array Architecture, Placement and Installation

Since a correlation of certain environmental conditions were derived from the historical data set analysis, specialized environmental sensor arrays were designed to measure certain parameters. A schematic of the Fog Monitoring System is shown in Figure 3.3.

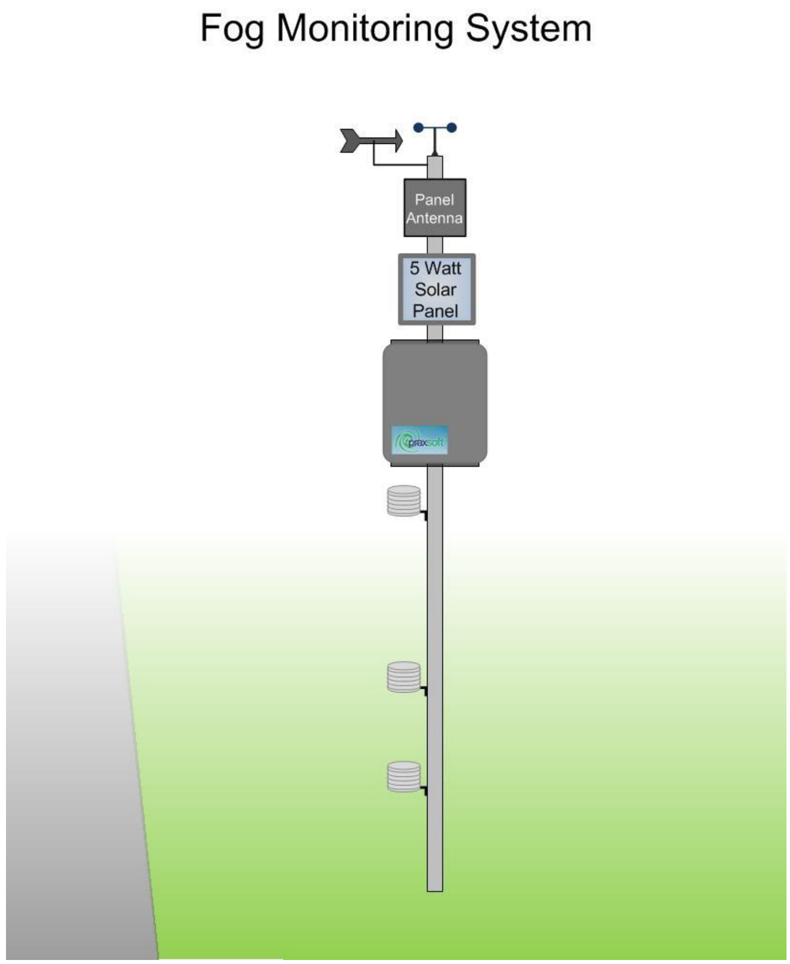

Figure 3.3 Fog Monitoring System

For purposes of this project, a Fog Monitoring Station (FMS) consists of three sensors at increasing elevations beginning at one foot one inch. A soil probe is inserted under the immediate ground surface. An anemometer is placed at every other FMS at a height of eight feet above the ground. The anemometer used was specifically chosen for its low-speed detection capabilities. A 5-watt solar panel and 12AH battery keep the FMS powered at all times so data is reported at 5-minute intervals 24/7. There are a total of eight FMS's spaced 0.25 miles apart. All sensors are secured to a 2-inch aluminum pole and a NEMA enclosure houses the battery, wiring, 802.15.4 radio, and Wireless Sensor

Node Microprocessor circuit board to handle the multiple sensor inputs while providing extremely low power consumption. This enables a high rate of data transmissions because of the very low power budget of the system. A photograph of one of the FMSs is shown in Figure 3.4 below.

Figure 3.4 Fog Monitoring Station

A more traditional meteorological sensor array, visibility sensor and camera were installed at the center point of the Fog Monitoring Stations to validate the data from the FMS units. Figure 3.5 is a diagram that illustrates the complete sensor architecture and layout of the system.

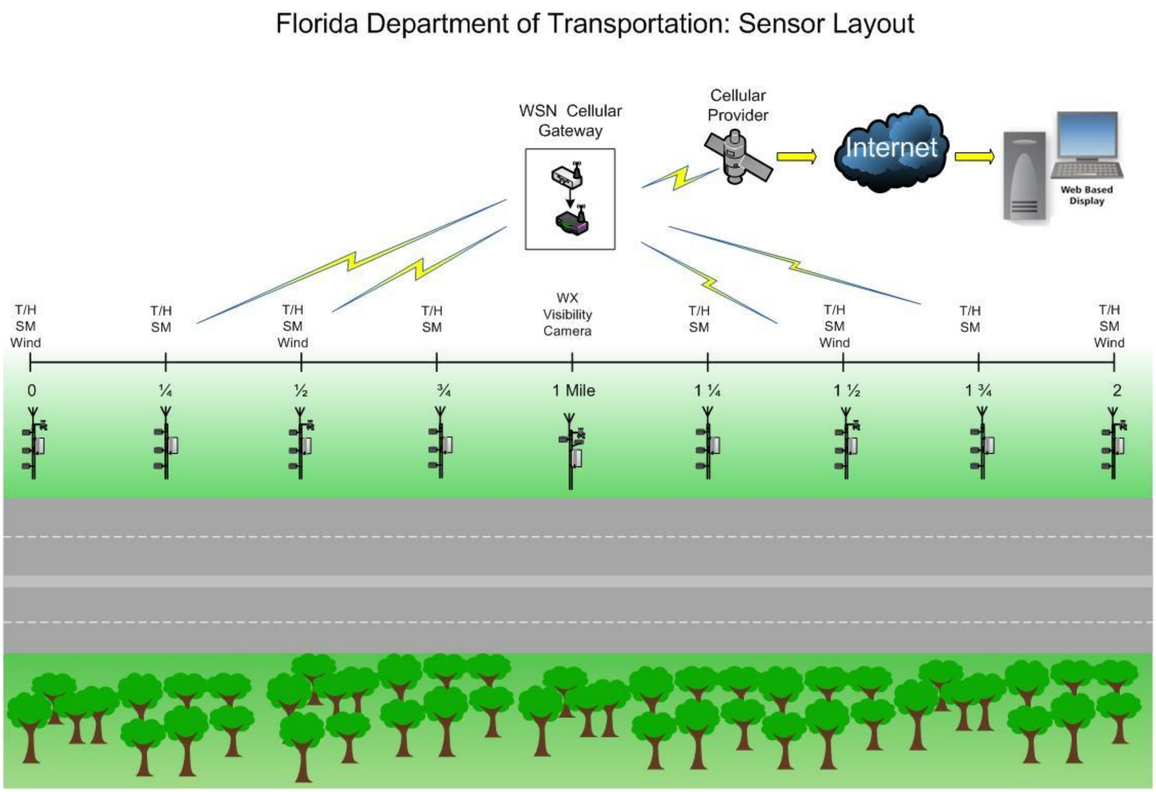

Figure 3.5 Sensor Architecture and Layout of the System

Also installed at the center location is the cellular back-haul and RF communications receiver that is responsible for collecting the data from the FMSs and delivering it to the PraxSoft database server via an "always-on" cellular gateway. This allows real-time access of data and images from the instrumented site. Each FMS communicates with the receiver via a point-to multipoint RF link with data packets sent out every 5 minutes (adjustable down to 1 minute). As each packet is received and acknowledged, it is sent to the server and inserted into an SQL database where the data is made available to selected users via a web application. The following photograph (Figure 3.6) shows the central collection point with the camera, visibility sensor, and meteorological sensor stack.

Figure 3.6 Camera, Visibility Sensor, and Meteorological Sensor Stack

Figure 3.7 below is the aerial view of the project study area located on I-4 between milepost 19 and milepost 23. The study area is roughly situated between State Road 559 and State Road 557. Each pinpoint marker represents the location of a multi-array sensor stack, and the distance between two consecutive yellow pinpoints is 0.25 miles.

Figure 3.7 Aerial View of the Study Area

Web Application

The web application is based on previous software developed by PraxSoft and modified for this project. It can be accessed at the following URL:

http://fdot.weatheractive.net:81/login.aspx

Credentials are required to login and access the data.

The web application provides real-time access to the data from the FMSs and other sensors via a GIS-based map interface as shown in Figure 3.8 below.

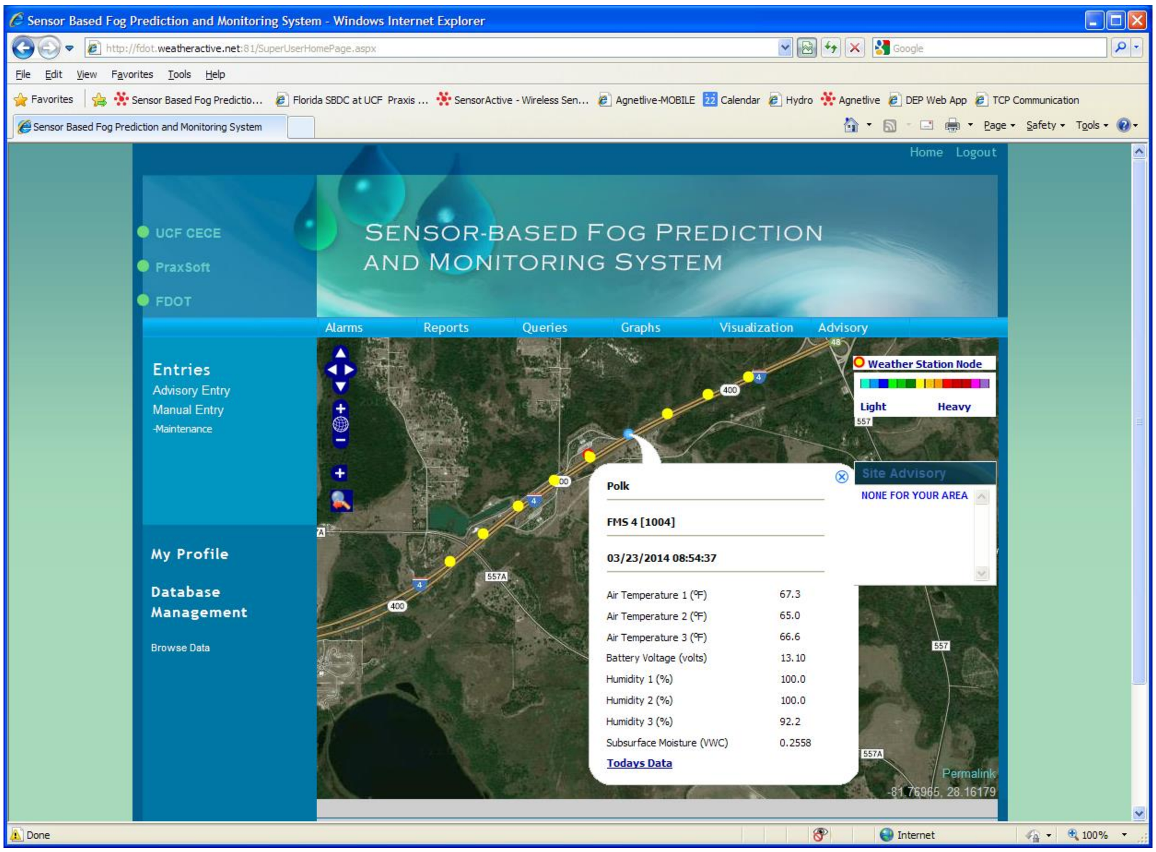

Figure 3.8 GIS-Based Map Interface

The web application includes an “Administrative” mode where the metadata used in determination of the Fog Detection Thresholds can be defined and adjusted.

This information along with the analysis of the data collected during the project will be explained in the following section.

3.4 Fog Algorithm and Visibility Determination

Measurements of environmental parameters from the Fog Measurement Stations were collected from sensors at different elevations above the ground. This data provided an objective micro-level assessment of the current state of the thermodynamic profile near the ground surface along with soil conditions to determine if a visibility constraint (fog) existed or was likely forming. The FMS sensor measurements were interrogated each 5-minute update cycle, seeking to identify conditions that exceeded certain defined fog detection thresholds for each unique location where FMS sensors are deployed.

Critical "threshold" values were identified for each measured FMS parameter, at each vertical level, that correlated to the presence of fog. Three distinct thresholds, one for low fog probability, one for medium fog probability, and one for high probability are assigned for each meteorological parameter. FMS measurements are continually monitored. As atmospheric conditions change, each FMS measurement at every vertical level along with soil moisture is compared to their corresponding fog thresholds. A resultant consolidated Mean Fog Index (MFI) is derived and is further refined by other geospatial factors. The MFI is then converted into an easy-to-understand numerical range value from 0 (no fog) to 3 (fog likely).

	Mean Fog Index	Description
High	3	Fog Likely
Moderate	2	Fog Likely Forming
Low	1	Monitor Trends
None	0	Good Visibility Likely

Initial test results have been encouraging. Once correlations of the presence of fog were validated by the FMS instrumentation, then continuous monitoring of the FMS measurements occurred over time looking for trends where parameters approached critical thresholds. This provided the opportunity for short-term prediction of the onset and dissipation of fog events. In some cases the system was able to not only indicate the onset of fog, but also provided a much longer pre-warning than we had originally anticipated. This is encouraging as it would allow officials more advance time to prepare for localized dense fog events. More research and more test data are suggested to further refine algorithms and also to reduce the chances of "false positives".

Test Case Verification

There were several data sets available for initial analysis to correlate observed fog episodes with the data gathered by the 8 FMS sites with "ground-truth" by the meteorological sensor array, visibility sensor and camera images.

In the initial test data sets shown below, two examples of radiation fog occurred on February 2nd and February 4th. In both cases the Mean Fog Index provided at least one hour advance notice prior to the formation of dense fog. Another shorter duration fog event occurred on January 20th which also showed the system at work.

February 2

On February 2nd, the data from the FMS sensors verified the presence of fog with the Mean Fog Index at "High" starting at 4:00 am, with all three FMS humidity sensors at

100% saturation and calm winds. The conventional visibility sensor started indicating lower readings at FMS station 1 at about 5:30 am. In this case the test FMS system provided over a full hour of advance warning of an ensuing fog event that ultimately became very dense.

Date	Time	FMS Station	SM	H1	H2	H3	Fog Index
2/2/2014	4:02:44	1	0.3701	100	100	100	High
2/2/2014	4:08:40	1	0.3701	100	100	100	High
2/2/2014	4:14:36	1	0.3701	100	100	100	High
2/2/2014	4:20:32	1	0.3701	100	100	100	High
2/2/2014	4:26:31	1	0.3701	100	100	100	High
2/2/2014	4:32:24	1	0.3701	100	100	100	High
2/2/2014	4:44:16	1	0.3701	100	100	100	High
2/2/2014	4:56:09	1	0.3701	100	100	100	High
2/2/2014	5:02:05	1	0.3701	100	100	100	High
2/2/2014	5:25:49	1	0.3701	100	100	100	High

Table 3.1: FMS Data 2/2/2014

Visibility sensor readings:

Visibility		
2/2/2014	5:27:51	2000
2/2/2014	5:34:35	1060
2/2/2014	5:48:03	2000
2/2/2014	6:01:31	274
2/2/2014	6:14:59	1074
2/2/2014	6:21:54	315
2/2/2014	6:28:38	96
2/2/2014	6:35:22	153
2/2/2014	6:42:06	241
2/2/2014	7:02:18	261
2/2/2014	7:09:03	184

Table 3.2: Visibility Data 2/2/2014

Camera images from this dense fog event are captured below:

5:34 am

7:15 am

9:30 am

Some time after sunrise (which occurred at 7:15 am) the fog began to lift and disperse as the winds increased. The humidity levels soon followed and the high risk was lowered.

Date	Time	FMS Station	SM	H1	H2	H3	Fog Index
2/2/2014	8:35:42	1	0.3653	100	100	100	High
2/2/2014	8:41:40	1	0.3653	100	100	100	High
2/2/2014	8:47:34	1	0.3653	100	100	100	High
2/2/2014	8:53:33	1	0.3653	100	100	100	High
2/2/2014	8:59:27	1	0.3653	100	100	100	High
2/2/2014	9:11:21	1	0.3653	100	100	100	High
2/2/2014	9:17:17	1	0.3653	100	100	100	High
2/2/2014	9:23:14	1	0.3653	100	100	100	High
2/2/2014	9:29:11	1	0.3653	100	100	100	High
2/2/2014	9:35:08	1	0.3653	100	100	100	High
2/2/2014	9:41:06	1	0.3653	100	100	100	High
2/2/2014	9:47:08	1	0.3653	98.2	100	100	High
2/2/2014	9:53:03	1	0.3653	98.6	100	100	High
2/2/2014	9:58:58	1	0.3653	98	98.8	100	High
2/2/2014	10:16:51	1	0.3653	93.8	94.4	96.4	Moderate
2/2/2014	10:22:48	1	0.3653	89.8	91.3	92.5	Moderate
2/2/2014	10:28:48	1	0.3653	86.7	88	89.3	Moderate

Table 3.1: Continued

February 4

The February 4th episode followed a similar pattern with a “High” Fog Index that preceded a fog event by more than one hour. Very light winds persisted for much of the night with saturated humidity levels resulting in fog in the early morning hours. This was followed by an increase in wind after sunrise, a decrease in humidity, and the lifting of the fog whereupon the Mean Fog Index was reduced.

Date	Time	FMS Station	SM	H1	H2	H3	Fog Index
2/4/2014	5:47:27	8	0.2796	100	100	100	High
2/4/2014	5:53:25	8	0.2796	100	100	100	High
2/4/2014	5:59:23	8	0.2796	100	100	100	High
2/4/2014	6:05:23	8	0.2796	100	100	100	High
2/4/2014	6:29:14	8	0.2796	100	100	100	High
2/4/2014	6:35:14	8	0.2749	100	100	100	High
2/4/2014	6:41:12	8	0.2749	100	100	100	High
2/4/2014	6:47:08	8	0.2796	100	100	100	High
2/4/2014	6:53:06	8	0.2796	100	100	100	High
2/4/2014	6:59:04	8	0.2796	100	100	100	High
2/4/2014	7:05:03	8	0.2796	100	100	100	High
2/4/2014	7:11:01	8	0.2796	100	100	100	High
2/4/2014	7:28:55	8	0.2796	100	100	100	High
2/4/2014	8:04:47	8	0.2749	100	100	100	High
2/4/2014	8:16:44	8	0.2749	100	100	100	High
2/4/2014	8:28:38	8	0.2749	100	100	100	High
2/4/2014	8:34:36	8	0.2749	100	100	100	High
2/4/2014	8:40:34	8	0.2749	100	100	100	High
2/4/2014	8:46:35	8	0.2749	100	100	100	High
2/4/2014	8:52:31	8	0.2749	100	100	100	High
2/4/2014	8:58:30	8	0.2749	100	100	100	High
2/4/2014	9:10:27	8	0.2749	100	100	100	High
2/4/2014	9:16:26	8	0.2749	100	100	100	High
2/4/2014	9:22:24	8	0.2749	100	100	100	High
2/4/2014	9:28:23	8	0.2749	100	100	100	High
2/4/2014	9:34:22	8	0.2749	100	100	100	High
2/4/2014	9:40:21	8	0.2749	100	100	100	High
2/4/2014	9:46:42	8	0.2749	100	100	100	High
2/4/2014	9:52:19	8	0.2749	100	100	100	High
2/4/2014	9:58:19	8	0.2749	98.1	98.2	99	High
2/4/2014	10:04:18	8	0.2749	94.4	92.5	96.3	High
2/4/2014	10:10:18	8	0.2749	86.9	86.3	92.3	Moderate
2/4/2014	10:16:19	8	0.2796	82	82.3	91.6	Moderate
2/4/2014	10:22:20	8	0.2749	79.6	80	87.4	Low

Table 3.3: FMS Data 2/4/2014

One note, the soil moisture (SM column) ticked down from 0.2796 to 0.2749 which may be expected as the fog persists and moisture slowly evaporates out of the soil. This was also noted in some of the FMS stations during the February 2nd event.

Visibility sensor readings:

Visibility		
2/4/2014	5:46:46	1271
2/4/2014	5:53:30	2000
2/4/2014	6:00:14	1188
2/4/2014	6:06:58	89
2/4/2014	6:20:26	242
2/4/2014	6:27:10	95
2/4/2014	6:33:54	258
2/4/2014	6:40:38	182
2/4/2014	6:47:22	220
2/4/2014	6:54:06	195
2/4/2014	7:00:51	216
2/4/2014	7:14:18	276
2/4/2014	7:27:46	177
2/4/2014	7:34:30	226
2/4/2014	7:41:14	149
2/4/2014	8:01:26	2000
2/4/2014	8:14:54	136
2/4/2014	8:28:22	289
2/4/2014	8:35:06	326
2/4/2014	8:41:50	1190
2/4/2014	8:48:34	1126
2/4/2014	8:55:18	198
2/4/2014	9:02:02	1190
2/4/2014	9:08:47	2000
2/4/2014	9:15:32	2000
2/4/2014	9:22:17	2000
2/4/2014	9:29:02	2000
2/4/2014	9:35:51	2000
2/4/2014	9:42:32	2000

Table 3.4: Visibility Data 2/4/2014

The lower visibility in this event, also correspond well with the visibility sensor readings, which just lag 40 or so minutes when the fog lifted. Below are camera images of the fog event for February 4th:

5:46 am 7:00 am 9:15 am

January 20

On January 20th there was a short duration radiation fog event. Even though it was of short duration, it was a radiation fog event with significantly reduced visibility. The event occurred right around sunrise. When the winds increased at just after 8:20 am, it began to break it up. The visibility sensor began indicating reduced visibility at 7:41 am, however the FMS indicated a “High” fog index at 6:06 am. From the pictures below it can be seen that there is indeed the beginning of reduced visibility at 6:06 am. Winds were calm and humidity levels were at saturation on all three levels of the FMS.

Visibility sensor for January 20th:

Visibility		
1/20/2014	6:06:49	2000
1/20/2014	6:26:58	2000
1/20/2014	6:33:41	2000
1/20/2014	6:40:24	2000
1/20/2014	6:47:07	2000
1/20/2014	6:53:50	2000
1/20/2014	7:00:33	2000
1/20/2014	7:07:16	1222
1/20/2014	7:13:59	2000
1/20/2014	7:20:42	2000
1/20/2014	7:27:25	2000
1/20/2014	7:41:02	174
1/20/2014	7:54:28	211
1/20/2014	8:07:57	72
1/20/2014	8:14:37	53
1/20/2014	8:21:20	2000
1/20/2014	8:28:06	2000
1/20/2014	8:34:49	2000
1/20/2014	8:41:31	2000
1/20/2014	8:48:18	2000
1/20/2014	8:54:59	2000

Table 3.5: Visibility Data 1/20/2014

Weather from station 1 for January 20th:

Date	Time	FMS Station	SM	H1	H2	H3	Fog Index
1/20/2014	6:06:32	1	0.332	100	100	100	High
1/20/2014	6:24:19	1	0.332	100	100	100	High
1/20/2014	6:30:14	1	0.332	100	100	100	High
1/20/2014	6:36:10	1	0.332	100	100	100	High
1/20/2014	6:42:05	1	0.332	100	100	100	High
1/20/2014	6:48:01	1	0.332	100	100	100	High
1/20/2014	6:59:52	1	0.332	100	100	100	High
1/20/2014	7:05:50	1	0.332	100	100	100	High
1/20/2014	7:11:45	1	0.332	100	100	100	High
1/20/2014	7:17:39	1	0.332	100	100	100	High
1/20/2014	7:23:35	1	0.332	100	100	100	High
1/20/2014	7:41:22	1	0.332	100	100	100	High
1/20/2014	7:53:13	1	0.332	100	100	100	High
1/20/2014	8:11:00	1	0.332	100	100	100	High
1/20/2014	8:16:57	1	0.332	100	100	100	High
1/20/2014	8:22:51	1	0.332	100	100	100	High
1/20/2014	8:34:42	1	0.332	100	100	100	High
1/20/2014	8:40:38	1	0.332	100	100	100	High
1/20/2014	8:46:36	1	0.332	100	100	100	High

Table 3.6: FMS Data 1/20/2014

6:06 am 7:40 am 8:21 am

Additionally, other events on the 21st and 28th of January, though they did not have a strong signature for radiation fog, produced reduced visibilities which started improving around sunrise with increased wind speeds.

3.5 Chapter Summary

The purpose of this chapter was to develop a proof of concept to validate that an array of low-cost environmental sensors, arranged at varying levels above the ground surface, could effectively detect the onset of fog and meet or exceed existing performance of traditional and much more expensive technologies. A combination of sensors and software algorithms were refined and augmented to work in concert to create derivative products that detect and provide the basis to predict the onset of fog. The design of the software is flexible enough to allow for the algorithms to be tuned and adjusted for micro-local conditions for improved accuracy. Visualization of category rankings of fog threat indices were also made available via an online portal. The validation during this initial project certainly justifies additional research and development that will lead to a final system which could be more broadly deployed.

4. DATA COLLECTION AND PREPARATION

4.1 Site Selection and Weather Sensor Installation

The site selected is based on the earlier report by UCF on I-4 in Polk County, mile posts 22.528-22.628 and 21.426-21.928 (see Figure 4.1). The system architecture and the aerial view of the selected study area are already shown in the previous chapter 3.

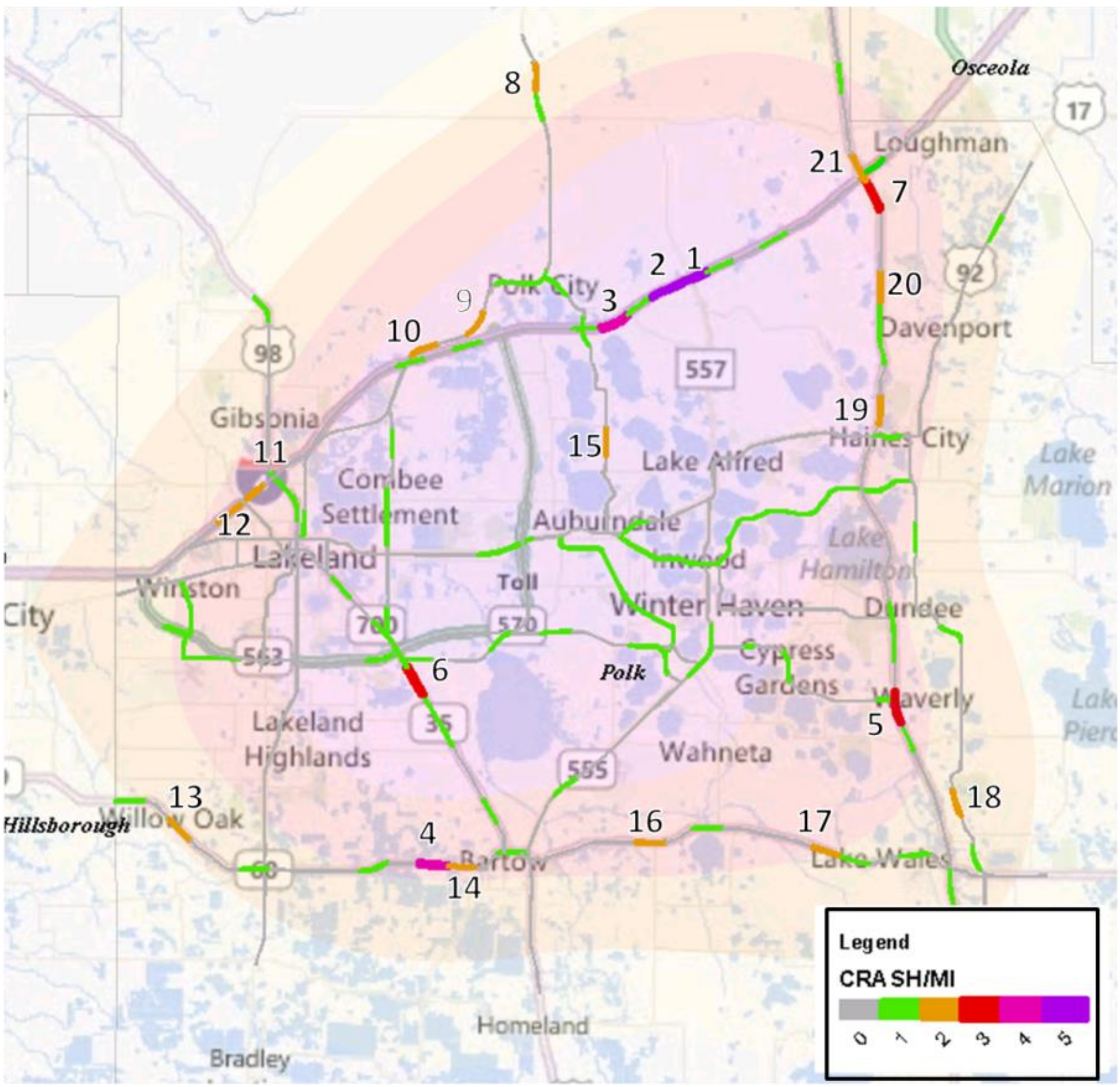

Figure 4.1 – Microscopic Analysis of Fog Crashes in Polk County (Abdel-Aty et al. 2012)

It is roughly situated between State road 559 and State road 557. On December 11 we were granted permission to visit the site to mark sensor and weather station locations. All FMS and WX are marked with stakes, flags, and orange paint. The RF field test results are listed below:

FMS 1: 100%, located 37 feet from pavement

FMS 2: 100%, located 37 feet from pavement, Located right at the fence

FMS 3: 99.4%, located 36 feet from pavement

FMS 4: 100%, located 36 feet from pavement, Located right at the fence

FMS 5: 100%, located 58 feet from pavement

FMS 6: 100%, located 69 feet from pavement

FMS 7: 100%, located 68 feet from pavement

FMS 8: 99.4%, located 69 feet from pavement

On December 11, 2013 we contacted the 811 underground utilities locator concerning the 2.5 mile stretch of I-4 West. On December 16th the locates were completed. The results are as follows:

- Brendan Lonergan, TransCore, request completed and any conflicts were marked with flags and spray paint.
- Gulfstream Natural Gas, close but not in conflict with the dig site area.
- Verizon, no conflicts.
- C/O Auburndale W/S/Street, no response yet
- Tampa Electric Company, no conflicts.

- AT&T, conflicts marked
- Ticket 345307883 FL : Polk County, POLK CITY Community I 4
- Ticket 345307655 FL : Polk County, POLK CITY Community I 4
- Ticket 345307779 FL : Polk County, POLK CITY Community

The NEXRAD weather radar data being integrated into the visualization module is of high quality and reliability, updating every 5 minutes (essentially the same update frequency as the NEXRAD radars themselves). A straightforward method to visualize this radar has been developed and the radar imagery is merged with base map information and highway networks.

The FMS have been setup in the PraxSoft lab and are collecting data to ensure all sensors and communications between nodes are working appropriately before field deployment. Data is being sent to a PraxSoft WSN receiver which is connected to the Internet.

4.2 Weather Data Collection

The weather data was then collected from those installed weather sensors in I-4 rest area. There are mainly two kinds of weather datasets. The first kind of dataset consists of twenty-one variables including air temperature, dewpoint, surface moisture, humidity, wind speed and some other important weather parameters such as barometric pressure and rainfall. The second kind of dataset consists of twelve variables including air temperature, surface moisture, humidity, wind speed and fog index which is used to predict the fog event. The Figure 4.2 and Figure 4.3 show a sample of these two kinds of datasets.

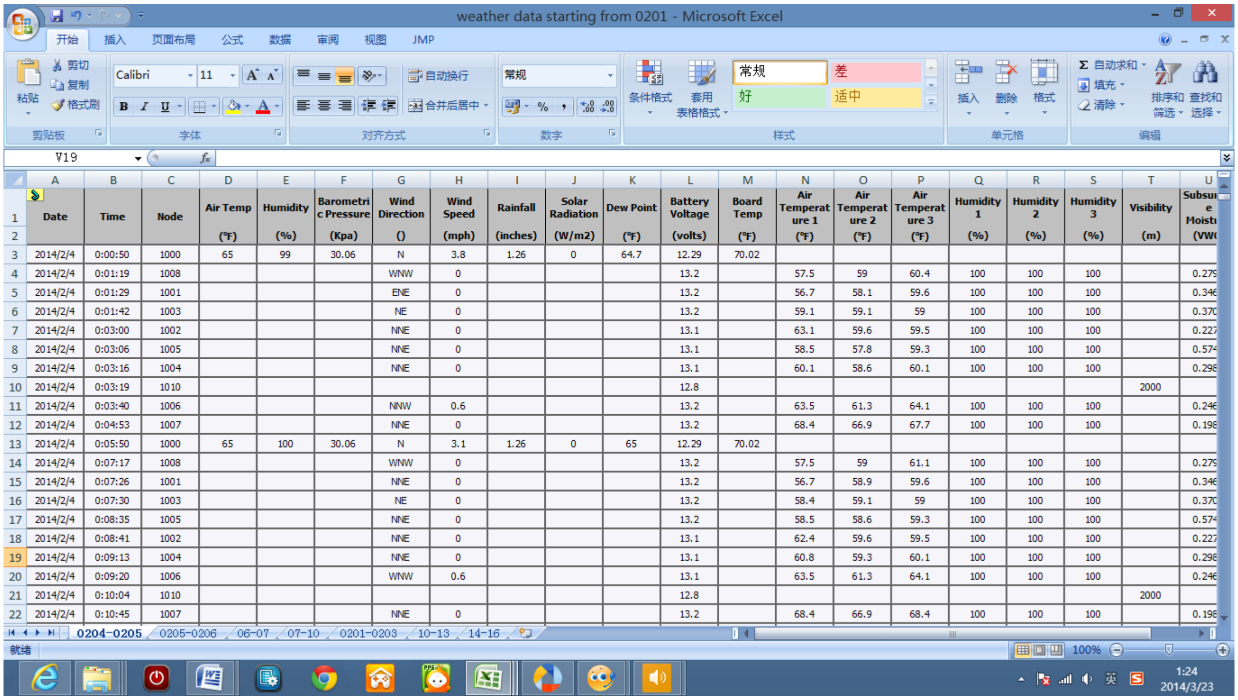

Date	Time	Node	Air Temp (°F)	Humidity (%)	Barometric Pressure (Kpa)	Wind Direction ()	Wind Speed (mph)	Rainfall (inches)	Solar Radiation (W/m2)	Dew Point (°F)	Battery Voltage (volts)	Board Temp (°F)	Air Temperature 1 (°F)	Air Temperature 2 (°F)	Air Temperature 3 (°F)	Humidity 1 (%)	Humidity 2 (%)	Humidity 3 (%)	Visibility (m)	Subsure Moistu (VW
2014/2/4	0:00:50	1000	65	99	30.06	N	3.8	1.26	0	64.7	12.29	70.02								
2014/2/4	0:01:19	1008				WNW	0				13.2		57.5	59	60.4	100	100	100		0.279
2014/2/4	0:01:29	1001				ENE	0				13.2		56.7	58.1	59.6	100	100	100		0.346
2014/2/4	0:01:42	1003				NE	0				13.2		59.1	59.1	59	100	100	100		0.370
2014/2/4	0:03:00	1002				NNE	0				13.1		63.1	59.6	59.5	100	100	100		0.227
2014/2/4	0:03:06	1005				NNE	0				13.1		58.5	57.8	59.3	100	100	100		0.574
2014/2/4	0:03:16	1004				NNE	0				13.1		60.1	58.6	60.1	100	100	100		0.298
2014/2/4	0:03:19	1010									12.8								2000	
2014/2/4	0:03:40	1006				NNW	0.6				13.2		63.5	61.3	64.1	100	100	100		0.246
2014/2/4	0:04:53	1007				NNE	0				13.2		68.4	66.9	67.7	100	100	100		0.198
2014/2/4	0:05:50	1000	65	100	30.06	N	3.1	1.26	0	65	12.29	70.02								
2014/2/4	0:07:17	1008				WNW	0				13.2		57.5	59	61.1	100	100	100		0.279
2014/2/4	0:07:26	1001				NNE	0				13.2		56.7	58.9	59.6	100	100	100		0.346
2014/2/4	0:07:30	1003				NE	0				13.2		58.4	59.1	59	100	100	100		0.370
2014/2/4	0:08:35	1005				NNE	0				13.2		58.5	58.6	59.3	100	100	100		0.574
2014/2/4	0:08:41	1002				NNE	0				13.1		62.4	59.6	59.5	100	100	100		0.227
2014/2/4	0:09:13	1004				NNE	0				13.1		60.8	59.3	60.1	100	100	100		0.298
2014/2/4	0:09:20	1006				WNW	0.6				13.1		63.5	61.3	64.1	100	100	100		0.246
2014/2/4	0:10:04	1010									12.8								2000	
2014/2/4	0:10:45	1007				NNE	0				13.2		68.4	66.9	68.4	100	100	100		0.198

Figure 4.2 Sample of Weather Data

Date	Time	Soil Moisture (VWC)	Temperature Level 1 (°F)	Humidity Level 1 (%)	Temperature Level 2 (°F)	Humidity Level 2 (%)	Temperature Level 3 (°F)	Humidity Level 3 (%)	Wind Speed (mph)	Wind Direction (&)	Fog Index
03/12/2014	0:00:19	0.232	64.7	86.4	65.3	85.9	64.6	87.4	0.6	SSW	Low
03/12/2014	0:11:52	0.232	64.7	87.6	65.3	86.8	64.6	88.7	1.5	SSW	Low
03/12/2014	0:17:48	0.232	64.7	88	65.3	87.3	64.6	89.1	0.9	SW	Low
03/12/2014	0:23:45	0.232	64.7	88.3	65.3	87.6	64.6	89.2	0.9	SW	Low
03/12/2014	0:29:43	0.232	64.7	88.3	65.3	87.5	64.6	89.3	0	SSW	Low
03/12/2014	0:35:38	0.232	64.7	88.4	65.3	87.6	65.3	89.3	0.3	WSW	Low
03/12/2014	0:59:24	0.232	64.7	88.7	65.3	87.9	64.6	89.6	1.8	SW	Low
03/12/2014	1:11:17	0.232	64.7	88	65.3	87.5	64.6	89.2	0.9	SW	Low
03/12/2014	1:17:14	0.232	64.7	87.3	65.3	86.6	64.6	88.2	2.1	WSW	Low
03/12/2014	1:23:10	0.232	64.7	87.5	65.3	86.7	64.6	88.4	1.5	SW	Low
03/12/2014	1:29:07	0.232	65.4	87.4	65.3	86.7	65.3	88.4	3.4	SSW	Low
03/12/2014	1:35:03	0.232	64.7	87.9	65.3	87.3	65.3	89.1	1.2	S	Low
03/12/2014	1:41:00	0.232	65.4	88.3	65.3	87.6	65.3	89.2	2.5	SSW	Low
03/12/2014	1:46:56	0.232	65.4	88.3	65.3	87.7	65.3	89.5	0.6	SSW	Low
03/12/2014	1:52:53	0.232	65.4	88.8	65.3	88.1	65.3	90	1.2	E	Low
03/12/2014	1:58:51	0.232	65.4	89.1	65.3	88.4	65.3	90.2	1.2	SW	Low
03/12/2014	2:22:36	0.232	65.4	91.3	65.3	90.7	65.3	92.7	1.5	ENE	Low

Figure 4.3 Sample of Weather Data including Fog Index

4.3 Installation of Wavetronix SmartSensor

In order to investigate the relationship between weather and traffic flow, a vehicle-based detector, Wavetronix SmartSensor HD, was installed to collect accurate traffic flow data, including vehicle speed, vehicle length and lane assignment. Augmenting the system with the unit Click 514 enables us to collect data for every vehicle so we can also calculate the headway.

The Installation Site

Figure 4.4 depicts is the aerial view of the selected study area on I-4 from milepost 19 to milepost 23. It is roughly situated between State road 559 and State road 557. The selected light pole to install the traffic detector is near the entrance of the rest area on the eastbound side (Figure 4.5). The offset from first detection lane to the light pole is 54 feet. The pictures of the street view of the light pole are provided from Figures 4.6 to 4.8.

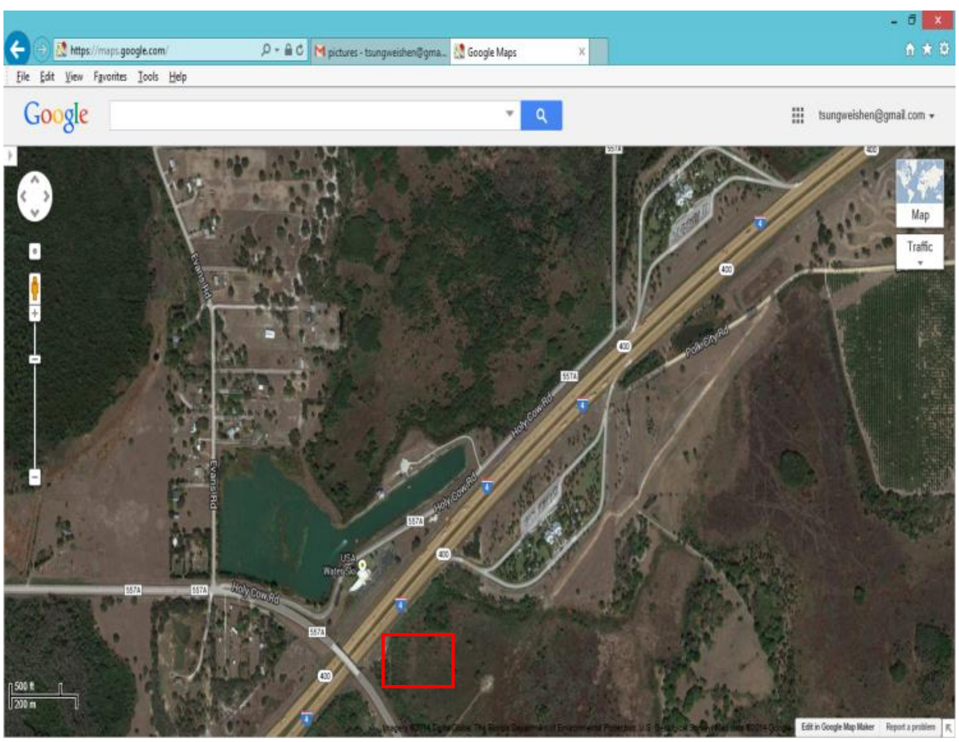

Figure 4.4 Rest area on the eastbound side of I-4

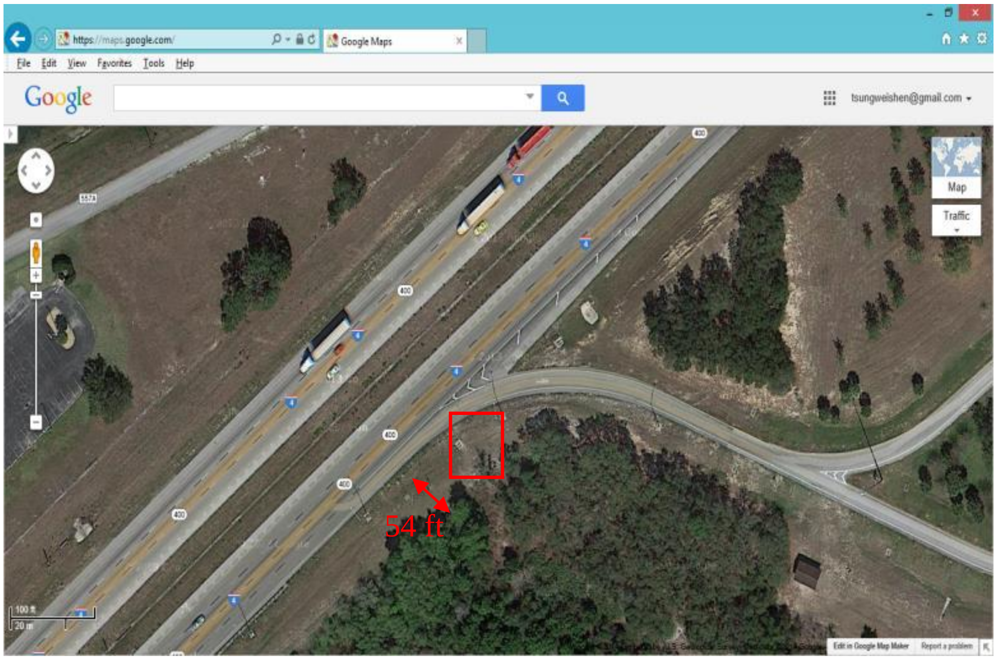

Figure 4.5 Light pole near the entrance of rest area

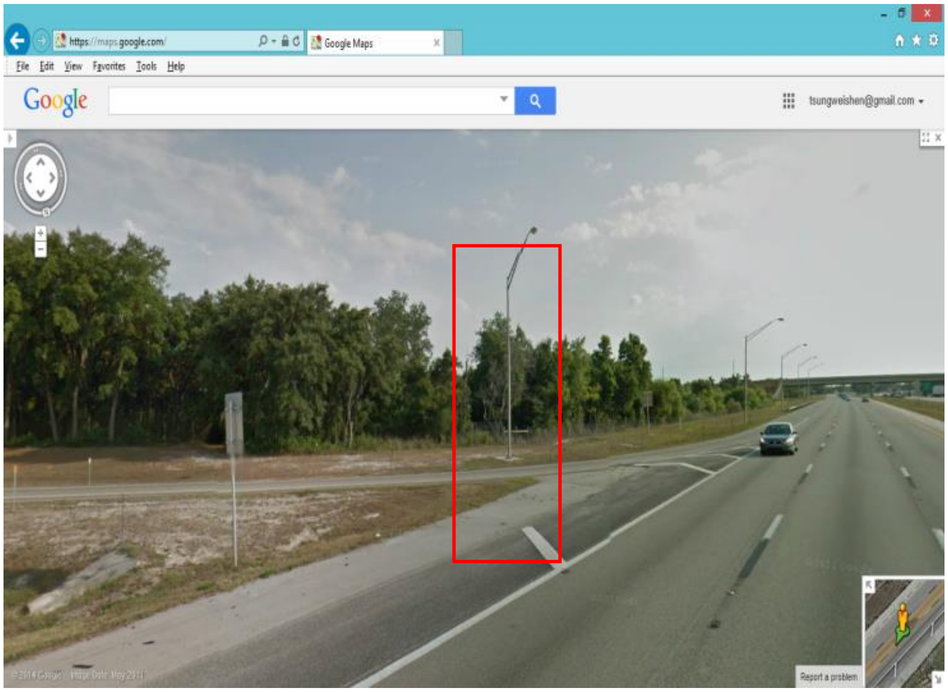

Figure 4.6 Street view of the light pole (1)

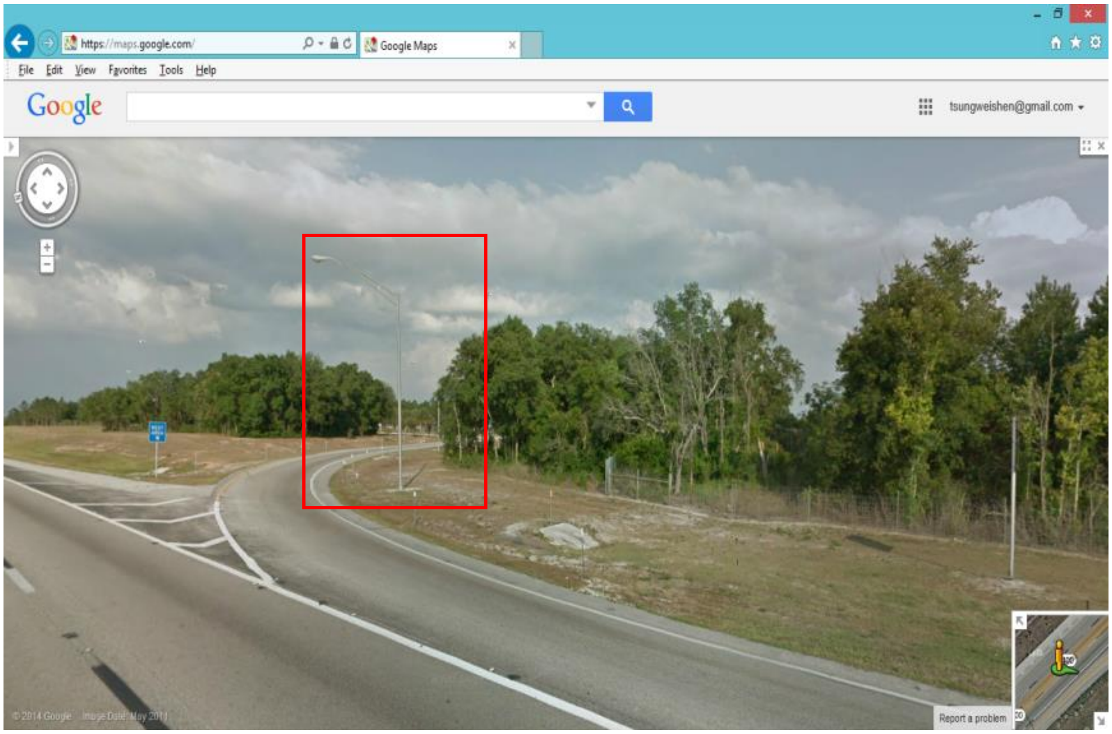

Figure 4.7 Street view of the light pole (2)

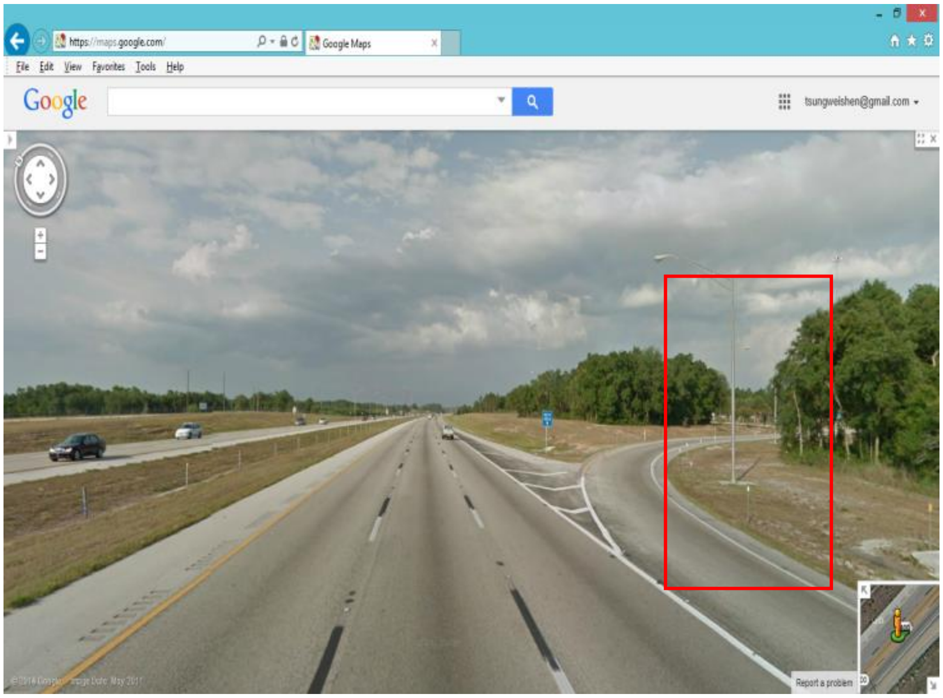

Figure 4.8 Street view of the light pole (3)

Components of the Traffic Sensor

There are three main parts of the detection systems: Wavetronix SmartSensor HD, pole-mount cabinet and power. The Wavetronix SmartSensor HD is a HD Digital Wave Radar which has a detection range of 250 feet and the ability to simultaneously detect up to 22 lanes of traffic (Figure 4.9). In the pole-mount cabinet, it has the Lightning surge protector (Click! 200) and the Event logger (Click 514). Lightning surge protector (Click! 200) protects devices from power surges over DC power and serial communication lines (Figure 4.10). Event logger (Click 514) monitors individual vehicle data pushed from SmartSensor HD and forwards it to data logger devices (Figures 4.11 to 4.13). In addition to the above two components, a DataBridge SDR-CF data logger was installed to save the vehicle-based traffic flow data (Figures 4.14 and 4.15). DataBridge SDR-CF is the tool for adding storage to any device. Two 12 V car batteries were connected in series to provide the power of the SmartSensor, event logger and data logger (Figure 4.16).

Figure 4.9 Wavetronix SmartSensor HD

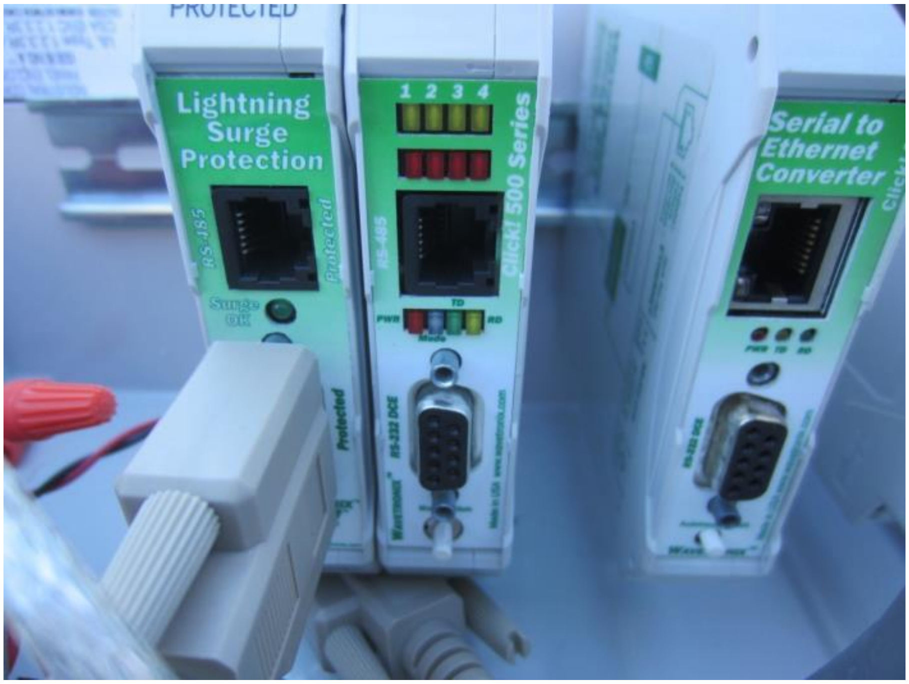

Figure 4.10 Lightning surge protector (First from left)

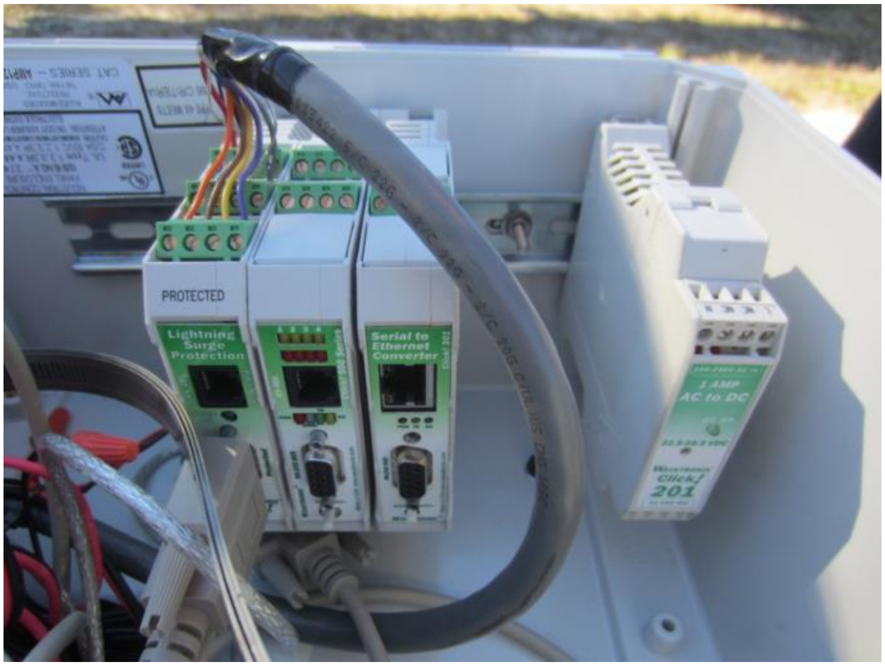

Figure 4.11 Event logger (Second from left)

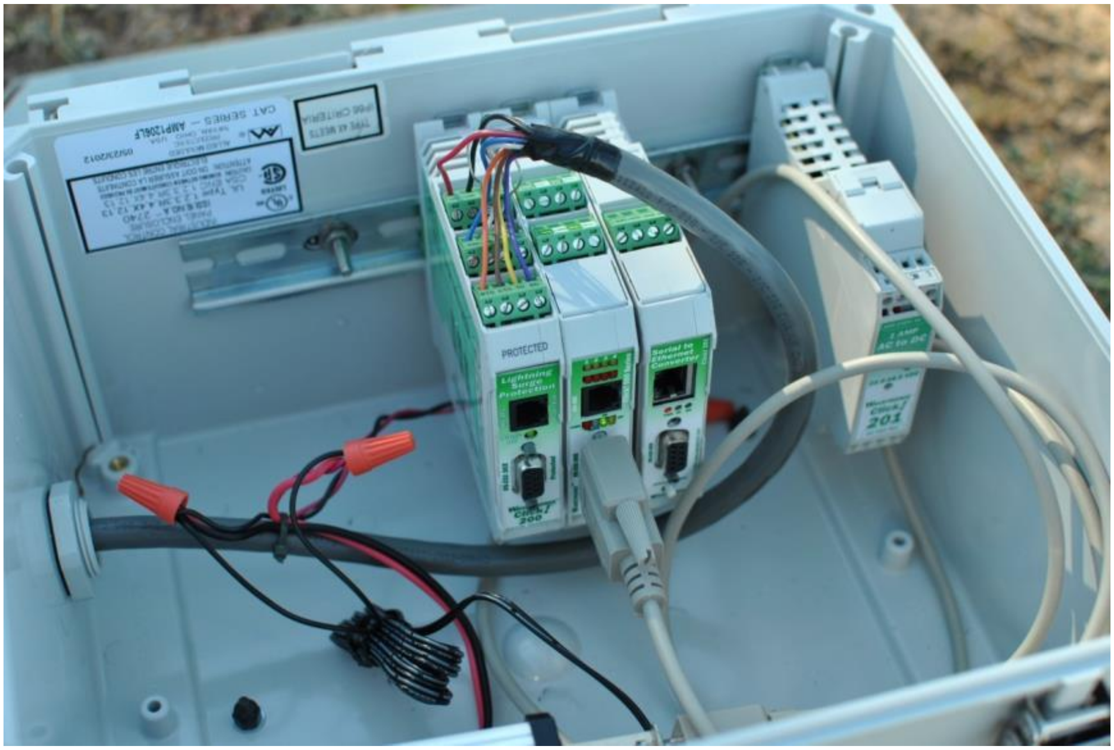

Figure 4.12 The connection between the lightning surge protector and the event logger

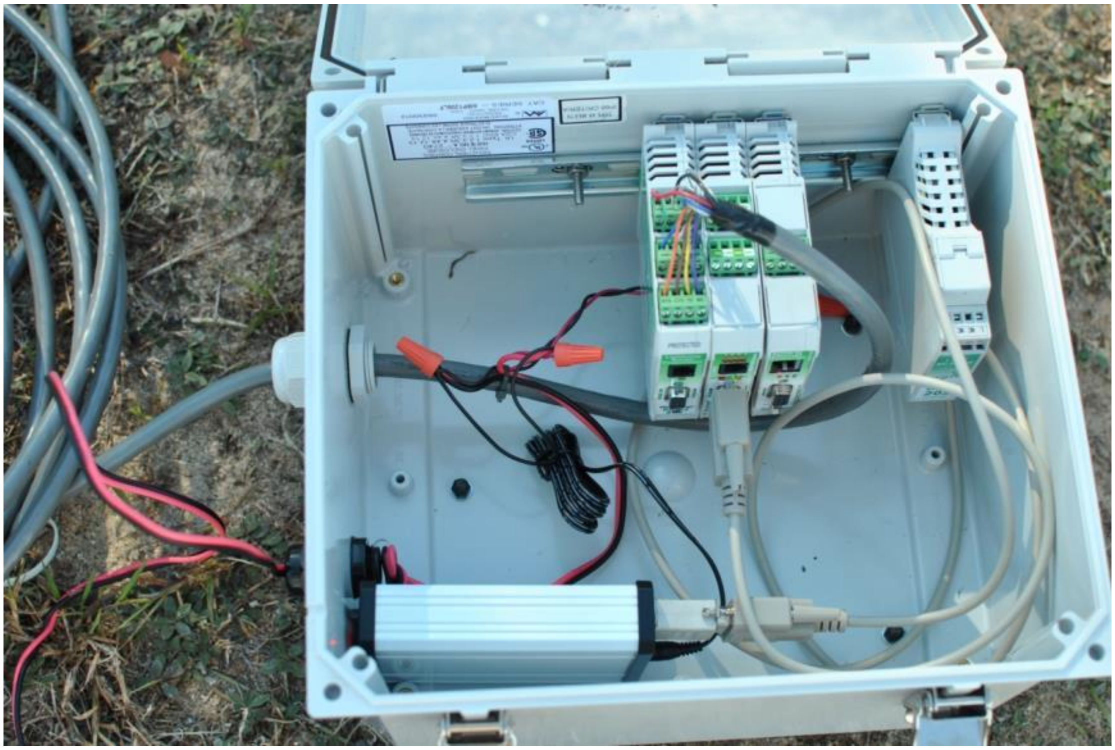

Figure 4.13 All components inside the cabinet

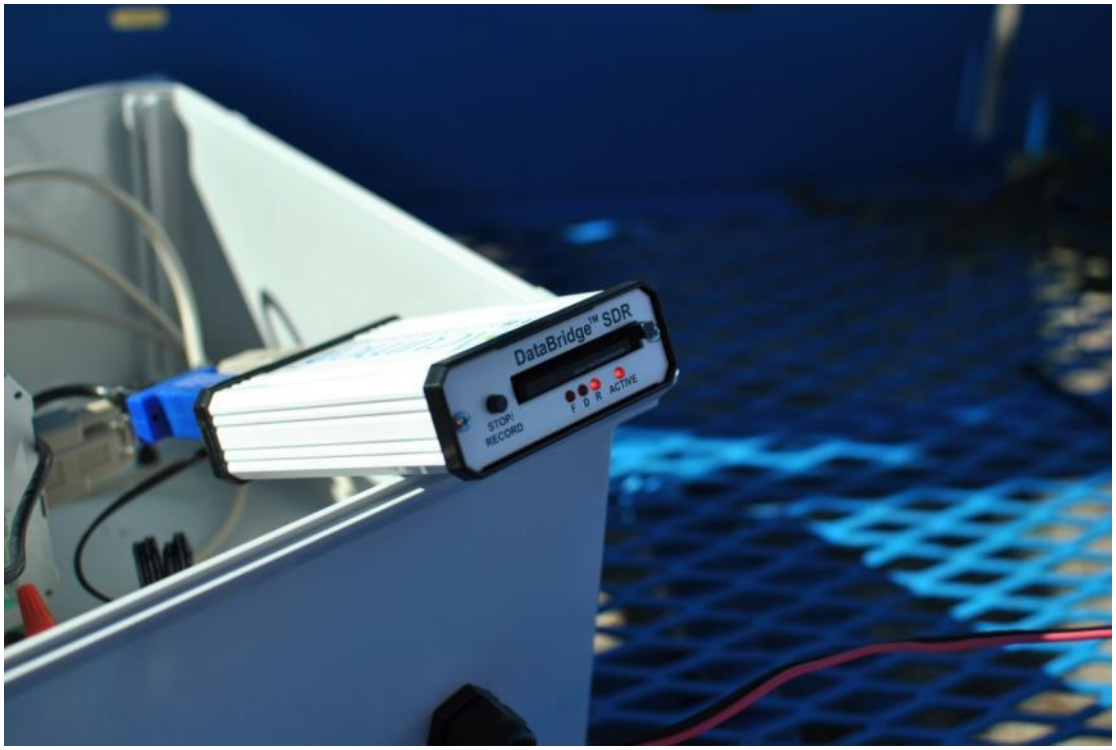

Figure 4.14 DataBridge SDR-CF data logger

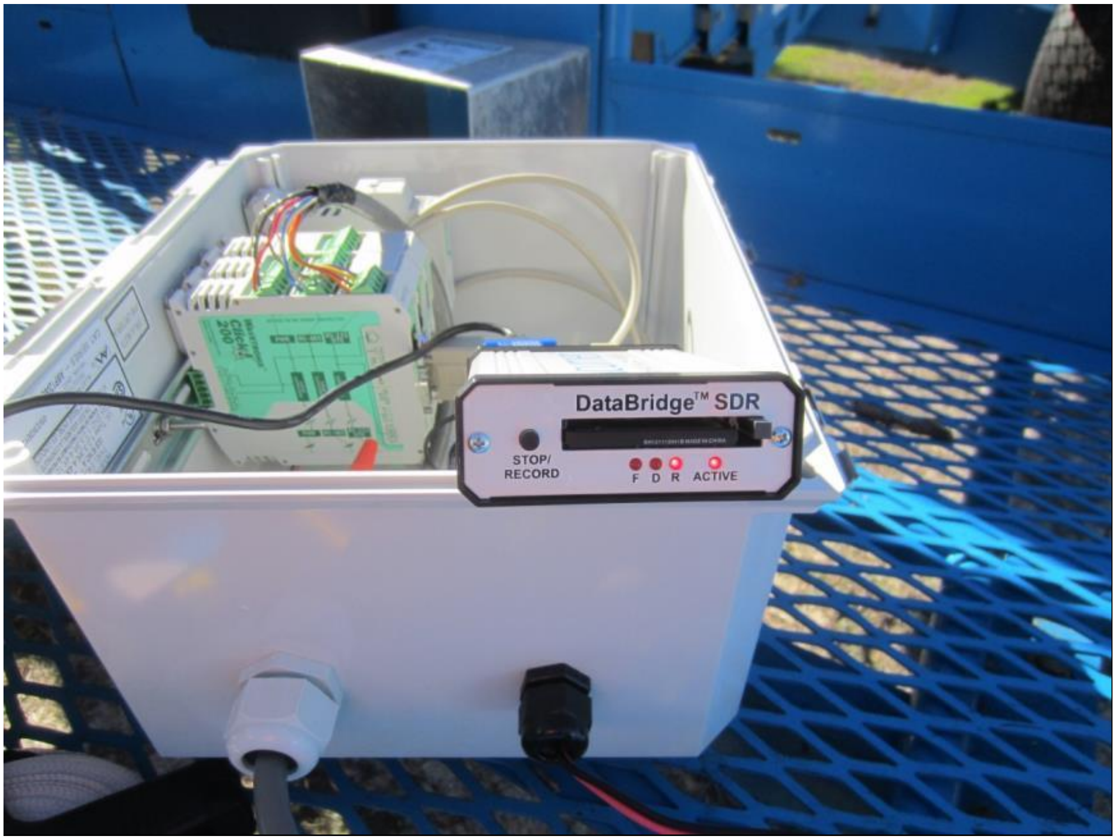

Figure 4.15 The LED indicators show the SDR's current recording status

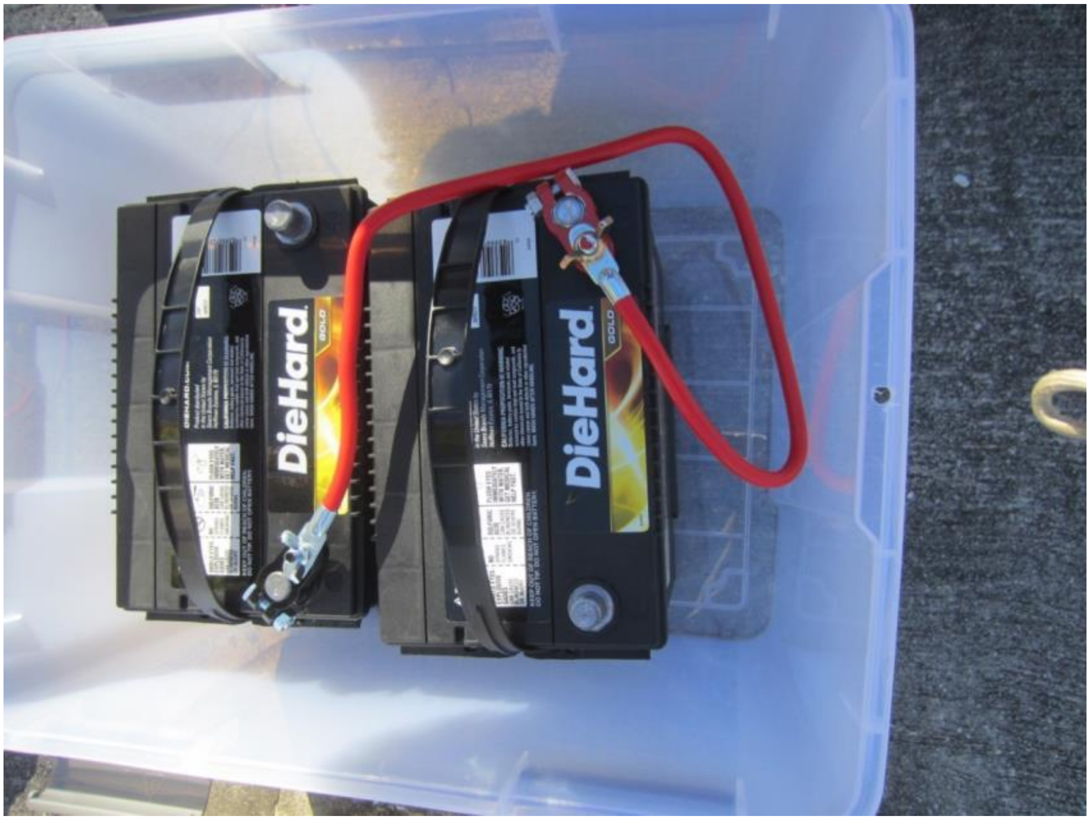

Figure 4.16 Batteries were connected in series

Installation of the Traffic Sensor

The installation of the traffic sensor system was in the morning of January 22, 2014. In order to capture the traffic flow for three lanes on each direction, the sensor was installed at more than 30 feet height. The side-to-side angle was set as close to perpendicular to the traffic flow as possible. The sensor alignment was done by the alignment tool of the SmartSensor HD Manager (SSMHD) software. Figures 4.17 to 4.22 show the process of the installation of the traffic sensor. Figure 4.23 shows the metal case for the batteries.

Figure 4.17 Preparation of the installation

Figure 4.18 The installation of Wavetronix SmartSensor HD (1)

Figure 4.19 The installation of Wavetronix SmartSensor HD (2)

Figure 4.20 The installation of the case

Figure 4.21 The installation of Wavetronix SmartSensor HD (3)

Figure 4.22 Test of the event logger and data logger

Figure 4.23 Battery case

4.4 Traffic Data Collection

The traffic data was then collected by Wavetronix SmartSensor HD installed in the above mentioned rest area. The dataset includes eight important variables related to traffic flow characteristics including vehicle speed, vehicle length, duration of detection and lane assignment. The headway of each vehicle can also be calculated from the original dataset. The dataset covers the period from January 31st, 2014 till April. Figure 4.24 shows a sample of the dataset.

	A	B	C	D	E	F	G	H	I
1	date	time	lane	speed	length	range	classification	duration	
2	02/12/201	21:08.8	1	73.7	17.8	72	1	219	
3	02/12/201	21:09.0	2	81.6	15.4	84	1	179	
4	02/12/201	21:09.6	3	76.7	18.1	157.1	1	213	
5	02/12/201	21:11.3	4	68.9	19.4	170.1	1	251	
6	02/12/201	21:11.6	1	80	16	72	1	187	
7	02/12/201	21:12.4	5	68.7	16.5	182.1	1	222	
8	02/12/201	21:15.5	2	77.8	17.4	85	1	205	
9	02/12/201	21:16.1	1	69.2	16.8	74	1	224	
10	02/12/201	21:18.0	4	70	22.6	170.1	1	278	
11	02/12/201	21:18.7	3	81.1	19.5	157.1	1	214	
12	02/12/201	21:19.6	4	76.4	18.7	169.1	1	220	

Figure 4.24 Sample of Traffic Dataset

4.5 Combined Dataset

It can be seen from Figure 4.2 and Figure 4.24 that there are two common variables in the weather dataset and the traffic dataset: date and time. Therefore, these two original datasets can be merged into one combined dataset which includes variables related to both traffic flow characteristics and weather parameters. The combined dataset can therefore be used to analyze the relationship between visibility and traffic flow characteristics. Figure 4.25 shows a sample of the dataset.

	A	B	C	D	E	F	G	H	I
1	date	time	lane	speed	length	range	classification	duration	visibility
2	02/12/201	21:08.8	1	73.7	17.8	72	1	219	2000
3	02/12/201	21:09.0	2	81.6	15.4	84	1	179	2000
4	02/12/201	21:09.6	3	76.7	18.1	157.1	1	213	2000
5	02/12/201	21:11.3	4	68.9	19.4	170.1	1	251	2000
6	02/12/201	21:11.6	1	80	16	72	1	187	2000
7	02/12/201	21:12.4	5	68.7	16.5	182.1	1	222	2000
8	02/12/201	21:15.5	2	77.8	17.4	85	1	205	2000
9	02/12/201	21:16.1	1	69.2	16.8	74	1	224	2000
10	02/12/201	21:18.0	4	70	22.6	170.1	1	278	2000
11	02/12/201	21:18.7	3	81.1	19.5	157.1	1	214	2000
12	02/12/201	21:19.6	4	76.4	18.7	169.1	1	220	2000
13	02/12/201	21:23.4	4	65.6	15.2	172.1	1	220	2000

Figure 4.25 Sample of Combined Dataset

4.6 Chapter Summary

This chapter presented the site selection and installation of weather sensors and the traffic sensor. The components of the traffic sensor were also introduced in detail. After that, a sample of collected weather data, traffic data and combined datasets were shown in this chapter.

5. ANALYSIS OF THE EFFECT OF WEATHER PARAMETERS ON REDUCED VISIBILITY

5.1 Analysis of Weather Parameters in a Fog Case

In this section we selected one fog period that occurred on the morning of Feb 2nd for the purpose of analyzing the impact of several important weather parameters on the fog formation. This fog occurrence is also addressed in Praxsoft's report. First the relationship between temperature difference of air temperature and dew point and visibility was analyzed. The dew point is the temperature at which the air can no longer hold all of the water vapor which is mixed with it, and some of the water vapor must condense into liquid water. It can be seen from Figure 5.1 that during the fog situation and also the period close to the fog situation, the air temperature and the dew point are identical. It can be concluded that the air temperature and dew point approaching each other is the sign of favorable fog conditions and the fog is most likely to form.

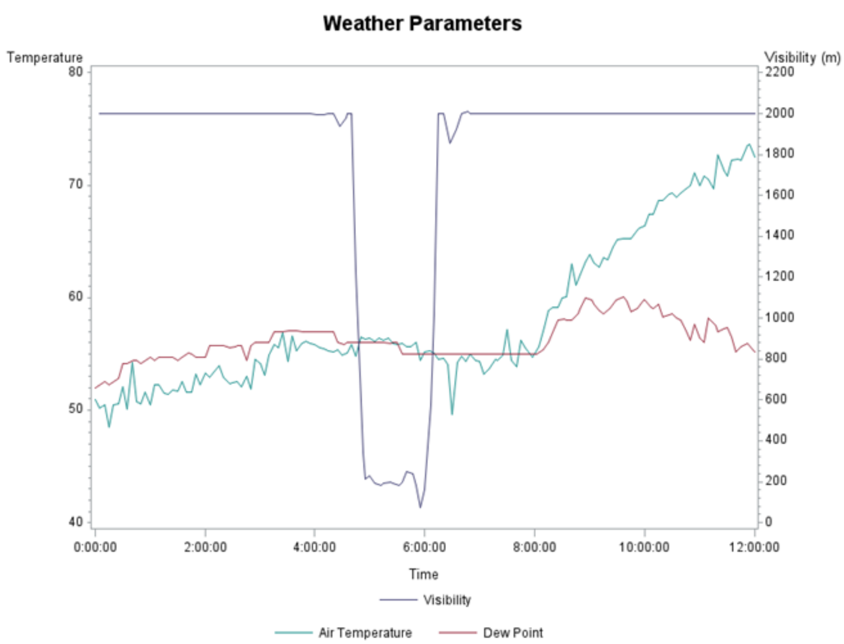

Figure 5.1 Analysis of Relationship between Temperature Difference and Visibility

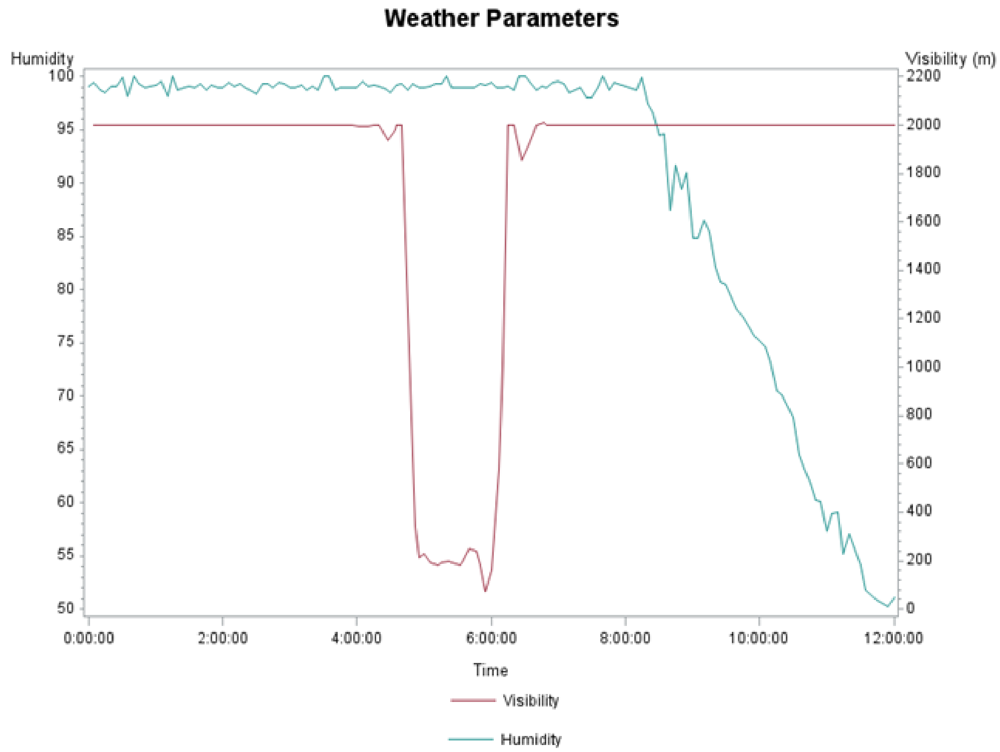

Figure 5.2 Analysis of Relationship Between Humidity and Visibility

Figure 5.2 shows the relationship between humidity and visibility during the fog period. It can be seen from this figure that the humidity is at 100% before the fog formation period and during the fog period. The humidity drops significantly around two hours after the fog disappeared. It can be concluded that the high humidity is the sign of favorable fog conditions and the fog is most likely to form.

5.2 Comparison of Weather Parameters between Fog Case and Clear Case

Four important weather parameters including humidity, subsurface moisture, wind speed and difference between air temperature and dew point were further compared using t-test to figure out the difference of these weather parameters in fog and clear cases. The weather dataset from Jan 1st to Mar 11th was divided into two subsets: weather dataset with good visibility and the dataset with reduced visibility. The sample size of the weather dataset with good visibility is 16017 while the sample size of the weather dataset with reduced visibility is 538.

5.2.1 Humidity Comparison

The comparison of the humidity under fog case and clear case is carried out by comparing the mean value of the humidity using the t-test. It is noted that the t-test used for comparing means of two independent samples in this report consists of two procedures. First, the Folded F test is used for checking the equality of variances of the two sample means. Secondly, the Pooled t-test is applied if the variances of two sample means are equal. On the other hand, the Satterthwaite t-test is applied if the variances of two sample means are not equal. Only the p-value for applied t-test is illustrated in the tables showing summary of the t-test. It can be seen from Table 5.1 that the value of the mean in fog case is 98.1%, while the value of the mean in clear case is 79.4%. The P-value showed to be less than 0.0001 which indicates that the mean value is significant different in both cases.

Table 5.1 Summary of t-test for Humidity

Parameter	Analysis Cases	
	Fog Case	Clear Case
Sample size	538	16017
Mean	98.11	79.37
95% CL Mean	97.29-98.93	79.04-79.70
Maximum Value	100	100
Minimum Value	32.00	18.00
Standard deviation	10.30	21.44
P-Value	<.0001	

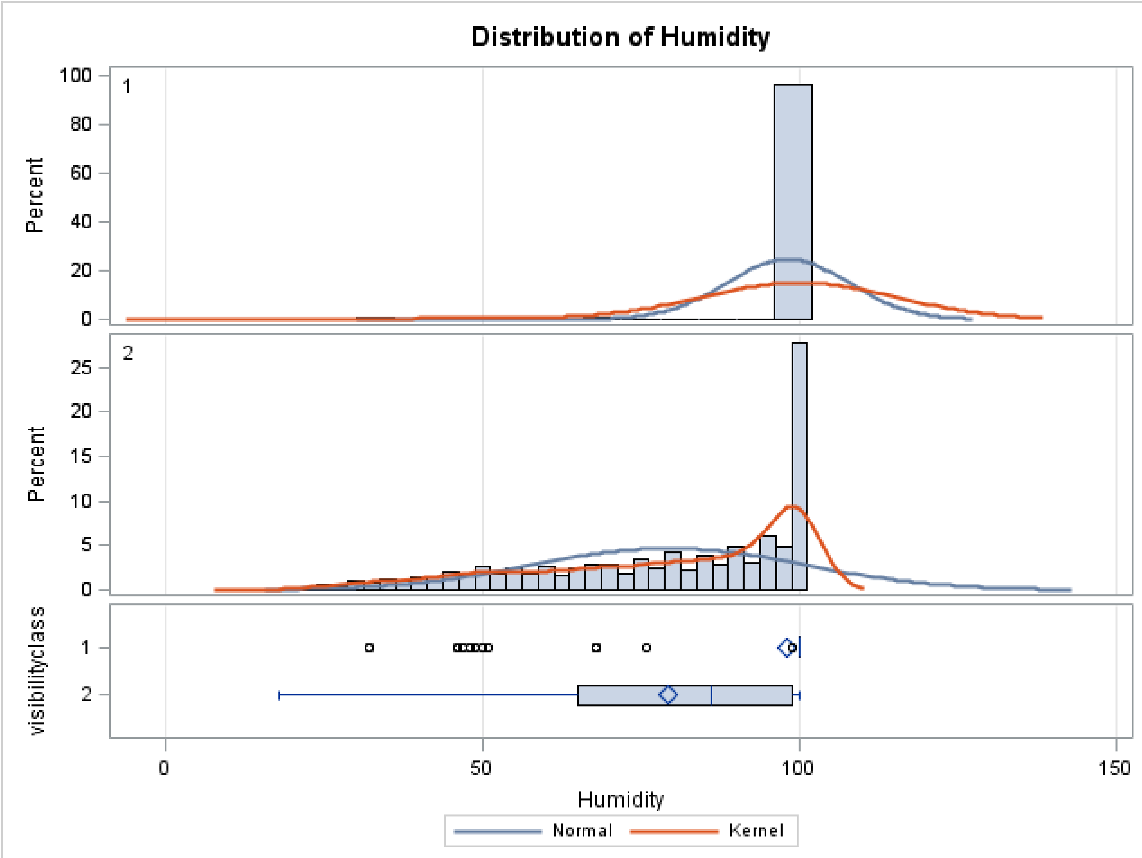

Figure 5.3 Distribution of Humidity

The distribution of value of humidity in both cases was shown in Figure 5.3. The top one is the distribution for the fog case and the bottom one is the distribution for the clear case. It can be seen from above figure that almost all the values of humidity in the fog case are 100% while the values of humidity in the clear case are much more various. There are a number of values below 100% for the clear case. It can be concluded from the figure that the fog is more likely to form when the humidity is higher and close to 100%.

5.2.2 Subsurface Moisture Comparison

The comparison of the subsurface moisture under fog case and clear case is carried by comparing the mean value of the subsurface moisture using the t-test. The value of the mean in fog case is 0.3122 volumetric water content (VWC), while the value of the mean in clear case is 0.2981 VWC. The P-value showed to be 0.0006 which indicates that the mean value is significantly different in both cases.

Table 5.2 Summary of t-test for Subsurface Moisture

Parameter	Analysis Cases	
	Fog Case	Clear Case
Sample size	538	16017
Mean	0.31	0.28
95% CL Mean	0.300-0.317	0.296-0.299
Maximum Value	0.5748	0.5843
Minimum Value	0.1368	0
Standard deviation	0.109	0.098
P-Value	0.0006	

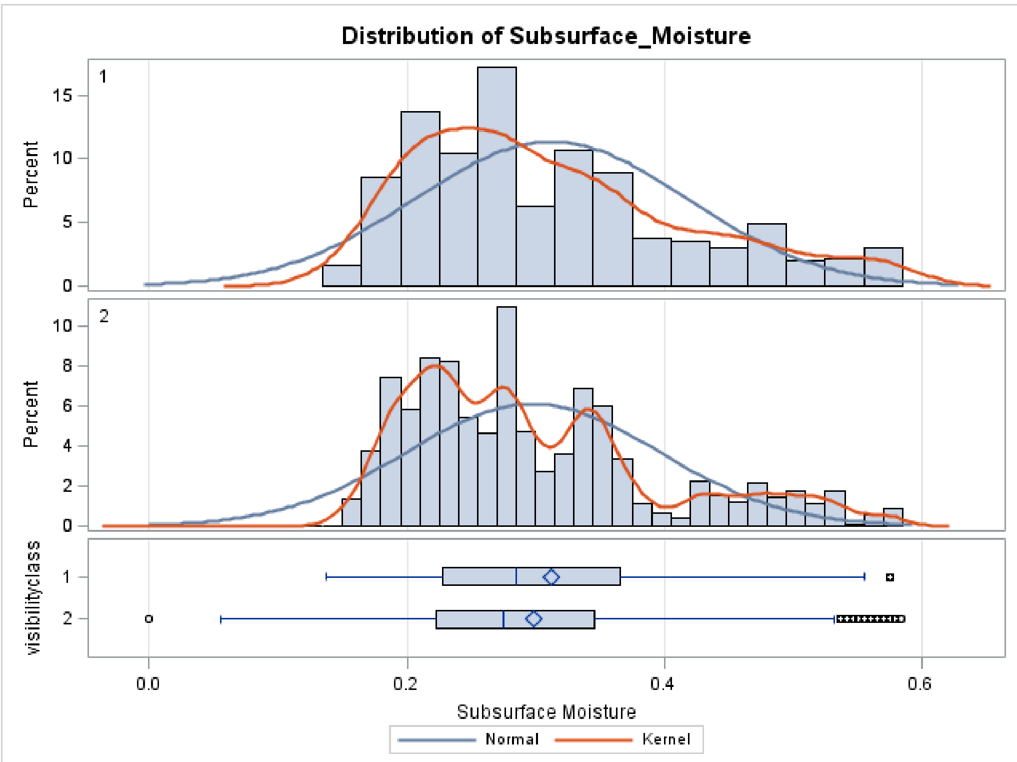

Figure 5.4 Distribution of Subsurface Moisture

The distribution of subsurface moisture in both cases was shown in Figure 5.4. The top one is the distribution for the fog case and the bottom one is the distribution for the clear case. It can be seen that the mean value of subsurface moisture in fog case is significantly higher than the mean value of subsurface moisture in clear case. It can be concluded that the fog is more likely to form when the subsurface moisture is higher.

5.2.3 Wind Speed Comparison

The comparison of the wind speed under fog case and clear case is carried by comparing the mean value of the wind speed using the T-test. The value of the mean in fog case is 1.809 mph, while the value of the mean in clear case is 2.996 mph. The P-value showed to be less than 0.0001 which indicates that the mean value is significant different in both cases.

Table 5.3 Summary of t-test for Wind Speed

Parameter	Analysis Cases	
	Fog Case	Clear Case
Sample size	538	16017
Mean	1.809	2.996
95% CL Mean	1.676-1.941	2.965-3.028
Maximum Value	9.4000	20.6000
Minimum Value	0	0
Standard deviation	1.662	2.084
P-Value	<.0001	

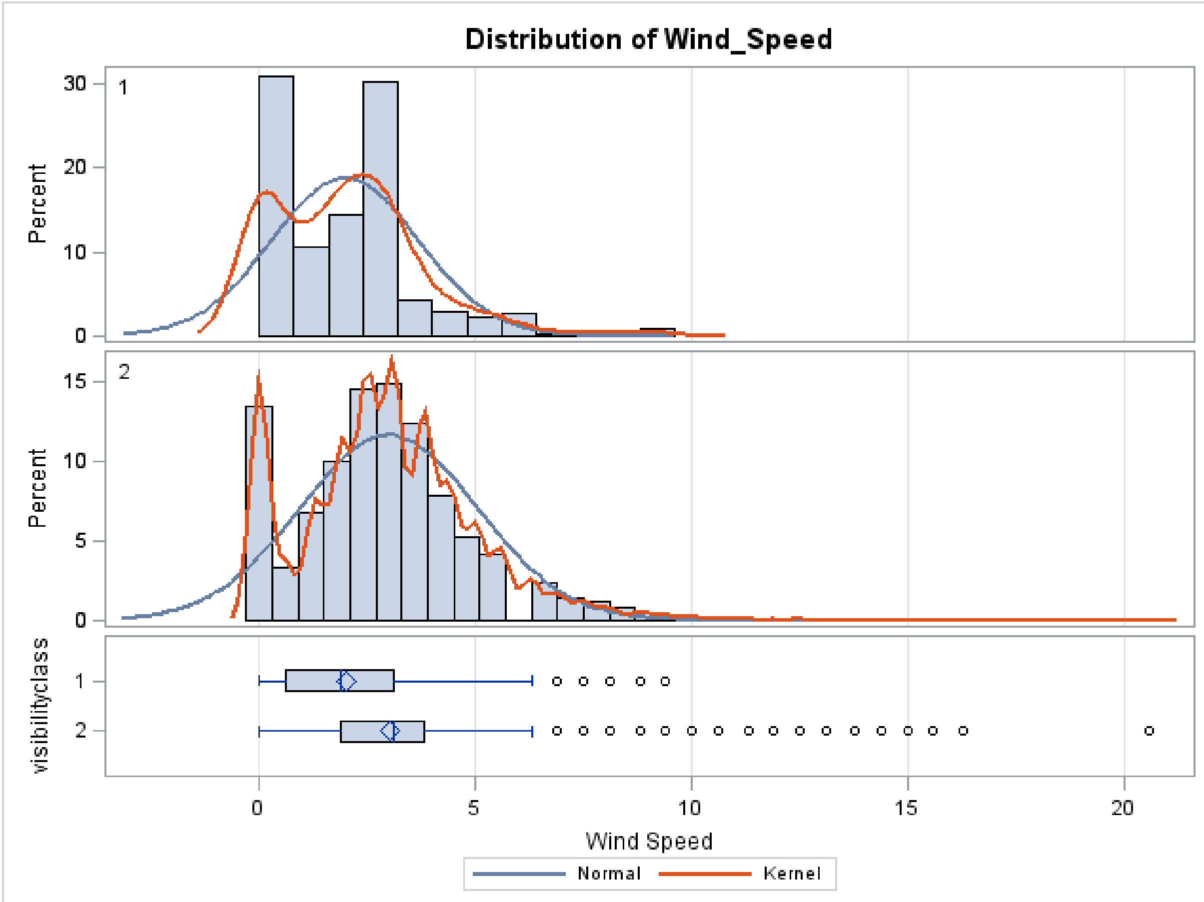

Figure 5.5 Distribution of Wind Speed

The distribution of wind speed in both cases was shown in Figure 5.5. The top one is the distribution for the fog case and the bottom one is the distribution for the clear case. It can be seen that the mean value of wind speed in fog case is significantly lower than the mean value of wind moisture in clear case. It is also noted that there is round 30 percent of wind speed equals to zero in the fog case compared to only around 13 percent of wind speed equals to zero in the clear case. It can be concluded that the fog is more likely to form when the wind speed is lower especially when the wind speed is equal to zero.

5.2.4 Difference Between Air Temperature And Dewpoint Comparison

The comparison of the temperature difference under fog case and clear case is carried by comparing the mean value of the temperature difference using the T-test. The value of the mean in fog case is 0.688°F, while the value of the mean in clear case is 7.586°F. The P-value showed to be less than 0.0001 which indicates that the mean value is significant different in both cases.

Table 5.4 Summary of t-test for Temperature Difference

Parameter	Analysis Cases	
	Fog Case	Clear Case
Sample size	538	16017
Mean	0.688	7.586
95% CL Mean	0.379-0.996	7.448-7.724
Maximum Value	29.320	44.010
Minimum Value	0	0
Standard deviation	3.643	8.888
P-Value	<.0001	

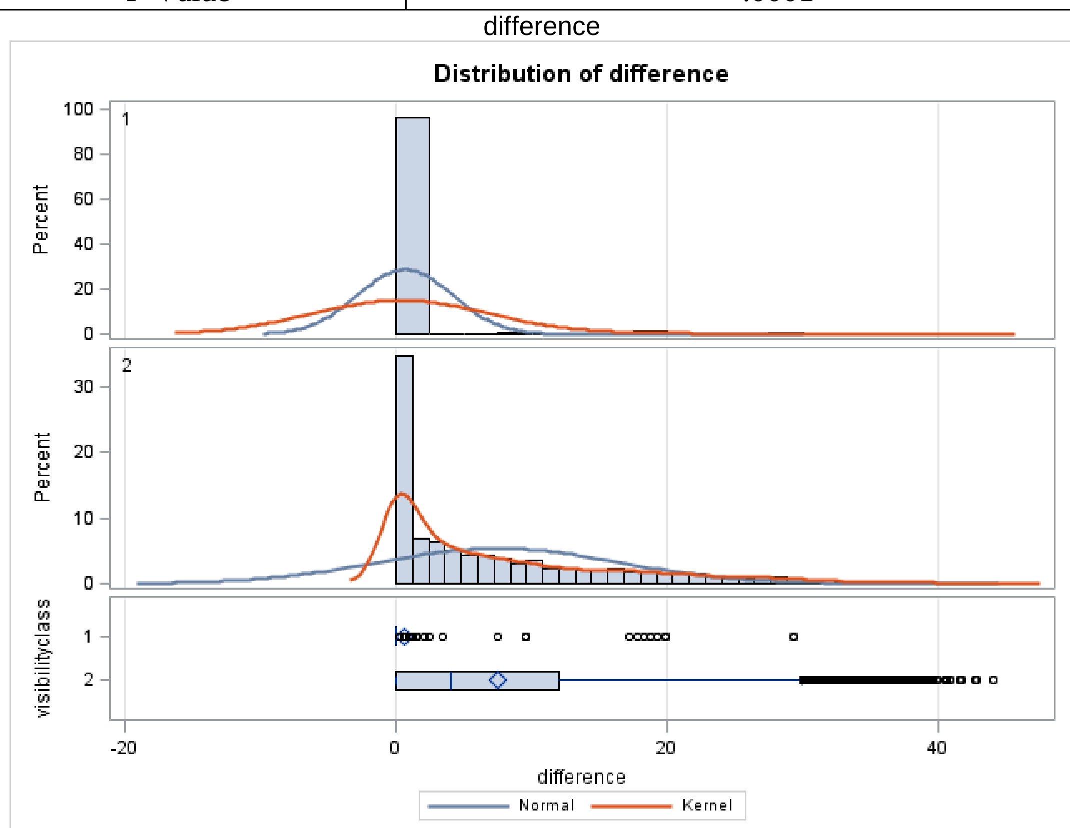

Figure 5.6 Distribution of Temperature Difference

The distribution of difference between air temperature and dew point in both cases is shown in Figure 5.6. The top one is the distribution for the fog case and the bottom one is the distribution for the clear case. It can be seen that the mean value of difference between air temperature and dew point in fog case is significantly lower than the mean value of wind moisture in clear case. It is noted that almost all the values of temperature difference equal to zero in the fog case compared to only around 34 percent of values equal to zero in the clear case. It can be concluded that the fog is more likely to form when the air temperature is very close to dew point.

5.3 Chapter Summary

Firstly, a fog case was analyzed to figure out the effects of weather parameters on reduced visibility. It can be concluded that the air temperature and dew point approach each other combined with the high humidity is the sign of favorable fog conditions and the fog is most likely to form. Four important weather parameters including humidity, subsurface moisture, wind speed and difference between air temperature and dew point were compared in further to figure out the difference of these weather parameters in fog and clear cases. It can be concluded from Figure 5.3-Figure 5.6 that the fog is more likely to form when the humidity is higher and close to 100%, the wind speed is lower, the subsurface moisture is higher and the air temperature is very close to the dew point.

6. DATA ANALYSIS OF IMPACT OF REDUCED VISIBILITY ON TRAFFIC FLOW CHARACTERISTICS

The impact of reduced visibility on traffic flow characteristics is analyzed in this section. Two fog cases were selected and analyzed by comparing them with clear cases to figure out the difference of traffic flow characteristics under different situations. Moreover, the vehicles were divided into two types including passenger cars and trucks in order to identify whether the impact of visibility on traffic flow characteristics is different for different vehicle types. After that, the traffic flow characteristics under different visibility levels and the effects of reduced visibility on different lanes were analyzed.

6.1 Preliminary Analysis of a Fog Case

6.1.1 Analysis of Traffic Flow Characteristics in a Fog Case

The fog case was selected on Feb 2nd morning. The period of fog formation is from 6:30am to 9:00am in the morning. The relationship between mean speed and visibility is shown in Figure 6.1. It can be seen from that there is a slight drop in speed during reduced visibility. The mean speed drops to around 70 mph during the fog period. The relationship between speed variation and visibility is shown in Figure 6.2. It is shown from this figure that the speed variation increases at the beginning of the fog formation and the speed variation is larger during the fog period.

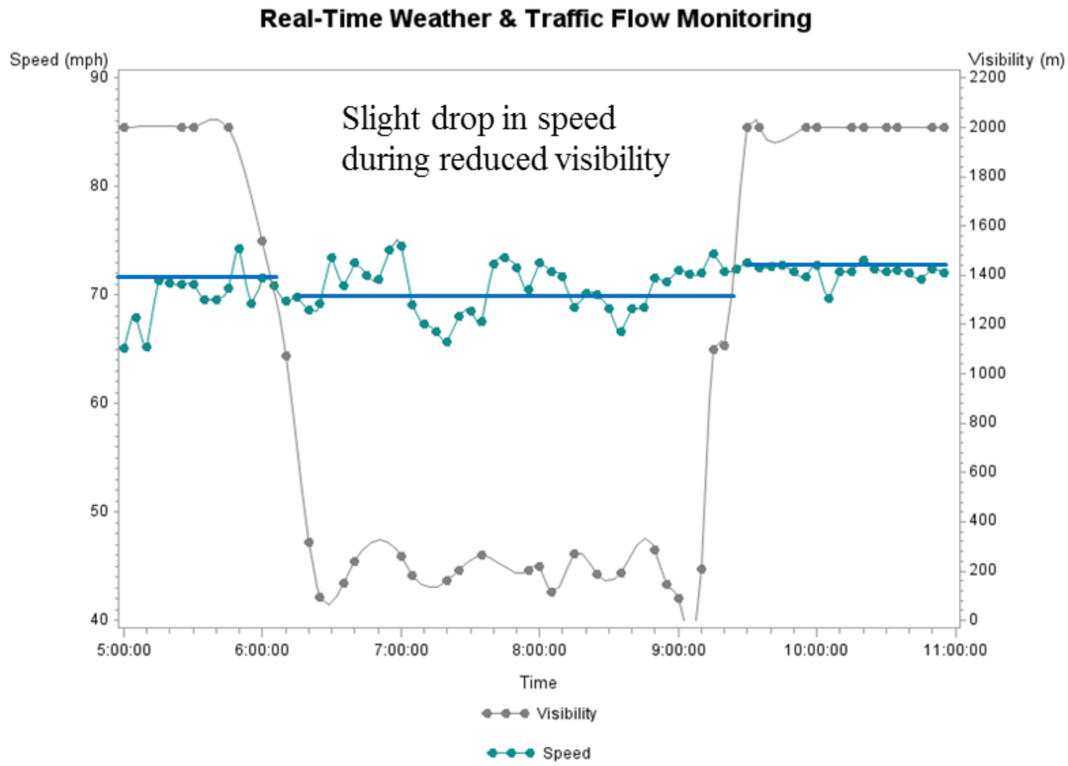

Figure 6.1 Relationship between Mean Speed and Visibility

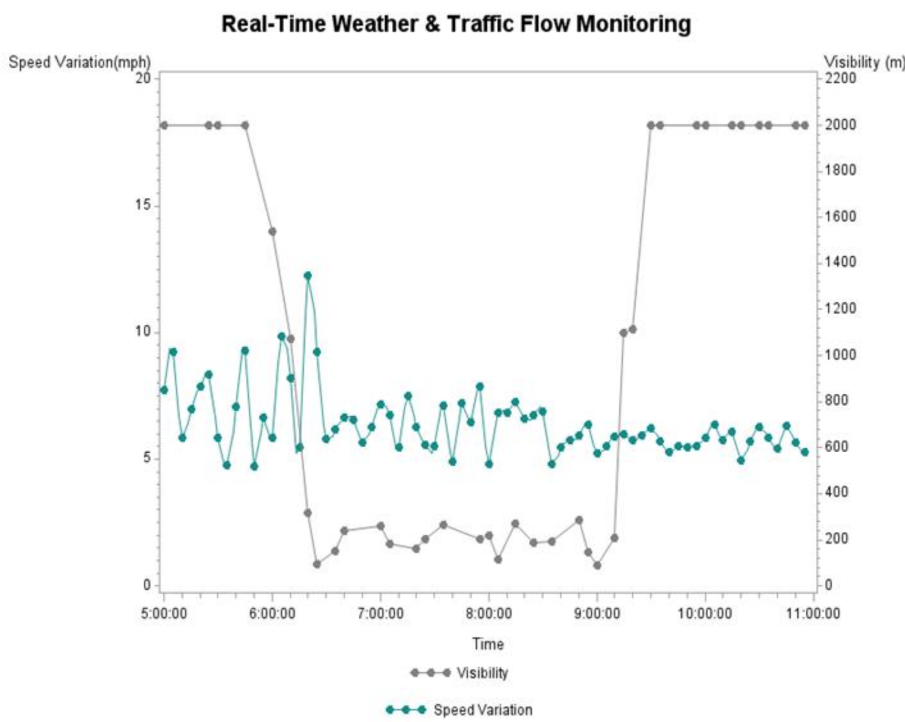

Figure 6.2 Relationship between Speed Variation and Visibility

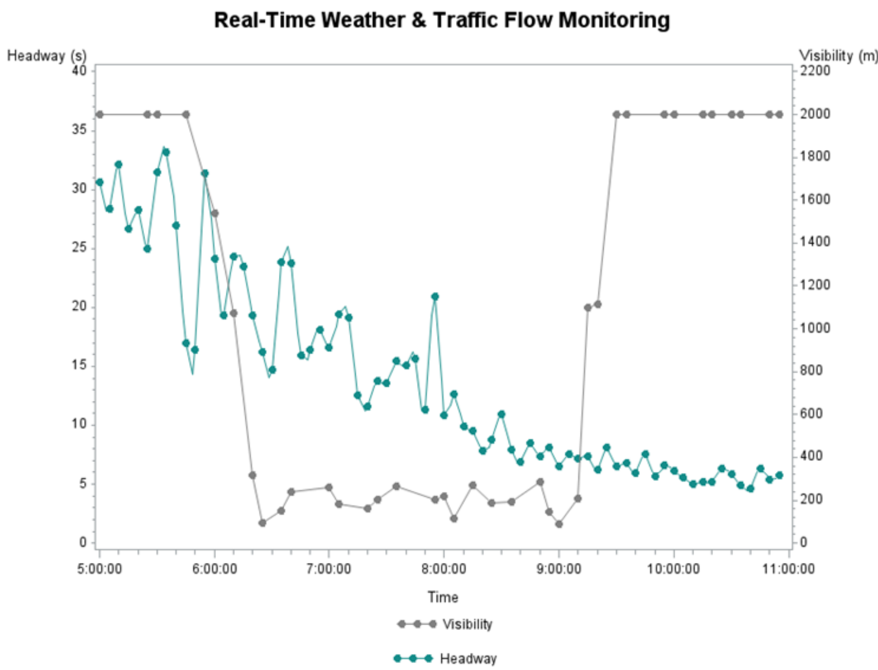

Figure 6.3 Relationship between Headway and Visibility

The relationship between headway and visibility is shown in Figure 6.3. It seems that the headway keeps decreasing during the fog period. The main reason for this is that the traffic volume also increases during this period. Therefore, the impact of reduced visibility on mean headway was not clearly shown from this Figure. It is easier to figure out the impact of reduced visibility on mean headway when the volume is more stable during the fog period. It can be seen from the figure that the headway variation is larger in the fog period.

6.1.2 Comparison of Traffic Flow Characteristics Between Fog Case and Clear Case

The same period from 6:30am to 9:00am on Feb 9th morning was selected as the clear case to compare the traffic flow characteristics between fog case and clear case. The reason to choose this date is that it is the same weekday as Feb 2nd. Therefore, the volume is expected to be similar in those two days and it will be easier to investigate the effect of reduced visibility. Five important traffic flow variables including headway, speed, speed variation, headway variation and volume were compared using t-tests to identify the difference of these variables in fog case and clear case.

6.1.2.1 Headway

The comparison of the headway under the fog and clear cases is carried by comparing the mean value of the logarithm of headway using the t-test. The value of the mean in fog case is 2.6708 seconds, while the value of the mean in clear case is 2.4351 seconds. The P- value showed to be less than 0.0001 which indicates that the mean value is significantly different in both cases.

Table 6.1 Summary of t-test for Logarithm of Headway

Parameter	Analysis Cases	
	Fog Case	Clear Case
Sample size	300	300
Mean	2.6708	2.4351
95% CL Mean	2.6125-2.7290	2.3836-2.4866
Maximum Value	4.2729	3.7710
Minimum Value	1.5064	1.3863
Standard deviation	0.5129	0.4535
P-Value	<.0001	

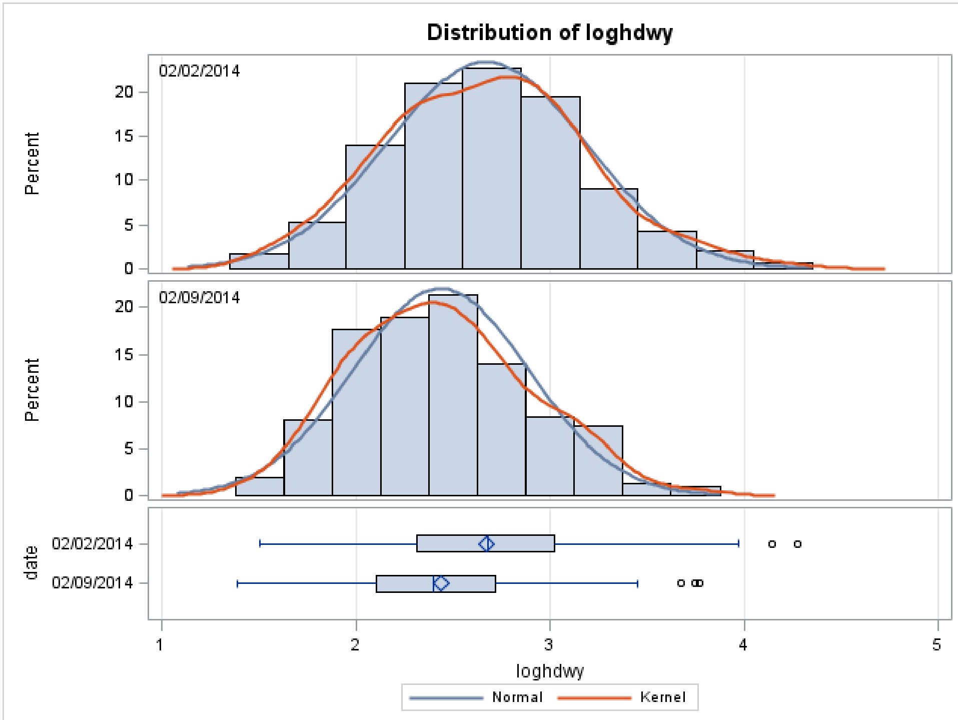

Figure 6.3 Distribution of Logarithm of Headway

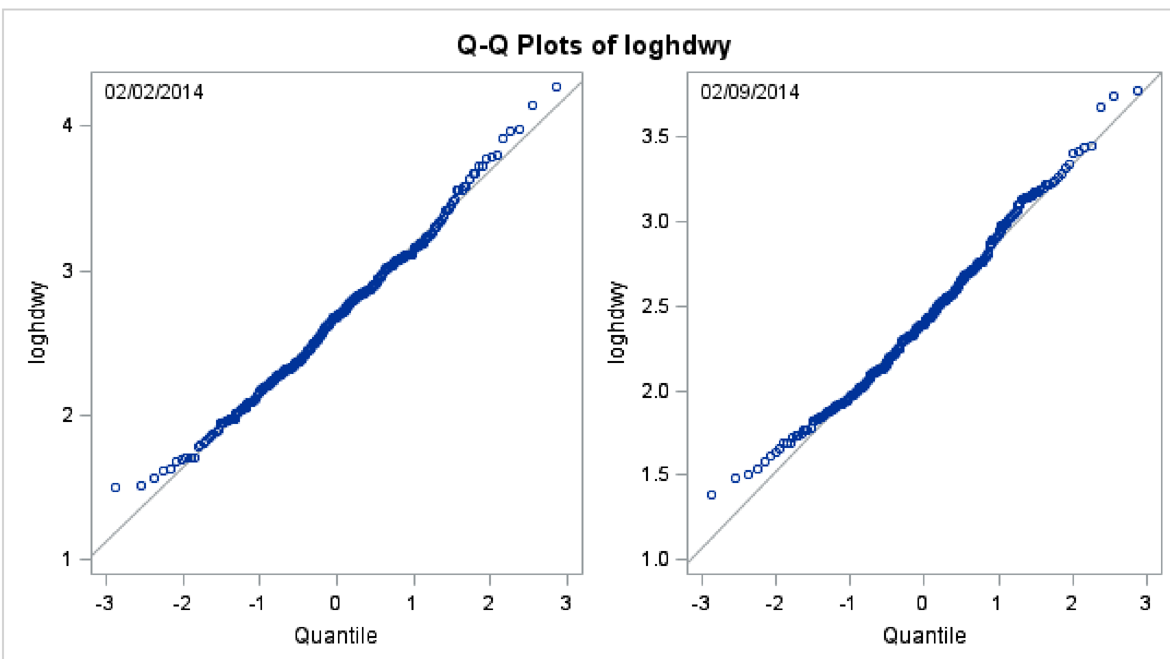

Figure 6.4 Q-Q Plots of Logarithm of Headway

The distribution of logarithm of headway in both cases is shown in Figure 6.4. The top one is the distribution for the fog case and the bottom one is the distribution for the clear case. It can be seen from above figure that the mean headway is significantly higher in the fog case. The Q-Q plot in shown in Figure 6.5 indicates that the logarithm of headway in both cases follows the normal distribution.

6.1.2.2 Mean Speed

The comparison of the mean speed under fog case and clear case is carried out by comparing the mean value of the mean speed using the t-test. The value of the mean in fog case is 70.61 mph, while the value of the mean in clear case is 73.37 mph. The P-value showed to be less than 0.0001 which indicates that the mean value is significantly different in both cases.

Table 6.2 Summary of t-test for Mean Speed

Parameter	Analysis Cases	
	Fog Case	Clear Case
Sample size	300	300
Mean	70.6139	73.3785
95% CL Mean	70.2258-71.0020	73.1235-73.6334
Maximum Value	84.1500	78.5658
Minimum Value	60.9567	65.5000
Standard deviation	3.4156	2.2442
P-Value	<.0001	

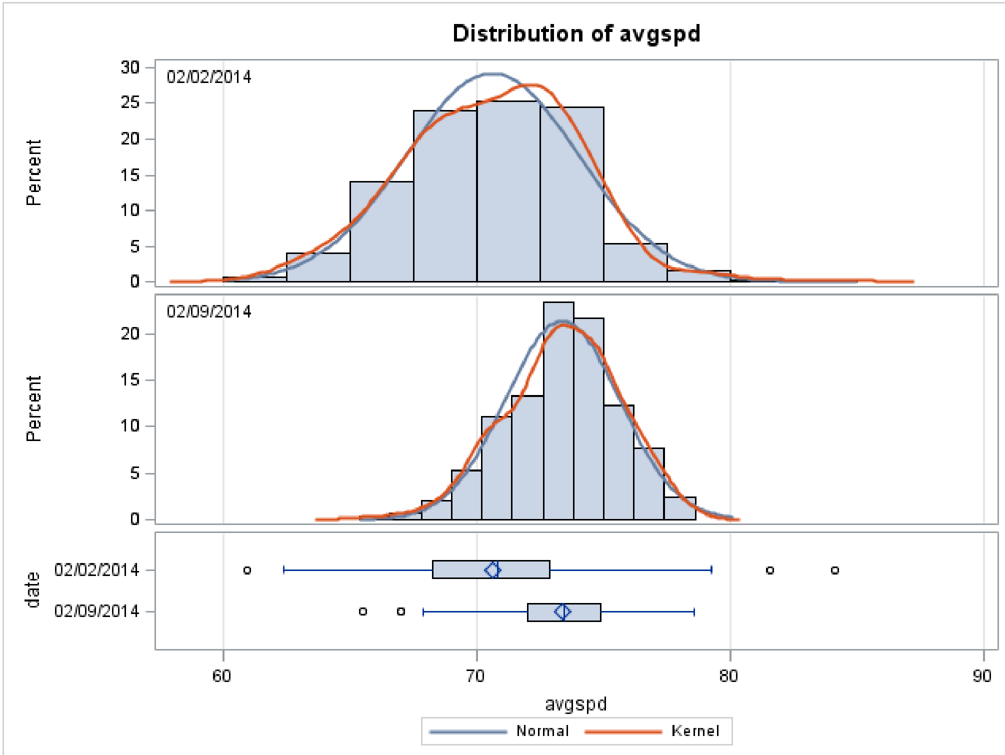

Figure 6.5 Distribution of Mean Speed

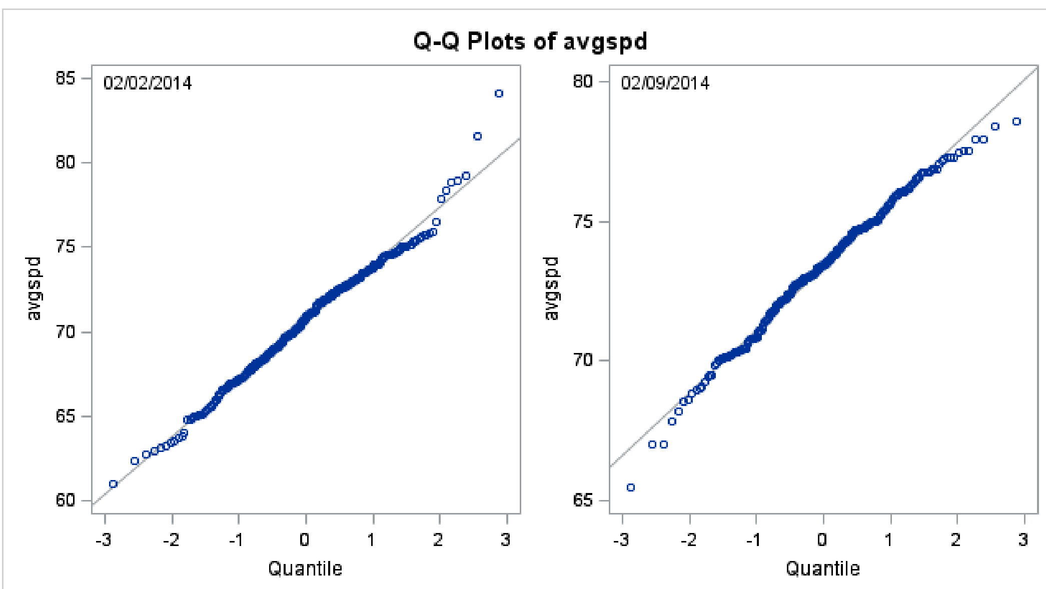

Figure 6.6 Q-Q Plots of Mean Speed

The distribution of mean speed in both cases is shown in Figure 6.6. The top one is the distribution for the fog case and the bottom one is the distribution for the clear case. It can be seen that the mean speed is significantly lower in fog case. The Q-Q plot illustrated in Figure 6.7 indicates that mean speed in both cases follows the normal distribution.

6.1.2.3 Standard Deviation of Speed

The comparison of the standard deviation of speed under fog case and clear case is carried out by comparing the mean value of the standard deviation of speed using the t-test. The P-value showed to be 0.48 which indicates that the mean value is not significant different in both cases, although it appears that the standard deviation of speed is higher in the fog condition.

Table 6.3 Summary of t-test for Standard Deviation of Speed

Parameter	Analysis Cases	
	Fog Case	Clear Case
Sample size	300	300
Mean	5.7945	5.6975
95% CL Mean	5.5828-6.0063	5.5226-5.8724
Maximum Value	12.4364	12.0994
Minimum Value	0.1768	1.8385
Standard deviation	1.8606	1.5397
P-Value	0.4871	

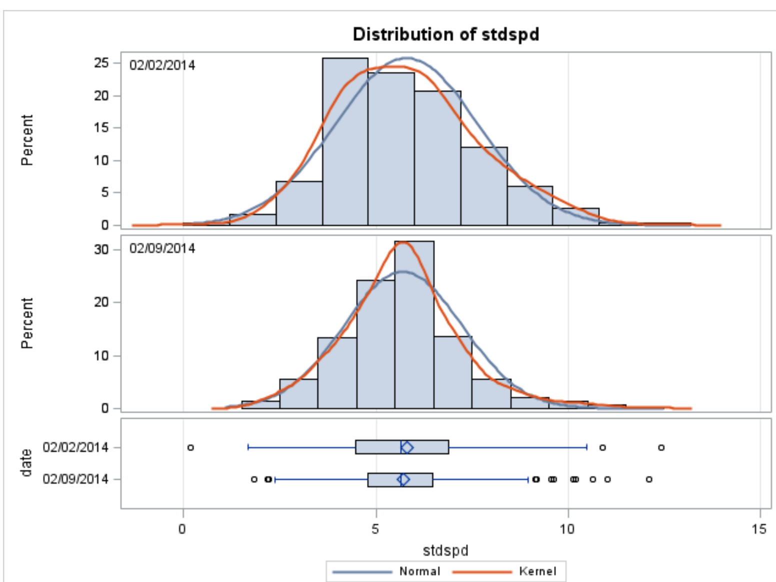

Figure 6.7 Distribution of Standard Deviation of Speed

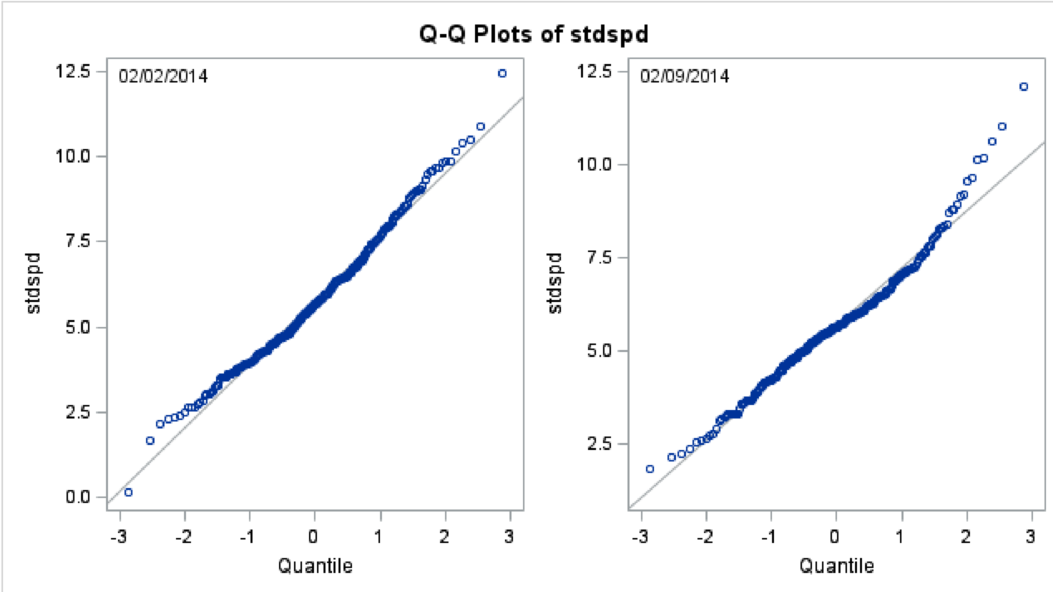

Figure 6.8 Q-Q Plots of Standard Deviation of Speed

The distribution of standard deviation of speed in both cases is shown in Figure 6.8. The top one is the distribution for the fog case and the bottom one is the distribution for the clear case. It can be seen that standard deviation of speed is slightly higher in fog case. The impact of reduced visibility on standard deviation of speed is not significant**.** The Q-Q plot in Figure 6.9 indicates that standard deviation of speed in both cases follows the normal distribution.

6.1.2.4 Standard Deviation of Headway

The comparison of the standard deviation of headway under fog case and clear case is carried by comparing the mean value of the standard deviation of headway using the T-test. The value of the mean in fog case is 15.705 s, while the value of the mean in clear case is 11.892 s. The P-value showed to be less than 0.05 which indicates that the mean value is significant different in both cases. The variance of standard deviation of headway is larger in fog case.

Table 6.4 Summary of t-test for Standard deviation of Headway

Parameter	Analysis Cases	
	Fog Case	Clear Case
Sample size	300	300
Mean	15.705	11.892
95% CL Mean	14.623-16.786	11.026-12.758
Maximum Value	68.32	74.74
Minimum Value	3.65	3.54
Standard deviation	0.8232	1.8632
P-Value	<0.0001	

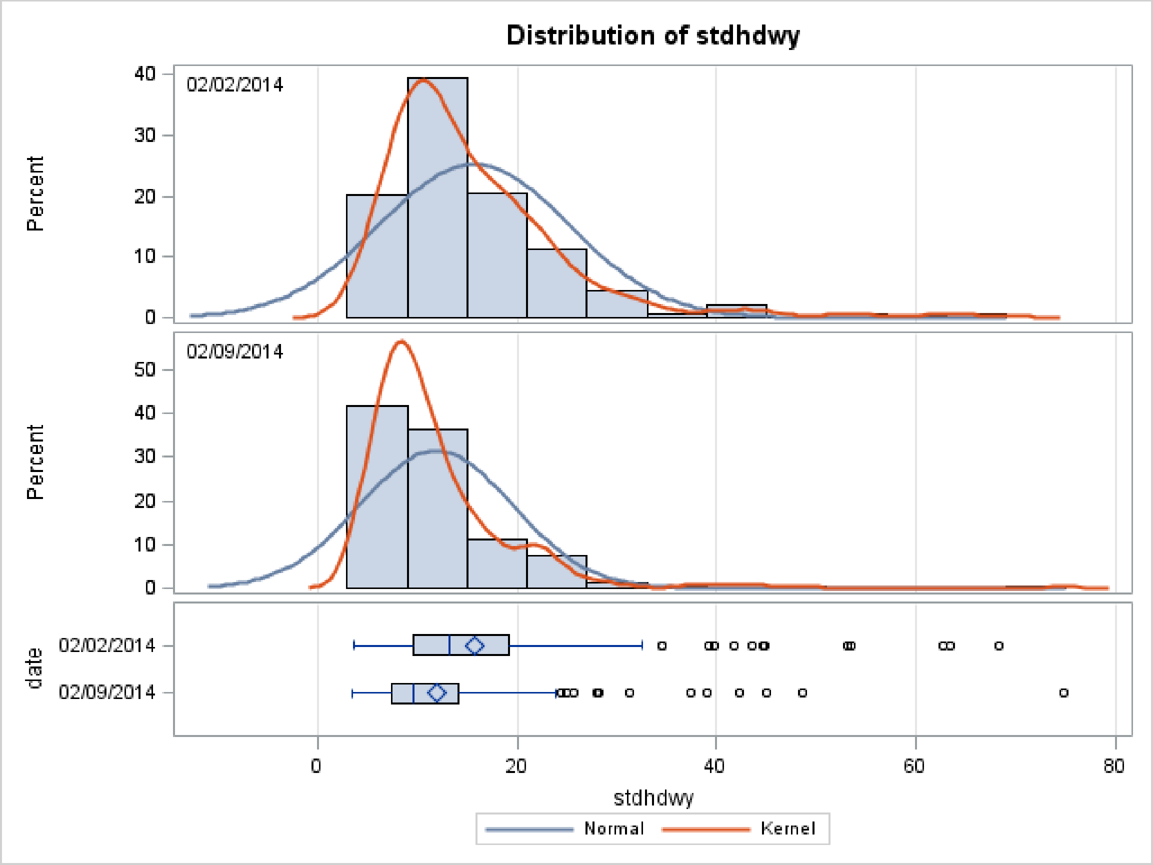

Figure 6.9 Distribution of Standard Deviation of Headway

The distribution of standard deviation of standard deviation of headway in both cases is shown in Figure 6.10. The top one is the distribution for the fog case and the bottom one is the distribution for the clear case. It can be seen that standard deviation of headway is higher in fog case.

6.1.2.5 Volume

The comparison of the volume under fog case and clear case is carried out by comparing the mean value of the volume using the t-test. The value of the mean in fog case is 13.85 vehicles per minute per direction, while the value of the mean in clear case is 17.15 vehicles per minute per direction. The P- value showed to be less than 0.0001 which indicates that the mean value is significantly different in both cases.

Table 6.5 Summary of t-test for Volume

Parameter	Analysis Cases	
	Fog Case	Clear Case
Sample size	300	300
Mean	13.8500	17.1500
95% CL Mean	12.9926-14.7074	16.2881-18.0119
Maximum Value	42.0000	42.0000
Minimum Value	1.0000	2.0000
Standard deviation	7.5461	7.5859
P-Value	<.0001	

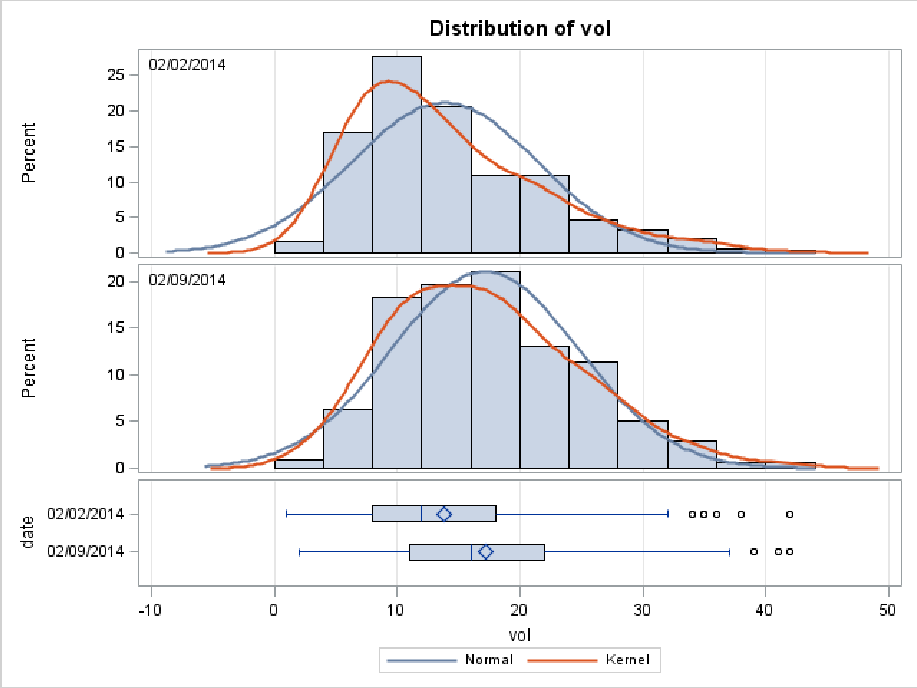

Figure 6.10 Distribution of Volume

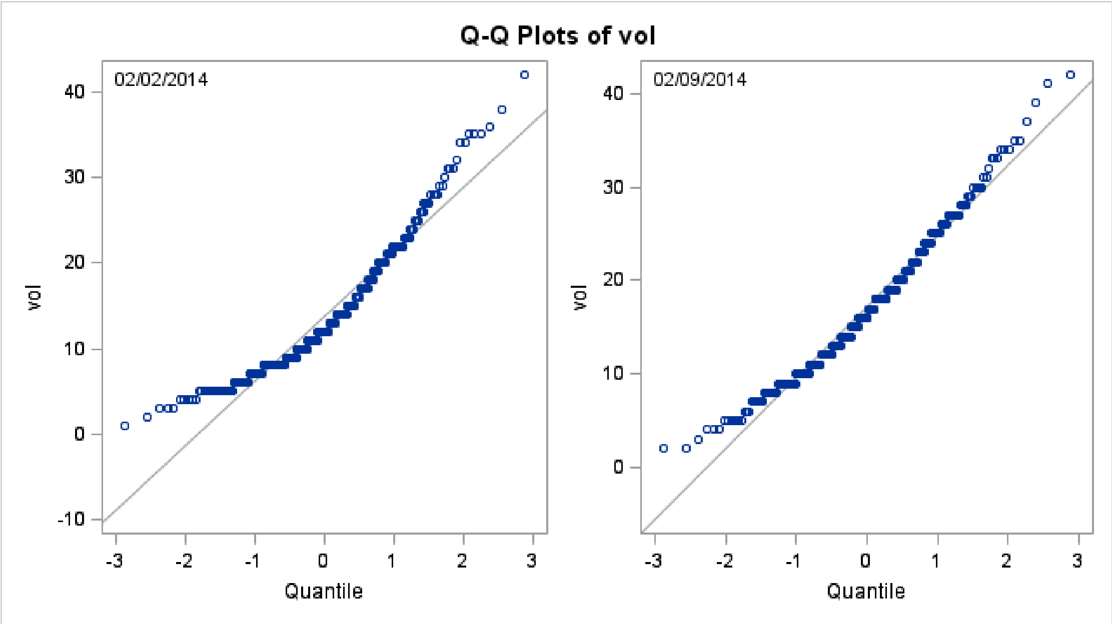

Figure 6.12 Q-Q Plots of Volume

The distribution of volume in both cases is shown in Figure 6.11. The top one is the distribution for the fog case and the bottom one is the distribution for the clear case. It can be seen that the volume is significant lower in fog case. The Q-Q plot in Figure 6.12

indicates that volume in clear case follows the normal distribution very well while the volume in fog case does not follow the normal distribution very well.

6.1.3 Scatterplot Analysis

The scatterplot was used to analyze the relationship between several traffic flow characteristics including speed, headway and volume in both fog case and clear case. The research team wants to figure out whether the relationship between several traffic flow characteristics is different in both cases.

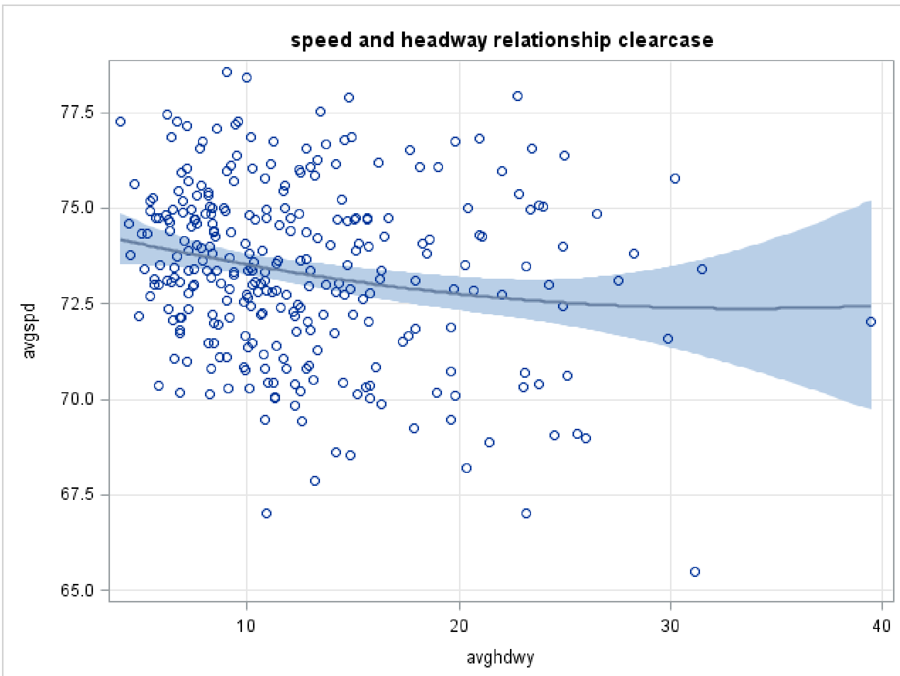

Figure 6.11 Speed and Headway Relationship in Clear Case

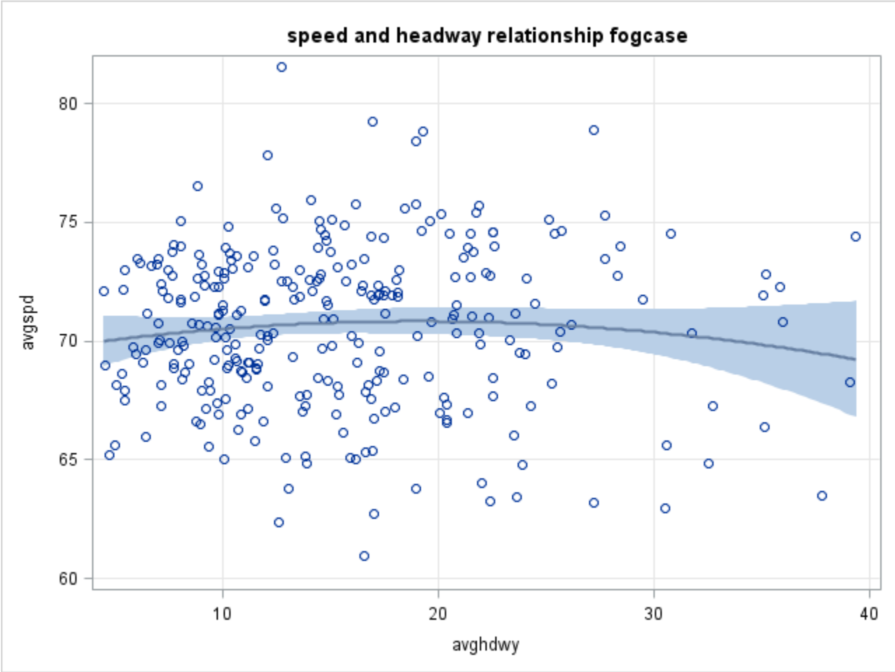

Figure 6.12 Speed and Headway Relationship in Fog Case

The speed and headway relationship in both cases is shown in Figures 6.13 and Figure 6.14. There is obvious difference in the relationship between speed and headway in both cases. It can be seen from the Figure 6.13 that the headway increases as the mean speed decreases in the clear case while this trend is not that obvious as it is shown in Figure 6.14. There is not significant change for the mean speed as the headway increases in the fog case.

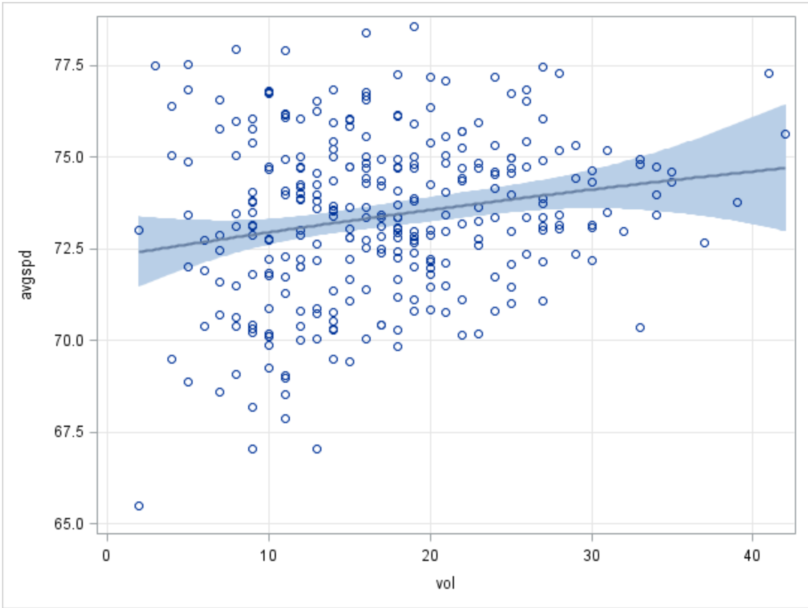

Figure 6.13 Speed and Volume Relationship in Clear Case

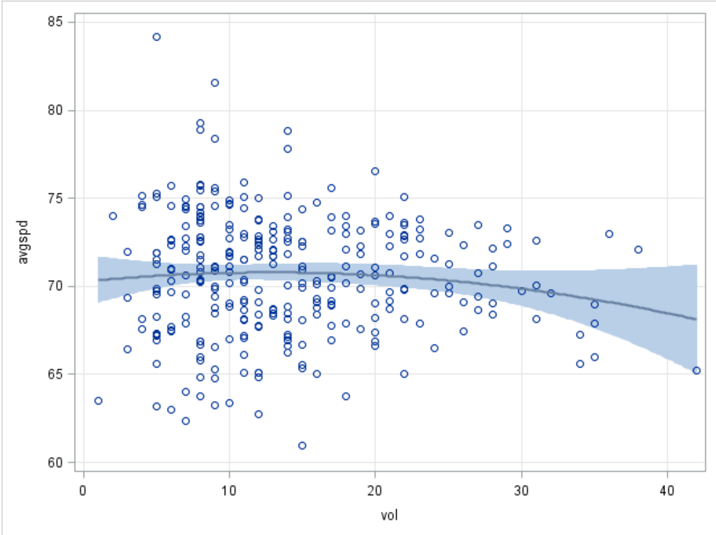

Figure 6.14 Speed and Volume Relationship in Fog Case

The speed and volume relationship in both cases is shown in Figures 6.15 and 6.16. There is also obvious difference in the relationship between speed and volume in both cases. It can be seen from Figure 6.15 that the volume increases as the mean speed increases in the clear case while the trend is not the same as it is shown in Figure 6.16. The mean speed remains constant or even slightly drops as the volume increases in the fog case.

6.2 Analysis of Impacts of Reduced Visibility on Different Types of Vehicles

In this section, the vehicles were divided into two types including passenger cars and trucks in order to figure out whether the impact of visibility on traffic flow characteristics is different in different vehicle types. The type of vehicles was divided based on the length of vehicles. The vehicle is considered as truck when the length of vehicle is above 30 feet and it is considered as passenger cars when the length of vehicle is equal to or less than 30 feet. The datasets used in this section were the combined data mentioned in section 4.5 which covers the period from Jan31th to Mar11th.

6.2.1 Comparison of Reduced Visibility on Speed

The comparison of the speed of both vehicle types under fog case and clear case is carried by comparing the mean value of the speed using T-test. The value of the mean for the passenger cars in fog case is 72.01 mph, while the value of the mean in clear case is 73.18 mph. The value of the mean for the trucks in fog case is 65.79 mph, while the value of the mean in clear case is 66.89 mph. It can be seen that the mean speed of both vehicle types decreases around 1.1 mph during the fog case. The P-value for both vehicle types showed to be less than 0.001 which indicates that the mean value is significantly different in both cases.

Table 6.6 Summary of t-test for Speed

Vehicle Type	Parameter	Analysis Cases	
		Fog Case	Clear Case
Passenger Cars	Sample size	367	7177
	Mean	72.01	73.18
	95% CL Mean	71.67-72.37	73.15-73.22
	Maximum Value	76.90	78.65
	Minimum Value	47.97	45.86
	Standard deviation	3.42	1.57
	P-Value	<0.001	
Truck	Sample size	365	7174
	Mean	65.79	66.89
	95% CL Mean	65.53-66.03	66.84-66.92
	Maximum Value	72.25	75.30
	Minimum Value	49.03	40.76
	Standard deviation	2.65	1.73
	P-Value	<0.001	

The distribution of speed in both cases is shown in Figure 6.17 and Figure 6.18. The top one in each figure is the distribution for the fog case and the bottom one is the distribution for the clear case. It can be seen from these two figures that the mean speed of both vehicle types is significantly lower in the fog case.

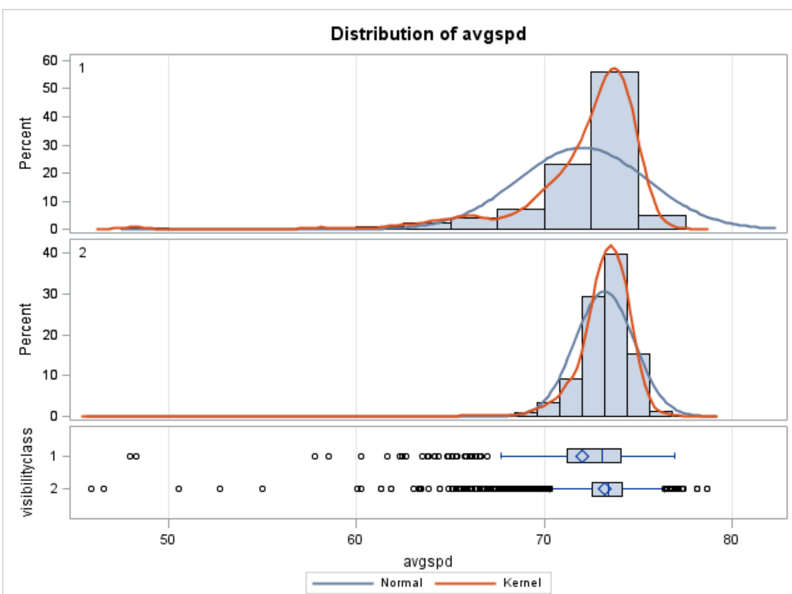

Figure 6.17 Distribution of Mean Speed for Cars

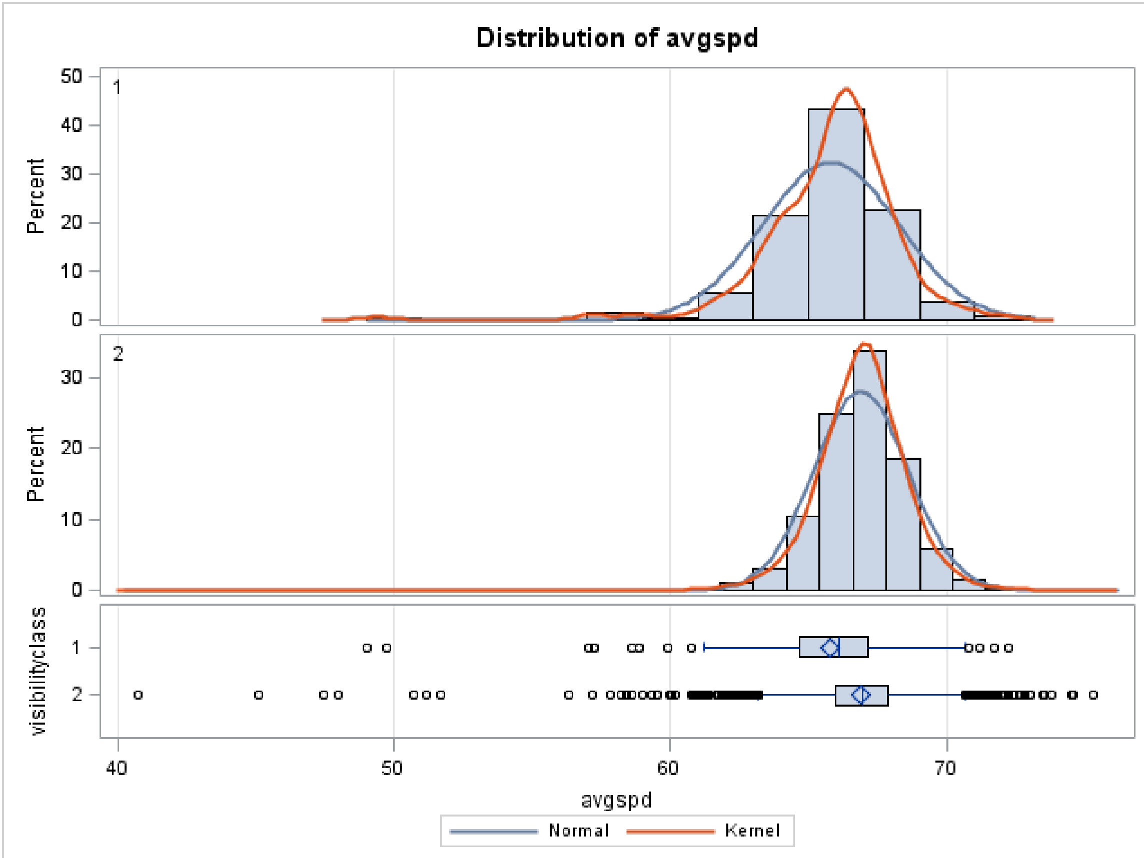

Figure 6.18 Distribution of Mean Speed for Trucks

6.2.2 Comparison of Reduced Visibility on Headway

The comparison of the headway of both vehicle types under fog case and clear case is carried by comparing the mean value of the logarithm of headway using T-test. The value of the mean for the passenger cars in fog case is 2.36 seconds, while the value of the mean in clear case is 1.99 seconds. The value of the mean for the trucks in fog case is 2.56 seconds, while the value of the mean in clear case is 2.27 seconds. It can be seen that the mean headway of passenger cars and trucks increases 0.37 seconds and 0.29 seconds separately during the fog case. The effect of reduced visibility on headway of passenger cars is larger compared to trucks. The P- value for both vehicle types showed to be less than 0.001 which indicates that the mean value is significant different in both cases.

Table 6.4 Summary of t-test for Logarithm of Headway

Vehicle Type	Parameter	Analysis Cases	
		Fog Case	Clear Case
Passenger Cars	Sample size	367	7177
	Mean	2.36	1.99
	95% CL Mean	2.29-2.44	1.97-2.00
	Maximum Value	3.81	0.82
	Minimum Value	1.27	4.10
	Standard deviation	0.78	0.79
	P-Value	<0.001	
Truck	Sample size	365	7174
	Mean	2.56	2.27
	95% CL Mean	2.50-2.63	2.25-2.29
	Maximum Value	4.05	4.26
	Minimum Value	1.60	0.35
	Standard deviation	0.67	0.64
	P-Value	<0.001	

The distribution of logarithm of headway in both cases is shown in Figure 6.19 and Figure 6.20. The top one in each figure is the distribution for the fog case and the bottom one is the distribution for the clear case. It can be seen from these two figures that the headway of both vehicle types is significantly higher in the fog case.

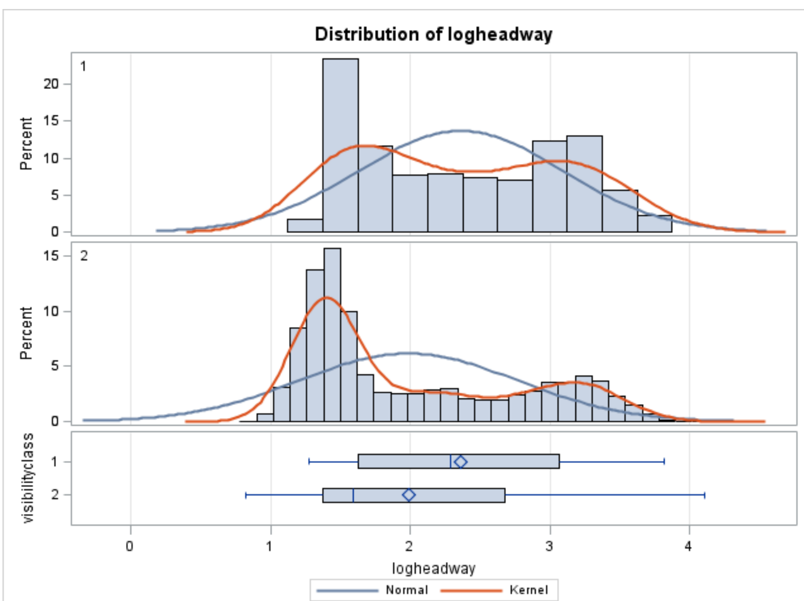

Figure 6.19 Distribution of Logarithm of Headway for Cars

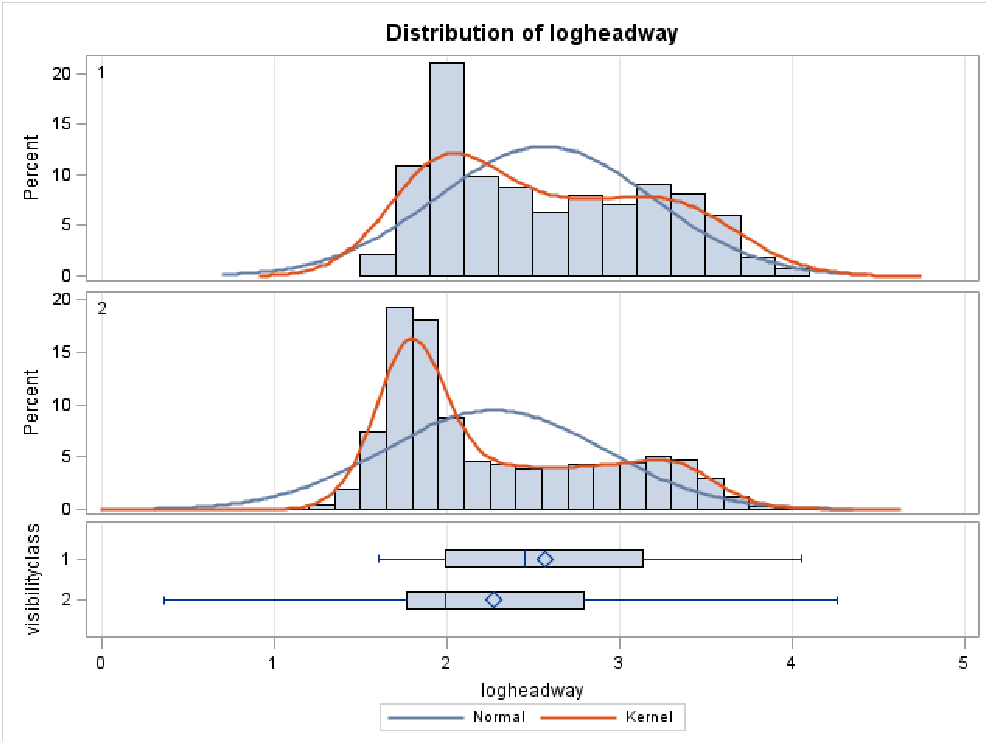

Figure 6.20 Distribution of Logarithm of Headway for Trucks

6.2.3 Comparison of Reduced Visibility on Speed Variation

The comparison of the speed variation of both vehicle types under fog case and clear case is carried by comparing the mean value of the standard deviation of speed using T-test. The value of the mean for the passenger cars in fog case is 6.10 mph, while the value of the mean in clear case is 5.77 mph. The value of the mean for the trucks in fog case is 5.62 mph, while the value of the mean in clear case is 5.60 mph. It can be seen that the standard deviation of speed of passenger cars and trucks increases 0.33 mph and 0.02 mph separately during the fog case. The effect of reduced visibility on standard deviation of trucks is not significant. The P-value for passenger cars showed to be less than 0.001 which indicates that the mean value is significantly different.

Table 6.5 Summary of t-test for Standard Deviation of Speed

Vehicle Type	Parameter	Analysis Cases	
		Fog Case	Clear Case
Passenger Cars	Sample size	367	7177
	Mean	6.10	5.77
	95% CL Mean	6.01-6.20	5.75-5.79
	Maximum Value	11.82	20.64
	Minimum Value	3.71	2.52
	Standard deviation	1.01	0.91
	P-Value	<0.001	
Truck	Sample size	365	7174
	Mean	5.62	5.60
	95% CL Mean	5.48-5.77	5.57-5.63
	Maximum Value	14.99	15.99
	Minimum Value	0.99	0.05
	Standard deviation	1.51	1.39
	P-Value	0.78	

The distribution of logarithm of headway in both cases is shown in Figure 6.21 and Figure 6.22. The top one in each figure is the distribution for the fog case and the bottom one is the distribution for the clear case. It can be seen from both figures that the speed variation of passenger cars is significantly higher in the fog case while the speed variation for the trucks is not.

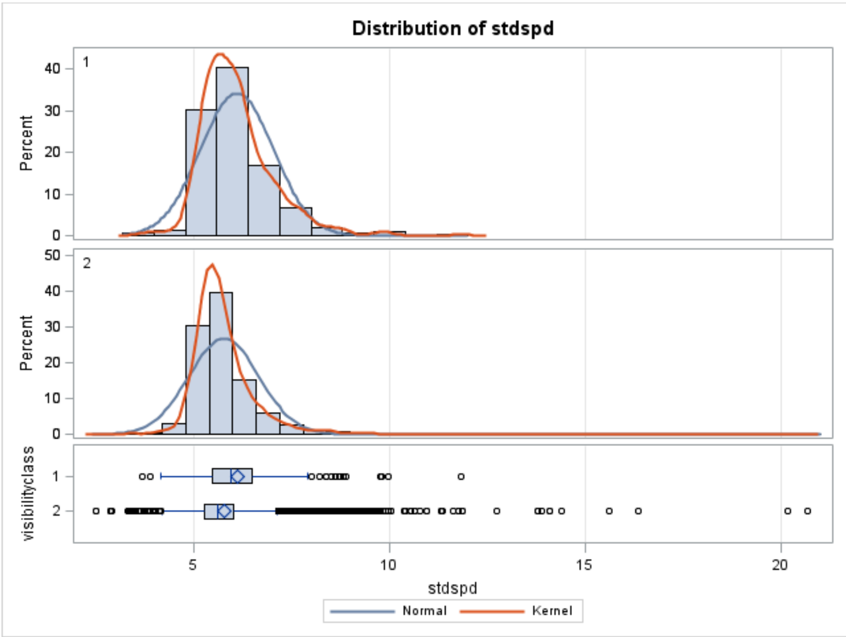

Figure 6.21 Distribution of Standard Deviation of Speed for Cars

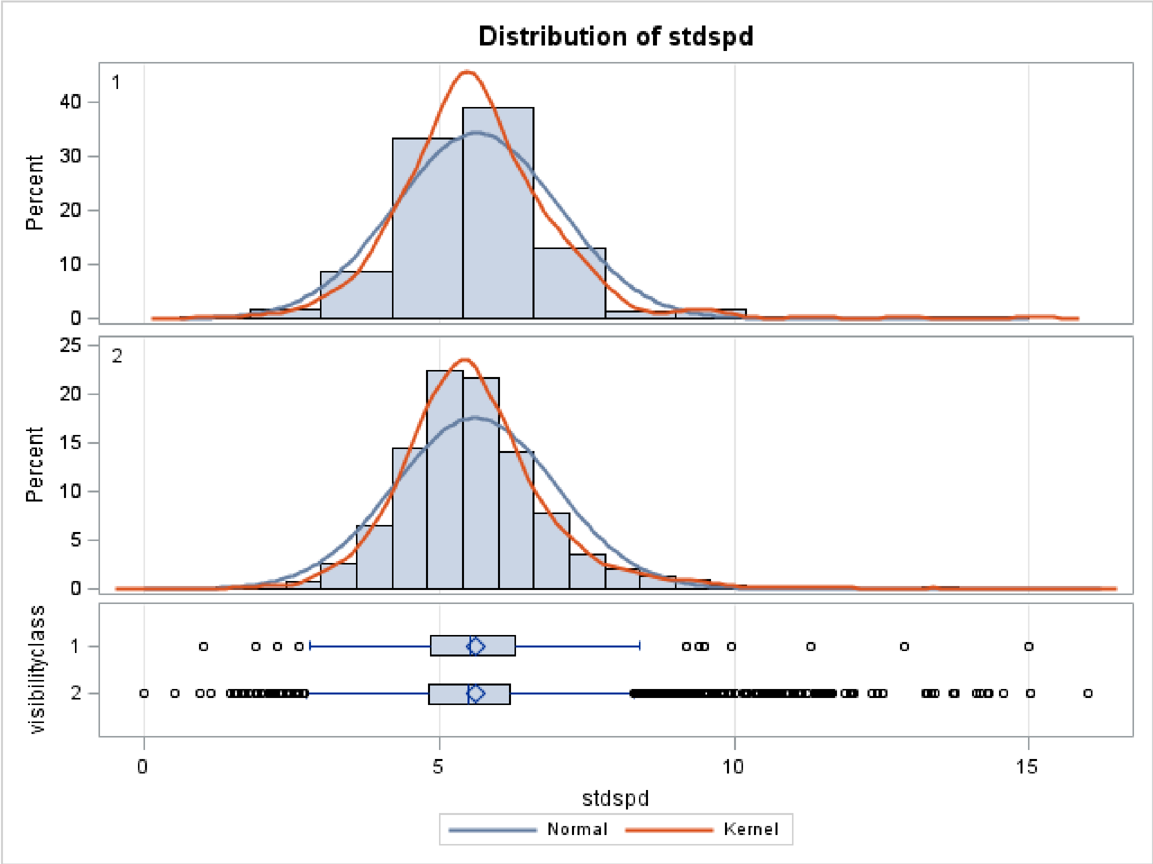

Figure 6.22 Distribution of Standard Deviation of Speed for Trucks

6.2.4 Comparison of Reduced Visibility on Headway Variation

The comparison of the standard deviation of headway under fog case and clear case is carried by comparing the mean value of the standard deviation of headway using the T-test. The value of the mean for the passenger cars in fog case is 13.03 seconds, while the value of the mean in clear case is 9.48 seconds. The value of the mean for the trucks in fog case is 12.59 seconds, while the value of the mean in clear case is 9.64 seconds. It can be seen that the standard deviation of headway of passenger cars and trucks increases 3.55 seconds and 2.95 seconds separately during the fog case. The effect of reduced visibility on standard deviation of headway of passenger cars is larger compared to trucks. The P- value for both vehicle types showed to be less than 0.001 which indicates that the mean value is significant different in both cases.

Table 6.6 Summary of t-test for Standard Deviation of Headway

Vehicle Type	Parameter	Analysis Cases	
		fog Case	clear Case
Passenger Cars	Sample size	367	7177
	Mean	13.03	9.48
	95% CL Mean	12.20-13.88	9.31-9.66
	Maximum Value	40.14	37.74
	Minimum Value	3.71	1.81
	Standard deviation	8.83	7.65
	P-Value	<0.001	
Truck	Sample size	365	7174
	Mean	12.59	9.64
	95% CL Mean	11.81-13.36	9.48-9.80
	Maximum Value	39.19	48.11
	Minimum Value	3.27	0.32
	Standard deviation	8.13	7.05
	P-Value	<0.001	

The distribution of standard deviation of headway in both cases is shown in Figure 6.23 and Figure 6.24. The top one in each figure is the distribution for the fog case and the bottom one is the distribution for the clear case. It can be seen from these two figures that standard deviation of headway of both vehicle types is significantly higher in the fog case.

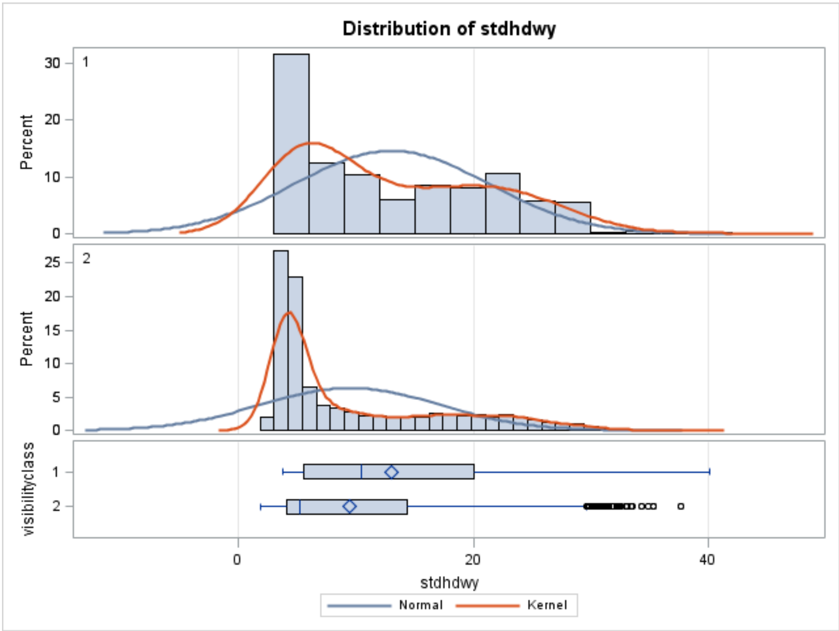

Figure 6.23 Distribution of Standard Deviation of Headway for Cars

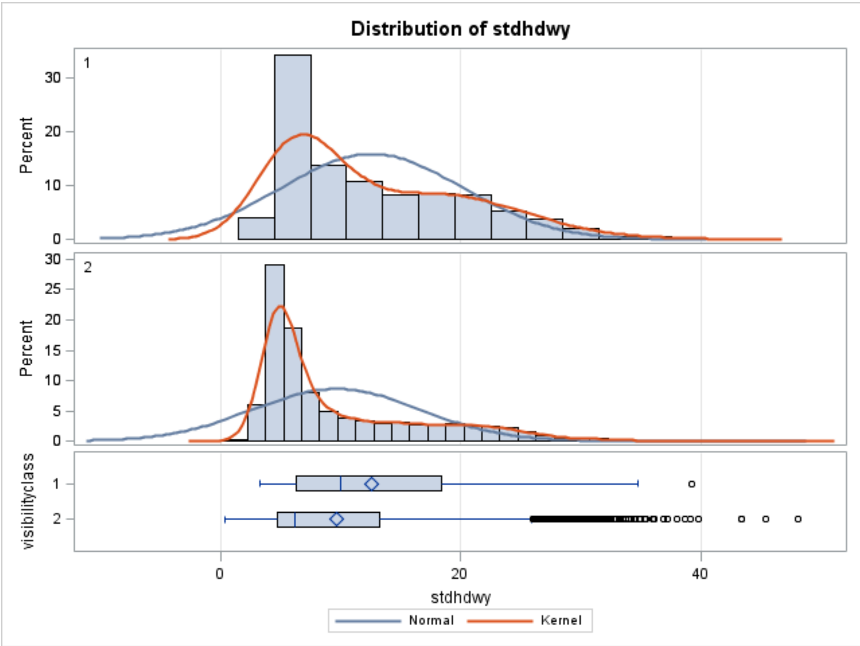

Figure 6.24 Distribution of Standard Deviation of Headway for Trucks

6.3 Effects of Reduced Visibility on Traffic Flow Characteristics using ANOVA

The method of Analysis of variance (ANOVA) is used in this project to compare the differences between several group means and their associated variations. This method provides a powerful statistical test of comparing means of more than two groups and it is a generalization of t-test. As doing multiple two-sample t-tests is not convenient and would result in an increased chance of errors, ANOVA is useful in comparing means of three or more groups for statistical significance. In this section ANOVA is used to further analyze the traffic flow characteristics under different visibility levels and the effects of reduced visibility on different lanes. The datasets used in this section were the combined dataset mentioned in section 4.5 which covers the period from Jan31th to Mar26th.

6.3.1Analysis of Effects of Different Visibility Levels

According to the characteristics of the weather dataset and some previous literature (Hassan and Abdel-Aty, 2011a), we divided the visibility into three levels using the same combined dataset analyzed above in order to further investigate the difference of traffic flow characteristics under different visibility levels. The visibility is considered as good visibility and classified as 1 in the ANOVA analysis when the visibility is greater than or equal to 2000 m. The visibility is considered as moderate visibility and classified as 2 if the visibility is less than 2000 m but greater than 300 m. The visibility is considered as low visibility and classified as 3 if the visibility is less than or equal to 300 m.

Headway comparison

The comparison of the headway under different visibility levels is carried out by comparing the mean value of the headway per direction. The distribution of means of headway under three different visibility levels is shown in Figure 6.25. It can be seen from the figure that the mean headway is significantly higher under low visibility.

It also can be seen in Table 6.10 that the differences of means of headway are all significant under different visibility levels. The mean of headway increases when the visibility drops. The difference of headway between good visibility and moderate headway is 2.0176 seconds and the difference between moderate visibility and low visibility is 1.8945 seconds.

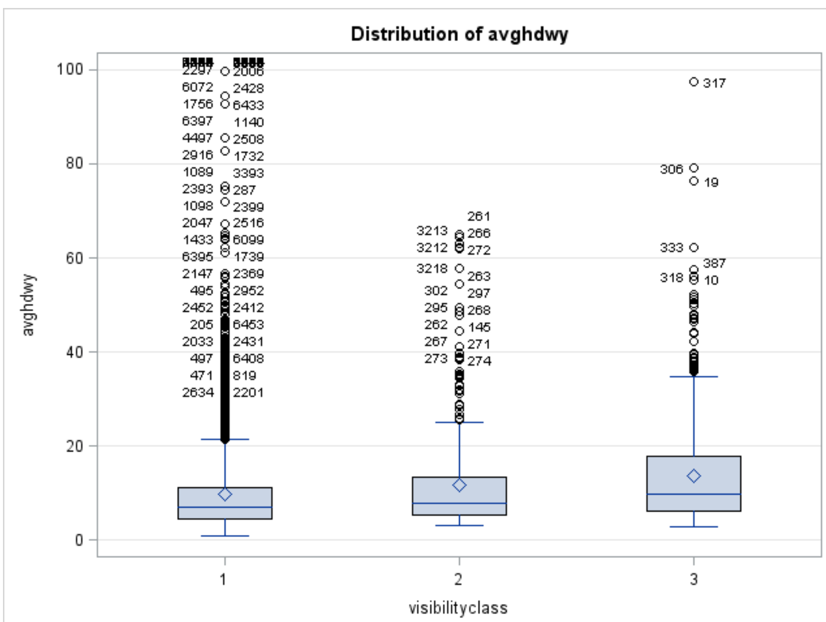

Figure 6.25 distribution of means of headway under different visibility levels

Table 6.7 Comparison of means of headway under different visibility levels

Comparison of different visibility levels	Difference Between Means	Simultaneous 95% Confidence Limits		
3 - 2	1.8945	0.6497	3.1392	***
3 - 1	3.9120	3.1780	4.6461	***
2 - 3	-1.8945	-3.1392	-0.6497	***
2 - 1	2.0176	0.9487	3.0864	***
1 - 3	-3.9120	-4.6461	-3.1780	***
1 - 2	-2.0176	-3.0864	-0.9487	***

*Note that *** indicates that the result is significant*

Speed comparison

The comparison of the speed under different visibility levels is performed by comparing the mean value of the speed per direction. The distribution of means of speed under three different visibility levels was shown in Figure 6.26. It can be seen that the mean speed is significantly lower under low visibility.

It also can be seen from Table 6.11 that the differences of mean speed are all significant under different visibility levels. The mean speed decreases when the visibility drops. The difference of speed between good visibility and moderate visibility is 0.2929 mph and the difference between moderate visibility and low visibility is 0.6588 mph.

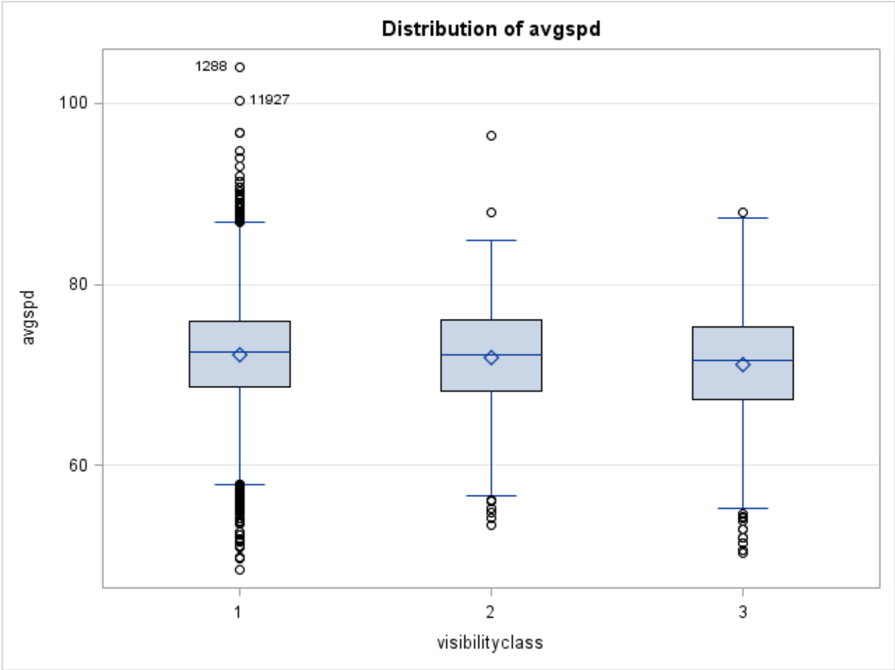

Figure 6.26 Distribution of means of speed under different visibility levels

Table 6.8 Comparison of means of speed under different visibility levels

Comparison of different visibility levels	**Difference Between Means**	**Simultaneous 95% Confidence Limits**		
1 - 2	0.29297	0.01564	0.57029	***
1 - 3	0.95181	0.76093	1.14268	***
2 - 1	-0.29297	-0.57029	-0.01564	***
2 - 3	0.65884	0.33533	0.98234	***
3 - 1	-0.95181	-1.14268	-0.76093	***
3 - 2	-0.65884	-0.98234	-0.33533	***

Variance of Headway comparison

The comparison of the variance of headway under different visibility levels is carried by comparing the mean value of the standard deviation of headway per direction. The distribution of standard deviation of headway under three different visibility levels was shown in Figure 6.27. It can be seen that the standard deviation of headway is significantly higher in low visibility.

It also can be seen from Table 6.12 that the differences of standard deviation of headway are all significant under different visibility levels. The mean of standard deviation of headway will increase when the visibility drops. The difference of standard deviation of headway between good visibility and moderate visibility is 0.8115 seconds and the difference between moderate visibility and low visibility is 1.7449 seconds.

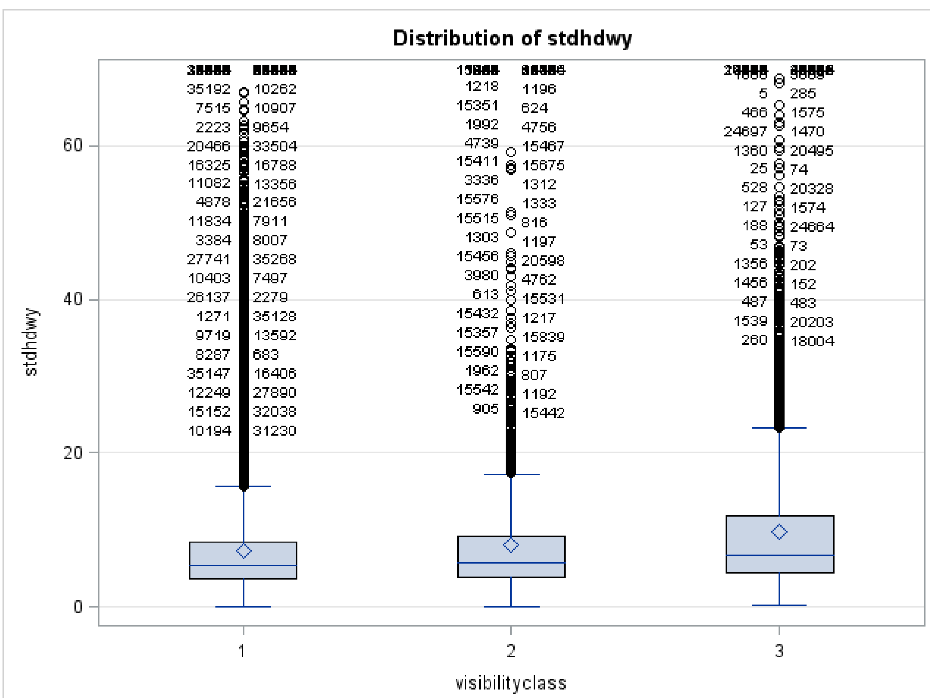

Figure 6.15 Distribution of standard deviation of headway under different visibility levels

Table 6.9 Comparison of standard deviation of headway under different visibility levels

Comparison of different visibility levels	Difference Between Means	Simultaneous 95% Confidence Limits		
3 - 2	1.74495	1.29903	2.19087	***
3 - 1	2.55647	2.29213	2.82082	***
2 - 3	-1.74495	-2.19087	-1.29903	***
2 - 1	0.81152	0.43065	1.19239	***
1 - 3	-2.55647	-2.82082	-2.29213	***
1 - 2	-0.81152	-1.19239	-0.43065	***

It is noted that the variance of speed under different visibility levels is also analyzed using the same method but the result shows that there is not significantly difference of variance of speed under different visibility levels.

6.3.2Analysis of Effects of Reduced Visibility on Different Lanes

There are three lanes in each direction for the site. The outer lane is labeled as 0 and the inner lane is labeled as 2 while the middle lane is labeled as 1 for the East Bound direction. The outer lane is labeled as 5 and the inner lane is labeled as 3 while the middle lane is labeled as 4 for the West Bound direction. In this section we will mainly make comparisons about the traffic flow characteristics in different lanes under different visibility levels. At first, the distributions of average speed and headway were compared for both directions. It can be seen from the Table 6.13 to Table 6.16 that the distribution of average speed and headway are very similar in both directions. The average speed for the inner lane is significantly higher than middle lane and outer lane while the average headway for the outer lane is significantly higher than middle lane and inner lane. In addition, further comparison under different visibility levels presents the similar results for both directions, therefore, this study focused on presenting the effects of reduced visibility on different lanes for the EB.

Table 6.13 Comparison of means of speed in different lanes for EB

Comparison of different visibility levels	**Difference Between Means**	**Simultaneous 95% Confidence Limits**		
2 - 1	4.41505	4.28185	4.54826	***
2 - 0	8.75264	8.61856	8.88672	***
1 - 2	-4.41505	-4.54826	-4.28185	***
1 - 0	4.33759	4.20458	4.47060	***
0 - 2	-8.75264	-8.88672	-8.61856	***
0 - 1	-4.33759	-4.47060	-4.20458	***

Table 6.14 Comparison of means of headway in different lanes for EB

Comparison of different visibility levels	Difference Between Means	Simultaneous 95% Confidence Limits		
0 - 2	5.1770	4.6939	5.6602	***
0 - 1	8.4569	7.9776	8.9362	***
2 - 0	-5.1770	-5.6602	-4.6939	***
2 - 1	3.2798	2.7998	3.7599	***
1 - 0	-8.4569	-8.9362	-7.9776	***
1 - 2	-3.2798	-3.7599	-2.7998	***

Table 6.15 Comparison of means of speed in different lanes for WB

Comparison of different visibility levels	Difference Between Means	Simultaneous 95% Confidence Limits		
5 - 3	-1.5589	1.1048	2.0131	***
5 - 4	4.6358	4.1876	5.0839	***
3 - 5	1.5589	-2.0131	-1.1048	***
3 - 4	3.0768	2.6234	3.5302	***
4 - 5	-4.6358	-5.0839	-4.1876	***
4 - 3	-3.0768	-3.5302	-2.6234	***

Table 6.16 Comparison of means of headway in different lanes for WB

Comparison of different visibility levels	Difference Between Means	Simultaneous 95% Confidence Limits		
5 - 3	1.5589	1.1048	2.0131	***
5 - 4	4.6358	4.1876	5.0839	***
3 - 5	-1.5589	-2.0131	-1.1048	***
3 - 4	3.0768	2.6234	3.5302	***
4 - 5	-4.6358	-5.0839	-4.1876	***
4 - 3	-3.0768	-3.5302	-2.6234	***

Speed comparison of outer lane in different visibility levels

The speed comparison of the outer lane under different visibility levels is carried out by comparing the mean speed. The distribution of means speed under three different visibility levels for the outer lane is shown in Figure 6.28. It is hard to see the difference of mean speed under different visibility levels but it can be seen from Table 6.17 that the mean speeds under good visibility level and moderate visibility level are both significantly higher than mean speed under low visibility level while the difference of mean speed under good visibility level and moderate visibility level is not significant. The difference of mean speed between good visibility and low visibility is 1.28 mph and the difference between moderate visibility and low visibility is 0.84 mph.

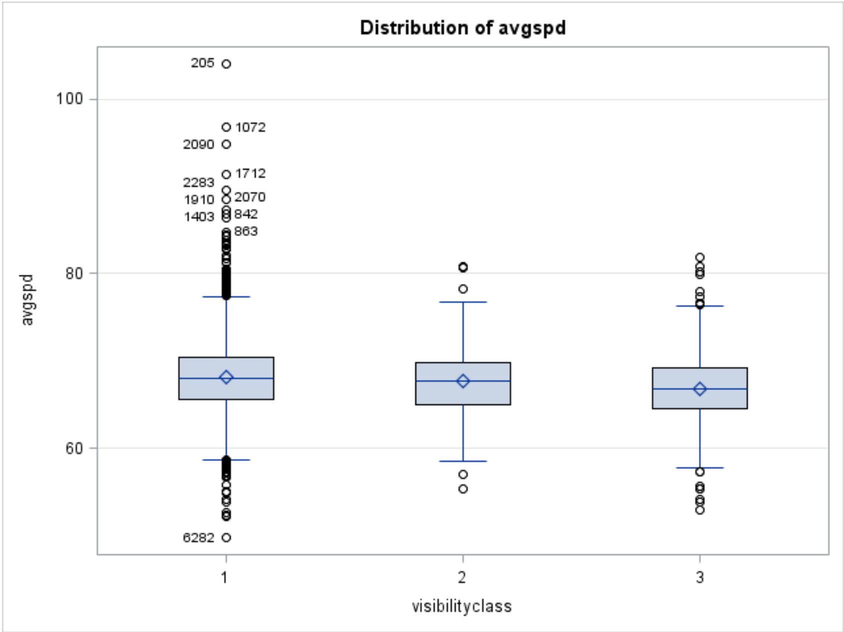

Figure 6.28 Distribution of means of speed for outer lane under different visibility levels

Table 6.10 Comparison of means of speed for outer lane under different visibility levels

Comparison of different visibility levels	Difference Between Means	Simultaneous 95% Confidence Limits		
1 - 2	0.44000	-0.08060	0.96061	
1 - 3	1.28185	0.92093	1.64277	***
2 - 1	-0.44000	-0.96061	0.08060	
2 - 3	0.84185	0.23303	1.45066	***
3 - 1	-1.28185	-1.64277	-0.92093	***
3 - 2	-0.84185	-1.45066	-0.23303	***

Speed comparison of middle lane in different visibility levels

The speed comparison of the middle lane under different visibility levels is also carried by comparing the mean speed. The distribution of means speed under three different visibility levels for the outer lane was shown in Figure 6.29. It can be seen from the Figure 6.29 that there is obvious difference of mean speed under different visibility levels. It also can be seen from the Table 6.18 that the mean speeds will increase as the visibility increases. The difference of mean speed between good visibility and low visibility is 1.01 mph and the difference between good visibility and moderate visibility is 0.36 mph.

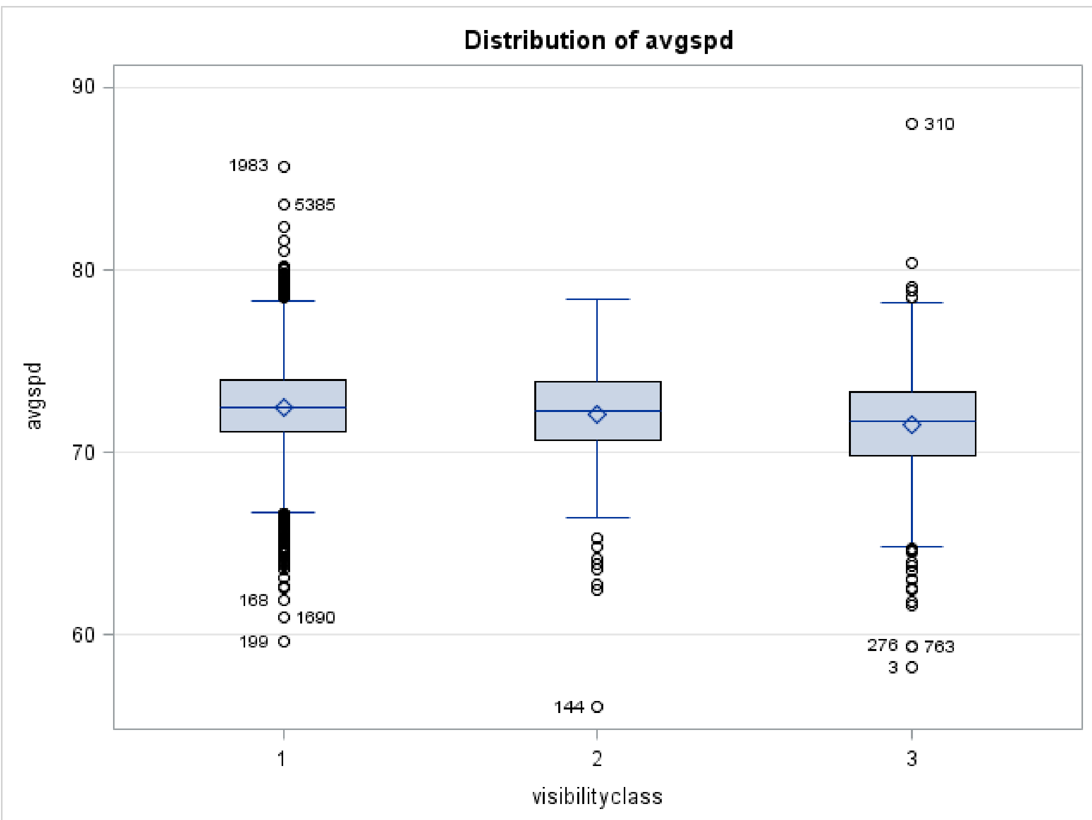

Figure 6.29 Distribution of means of speed for middle lane under different visibility levels

Table 6.11 Comparison of means of speed for middle lane under different visibility levels

Comparison of different visibility levels	Difference Between Means	Simultaneous 95% Confidence Limits		
1 - 2	0.36757	0.03969	0.69546	***
1 - 3	1.01375	0.78870	1.23881	***
2 - 1	-0.36757	-0.69546	-0.03969	***
2 - 3	0.64618	0.26424	1.02813	***
3 - 1	-1.01375	-1.23881	-0.78870	***
3 - 2	-0.64618	-1.02813	-0.26424	***

speed comparison of inner lane in different visibility levels

The speed comparison of the inner lane under different visibility levels is shown in the Figure 6.30 and Table 6.19. The distribution of means speed under three different visibility levels for the inner lane was shown in Figure 6.30. It is hard to see the difference of mean speed under different visibility levels but it can be seen from Table 6.19 that the mean speeds under good visibility level and moderate visibility level are both significantly higher than mean speed under low visibility level while the difference of mean speed under good visibility level and moderate visibility level is not significant. The difference of mean speed between good visibility and low visibility is 0.96 mph and the difference between moderate visibility and low visibility is 0.77 mph.

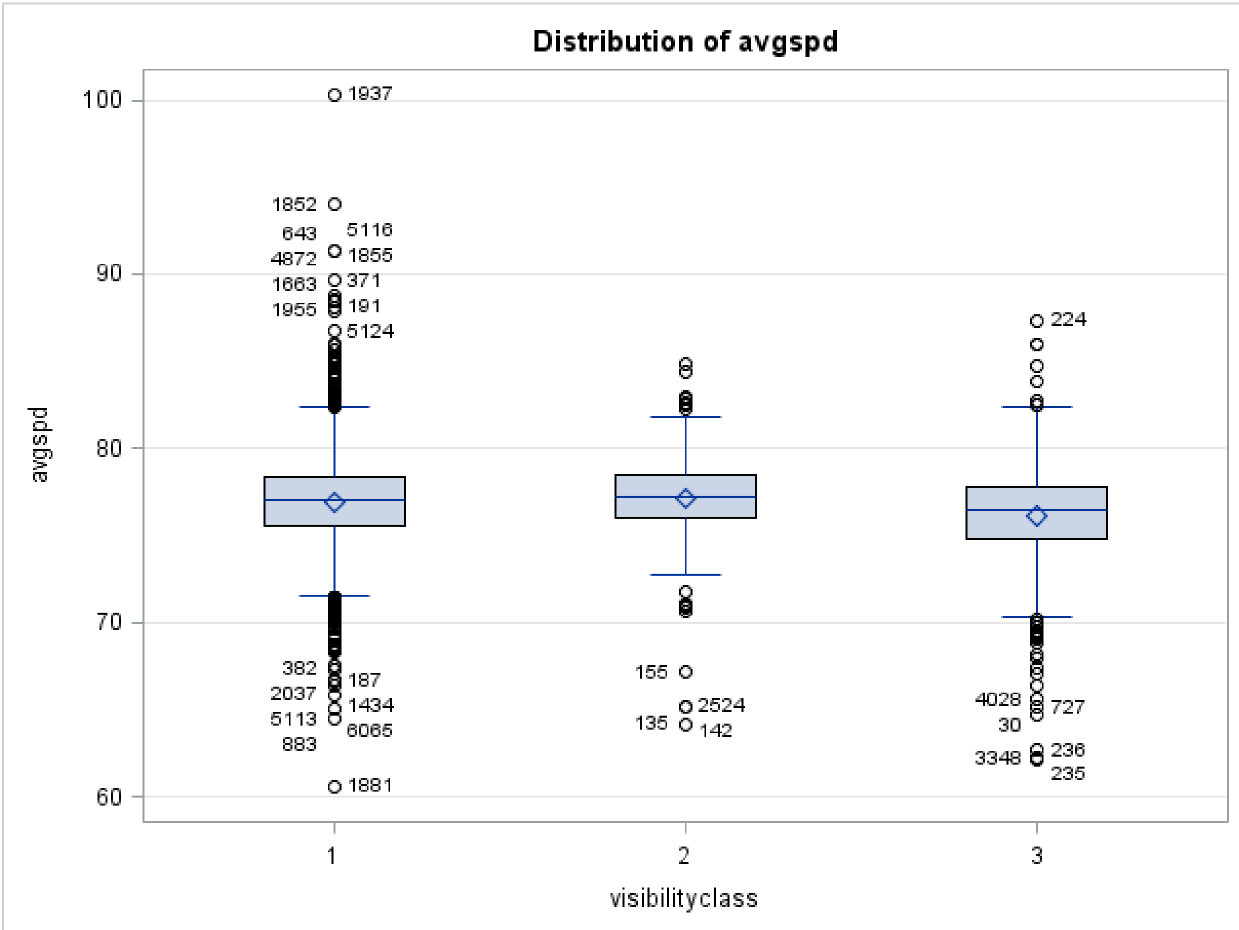

Figure 6.30 Distribution of means of speed for inner lane under different visibility levels

Table 6.12 Comparison of means of speed for inner lane under different visibility levels

Comparison of different visibility levels	Difference Between Means	Simultaneous 95% Confidence Limits		
2 - 1	0.18868	-0.14793	0.52528	
2 - 3	0.96323	0.57122	1.35524	***
1 - 2	-0.18868	-0.52528	0.14793	
1 - 3	0.77455	0.54413	1.00497	***
3 - 2	-0.96323	-1.35524	-0.57122	***
3 - 1	-0.77455	-1.00497	-0.54413	***

In summary, we can conclude that the mean speed will not drop significantly as the visibility starts to decrease especially in inner lane and outer lane. The mean speed will reduce significantly as the visibility drop to below 300m for all the lanes.

Headway comparison of inner lane in different visibility class

The headway comparison of the inner lane under different visibility levels is shown in the Figure 6.31 and Table 6.20. The distribution of means speed under three different visibility levels for the inner lane was shown in Figure 6.31. It can be seen from that there is obvious difference of headway under different visibility levels. It also can be seen from the Table 6.20 that the mean headway will decrease as the visibility increases. The difference of mean headway between good visibility and low visibility is 4.4734 seconds and the difference between good visibility and moderate visibility is 2.4157 seconds.

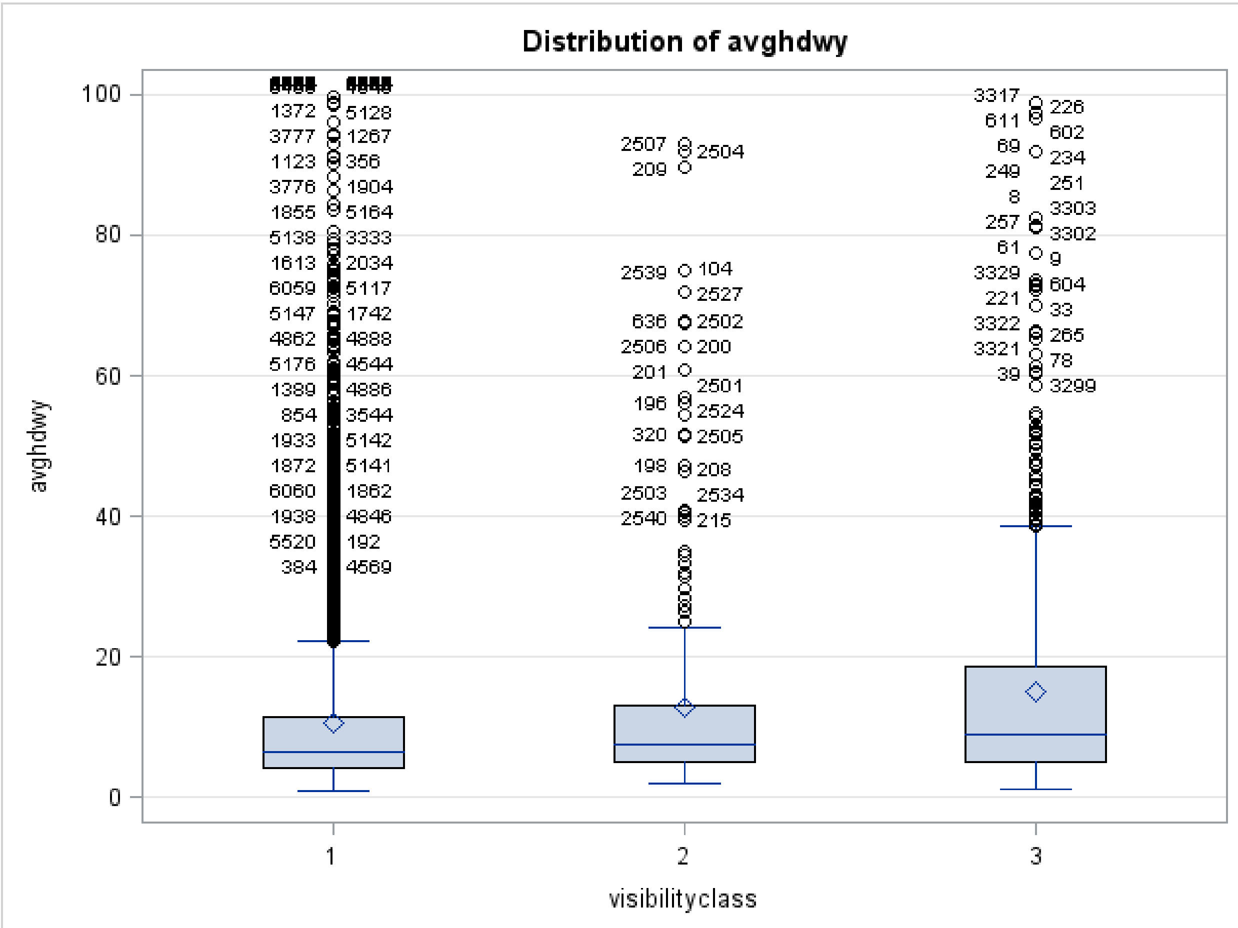

Figure 6.31 Distribution of means of headway for inner lane under different visibility levels

Table 6.20 Comparison of means of headway for inner lane under different visibility levels

Comparison of different visibility levels	Difference Between Means	Simultaneous 95% Confidence Limits		
3 - 2	2.0577	0.0936	4.0218	***
3 - 1	4.4734	3.3189	5.6279	***
2 - 3	-2.0577	-4.0218	-0.0936	***
2 - 1	2.4157	0.7292	4.1022	***
1 - 3	-4.4734	-5.6279	-3.3189	***
1 - 2	-2.4157	-4.1022	-0.7292	***

Headway comparison of middle lane in different visibility class

The headway comparison of the middle lane under different visibility levels is shown in the Figure 6.32 and Table 6.21. The distribution of means speed under three different visibility levels for the middle lane was shown in Figure 6.32. It can be seen that the mean headway increases as the visibility drops and it can be seen from Table 6.21 that the mean headway under good visibility level are significantly higher than both mean headways under low visibility level and moderate visibility level while the difference of mean headway under low visibility level and moderate visibility level is not significant. The difference of mean headway between good visibility and low visibility is 2.48 seconds and the difference between good visibility and moderate visibility is 2.12 seconds.

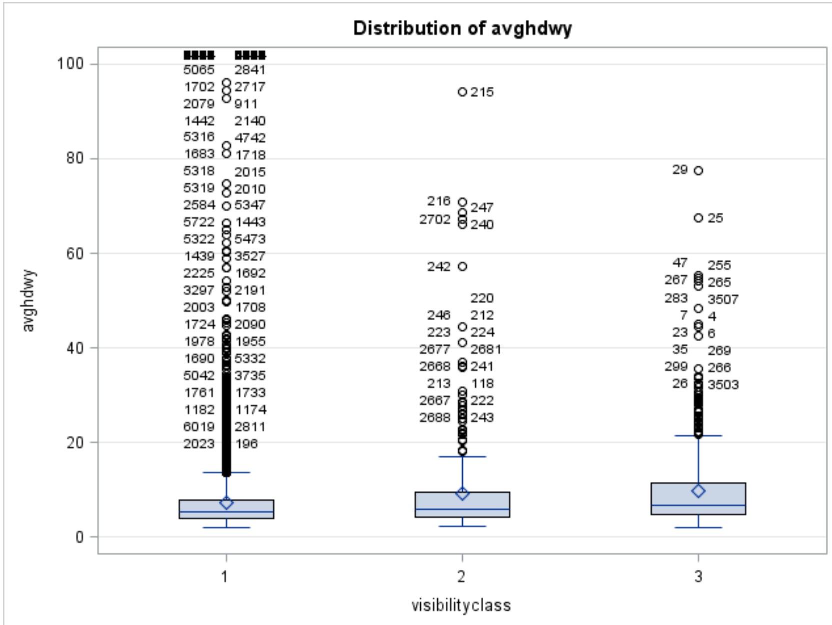

Figure 6.32 Distribution of means of headway for middle lane under different visibility levels

Table 6.13 Comparison of means of headway for middle lane under different visibility levels

Comparison of different visibility levels	Difference Between Means	Simultaneous 95% Confidence Limits		
3 - 2	0.3600	-0.7359	1.4558	
3 - 1	2.4892	1.8435	3.1349	***
2 - 3	-0.3600	-1.4558	0.7359	
2 - 1	2.1292	1.1885	3.0700	***
1 - 3	-2.4892	-3.1349	-1.8435	***
1 - 2	-2.1292	-3.0700	-1.1885	***

Headway comparison of Outer lane in different visibility class

The headway comparison of the inner lane under different visibility levels is shown in the Figure 6.33 and Table 6.22. The distribution of mean headway under three different visibility levels for the inner lane was shown in Figure 6.33. The results are very similar to the results related to middle lane. The mean headway increases as the visibility drops and it can be seen from Table 6.22 that the mean headway under good visibility level are significantly higher than both mean headways under low visibility level and moderate visibility level while the difference of mean headway under low visibility level and moderate visibility level is not significant. The difference of mean headway between good visibility and low visibility is 4.70 seconds and the difference between good visibility and moderate visibility is 3.17 seconds, which are both larger than those of middle lane.

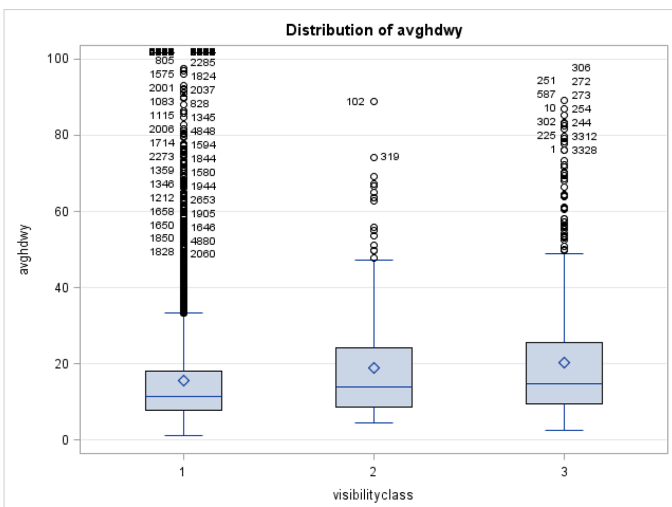

Figure 6.33 Distribution of means of headway for outer lane under different visibility levels

Table 6.14 Comparison of means of headway for outer lane under different visibility levels

Comparison of different visibility levels	Difference Between Means	Simultaneous 95% Confidence Limits		
3 - 2	1.5334	-0.5493	3.6161	
3 - 1	4.7072	3.4726	5.9419	***
2 - 3	-1.5334	-3.6161	0.5493	
2 - 1	3.1738	1.3929	4.9548	***
1 - 3	-4.7072	-5.9419	-3.4726	***
1 - 2	-3.1738	-4.9548	-1.3929	***

6.4 Chapter Summary

This chapter mainly analyzed the effect of reduced visibility on traffic flow characteristics. The mean headway and headway variation are significantly higher while the mean speed and volume are significantly lower in fog case. The impact of reduced visibility on passenger cars is more significant compared to trucks. In comparison, there isn't significant difference in the standard deviation of speed for trucks. The difference of mean speed, headway and standard deviation of headway between fog cases and clear cases for passenger cars are all larger than trucks.

The differences of means of headway are all significant under different visibility levels. The mean of headway will increase when the visibility drops. The mean speed will decrease when the visibility drops. The mean of standard deviation of headway will increase when the visibility drops.

The distribution of traffic flow characteristics is very similar in both directions and the effect of reduced visibility on both directions is also similar. The effects of reduced visibility on different lanes are different.

7. ANALYSIS OF THE DISTRIBUTION AND FACTORS OF FOG DURATION

Fog duration time is the period starting from the time a fog appears to the time it disappears. The main objective of this section is to explore the distribution of the fog duration time and its influencing factors.

7.1 Data Collection and Preparation

The data were obtained from the project of sensor-based fog prediction and monitoring system and the website (http://fdot.weatheractive.net:81/login.aspx). The original data contains several important weather variables including visibility, air_temp, board_temp, humidity, barometric_pressure, wind_speed, solar_radiation, dew_point and subsurface_moisture. It is known that fog may have an effect on traffic flow. Therefore, weather variables were considered as the potential influencing factors on the fog duration in this study.

We need to obtain the duration times of fog events and the corresponding values of weather variables. Whether fog appears was determined by the visibility variable aggregated by 5-mintues interval. After excluding the days with significant wind, rain and snow, we define that fog appears when the visibility is less than 2000 meters, and there is no fog if the visibility is equal or better than 2000 meters. A fog event is that a fog appears (the visibility<2000) and lasts to disappears (the visibility≥2000). Duration time of a fog event is the period starting from the time it appears to the time it disappears. It is a sum of several successive 5-mintues time intervals. The average value of each weather variable in the fog duration time is the corresponding value of the potential factor of the sample. For example, the fog event is a valid sample and its duration time is 1.5 hours if a fog event starts at 6:00 AM and lasts to end at 7:30 AM. The average values of weather variables from 6:00 AM to 7:30 AM are the corresponding values of the variables in this sample.

7.2 Duration Model

Hazard-based duration models have been used in the biometrics and industrial engineering fields as a means of determining causality in duration data and they have recently been applied in the transportation field. In the transportation field, duration models have been used in accident analysis (Nam and Mannering, 2000; Chung, 2010), travel activity behavior (Bhat, 1996, 2004; Lee and Timmermans, 2007; Berg et al., 2012), automobile ownership (Yamamoto et al., 2004; Chen and Niemeier, 2005; Chang and Yeh, 2007) and vehicle delay (Paselk and Mannering, 1994; Guo et al., 2012; Yang et al., 2012).

The variable of interest in duration model is the survival time that elapsed from the beginning of an event until its end. In our study, fog duration time can be regarded as the fog duration that starts when a fog appears and ends when it disappears. Therefore, a duration model is very appropriate to be used to study fog duration event.

Let T denote fog duration time. Then, the survival function is denoted by $S(t)$. It is also called endurance probability or survivor probability in duration literature. It represents the probability that the duration time does not elapse before time t.

$$S(t) = \Pr(T > t) \tag{7.1}$$

The failure probability, which is known as the cumulative distribution of T, is then

$$F(t) = \Pr(T \le t) = 1 - S(t) \tag{7.2}$$

The fog duration time T has a probability density function defined as the limit of the probability of failure in a small interval per unit time. It can be expressed as

$$f(t) = \frac{\partial F(t)}{\partial t} = \lim_{\Delta t \to 0} \frac{P\left(t \le T < t + \Delta t\right)}{\Delta t} \tag{7.3}$$

The density function is also known as the unconditional failure rate.

The hazard function $h(t)$ of duration time T gives the conditional failure rate. In this study, The hazard function is the instantaneous rate at which the fog duration will end in an infinitesimally small time period, Δt, after time t, given that the duration time has lasted to time t seconds:

$$h(t) = \lim_{\Delta t \to 0} \frac{\Pr(t \le T < t + \Delta t \mid T \ge t)}{\Delta t} = \frac{f\left(t\right)}{S\left(t\right)} = \frac{-d \ln S(t)}{dt} \tag{7.4}$$

The shape of the hazard function has important implications for the modeling approach. Depending on the underlying event and the duration process, the hazard function may take different shapes. Note that fog duration times may be influenced by various factors. The influential factors can be defined as a vector of explanatory variables, $\mathbf{x} = \left(x_1, x_2, \cdots, x_p\right)'$. To accommodate the effects of these influential factors, the most commonly used approach to model duration data is the proportional hazard model (Bhat, 1996). The proportional hazard models for duration data usually assume that the explanatory variables take a constant proportional effect on an unspecified baseline hazard function. Although this assumption may relieve the estimation efforts of the model, it may not be applicable when the constant proportional assumption is violated. An alternative approach is the accelerated hazard model, which is mainly used in reliability theory and industrial experiments. In our study, a parametric hazard approach is adopted because its hazard function can be chosen flexibly.

In the accelerated hazard model, the natural logarithm of the duration time, log t, is expressed as a linear function of the covariates, yielding the linear model

$$\log t_j = \mathbf{X}_j \boldsymbol{\beta} + \varepsilon_j \tag{7.5}$$

where x_j is a vector of covariates, β is a vector of regression coefficients, and ε_j is the error with density f(ε). The distributional form of the error term determines the regression model. If we let f(ε) be the logistic density, the log-logistic regression is obtained. If we let f(ε) be the standard normal density, the lognormal regression is obtained. Setting f(ε) equal to the extreme-value density yields the exponential and the Weibull regression models. Several parametric distributions for the accelerated hazards can be assumed including Exponential, Weibull, lognormal and Log-logistic. Parametric hazard models can be estimated by maximum likelihood method. These common distributions and the detailed estimation methods can be found in Lee and Wang (2003).

The AIC (Akaike Information Criterion) and the BIC (Baysian Information Criterion) procedure approaches can be applied to select the best parametric model. The AIC and BIC are two popular measures for comparing maximum likelihood models. AIC and BIC are defined as

$$AIC = -2*\ln(L) + 2*k \tag{7.6}$$

$$BIC = -2*\ln(L) + \ln(N)*k \tag{7.7}$$

where, k = number of parameters estimated, N = number of observations, L = the maximized value of the likelihood function for the estimated model. Given two models fit on the same data, the model with the smaller value of the information criterion is considered to be better.

7.3 Results and Discussions

Descriptive statistics

A total of 65 valid samples were obtained from four months of weather data from January 1 to April 30, 2014. Sometimes there are several fog duration (i.e. low visibility) events in one day. Meanwhile, sometimes there is not one low-visibility event in several successive days. The average duration time of all samples was 0.816 hour, with a standard deviation of 1.492 hours. The median duration time was 0.333 hour (i.e. 20 minutes). It means that half of all low-visibility events last 20 minutes or less. The maximum low-visibility duration was 8.25 hours while the minimum was 5 minutes. Figure 7.1(a) presents the sample distribution of fog duration times with 0.5 hour in each interval. Figure 7.1(b) shows the cumulative distribution of fog duration times. From these two Figures, it is shown that 67.7% of all samples last no more than 0.5 hour. 84.6% of all samples last no more than one hour.

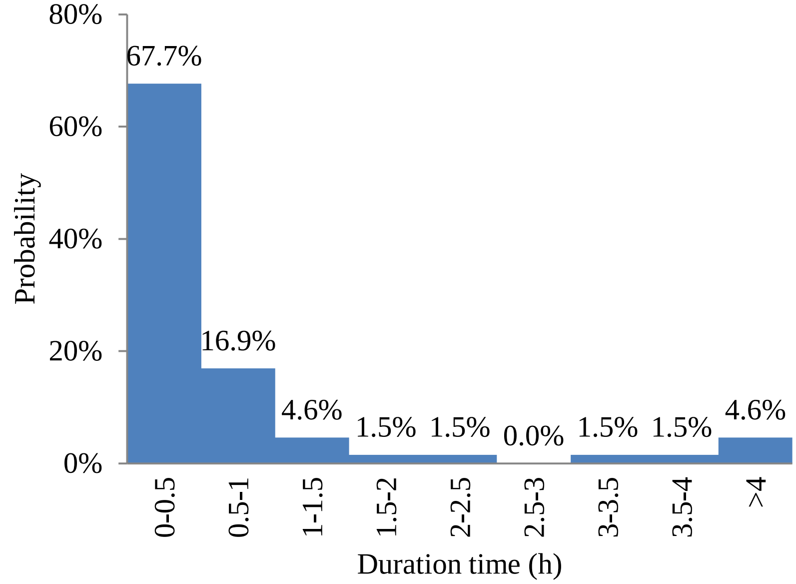

a. Histogram of fog duration time

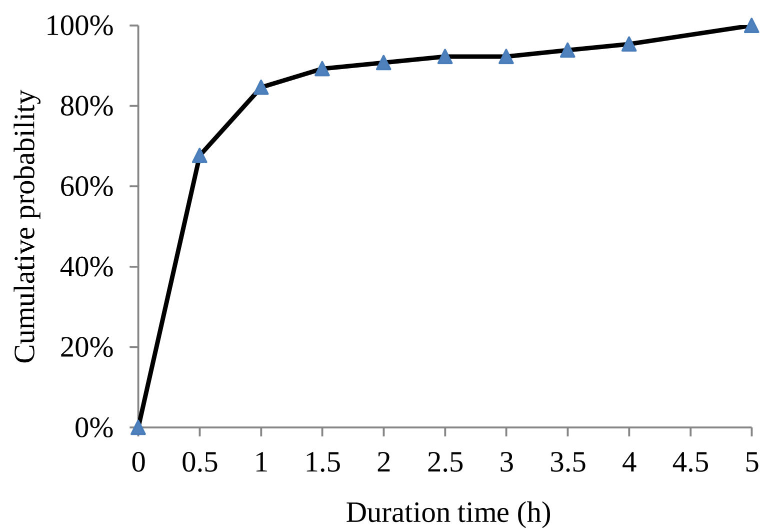

Figure 7.1 Cumulative distribution Table of fog duration time

Estimated results without covariates

Considering the fog duration times of the 65 fog events , we obtain the MLE (Maximum Likelihood Estimation) of the parameters and the log-likelihoods for the exponential, Weibull, lognormal, and log-logistic distributions using STATA. The results are shown in Table 7.1. For example, the MLE of λ in the exponential distribution is $\exp^{(0.203)}$ and the corresponding log-likelihood is -119.401, and the MLE of the two parameters in the Weibull distribution are λ=exp(0.413*0.764) and γ=0.764 and the corresponding log-likelihood is -113.654.

Table 7.1 Goodness-of-fit tests of models without the covariates for fog duration data

Model	Estimated Parameters		LL[c]	BIC	AIC
	A[a]	B[b]			
Exponential	-0.203	*None*[d]	-119.401	242.976	240.801
Weibull	-0.413	0.764	-113.654	235.657	231.308
Lognormal	-1.104	1.189	-103.509	**215.366**	**211.017**
Log-logistic	-1.602	0.679	-104.040	216.430	212.081

[a]A=-lnλ for the exponential and log-logistic, =-(1//γ)lnλ for the Weibull, =μ for the lognormal distribution.

[b]B=γ for the Weibull and log-logistic, =σ for the lognormal distribution.

[c]LL, Log-likelihood.

[d]*None*, this parameter does not exist in the exponential model.

The values of the BIC and AIC for the various distributions considered in fog duration data are listed in the last two columns in Table 7.1. Based on Table 7.1, the lognormal distribution would be selected by either the BIC or AIC procedure.

The lognormal distribution model gives the best description of fog duration without covariates (see Figure 7.2). Based on the lognormal distribution model, density function and cumulative distribution function of fog duration using our sample data can be written as

$$f(t)=\frac{1}{t\sigma\sqrt{2\pi}}\exp\{\frac{-1}{2\sigma^2}[\log(t)-\mu]^2\}=\frac{1}{1.189t\sqrt{2\pi}}\exp\{-0.354[\log(t)+1.040]^2\} \quad (7.8)$$

$$F(t)=\Phi\{\frac{\log(t)-\mu}{\sigma}\}=\Phi\{0.841\log(t)+0.875\}. \quad (7.9)$$

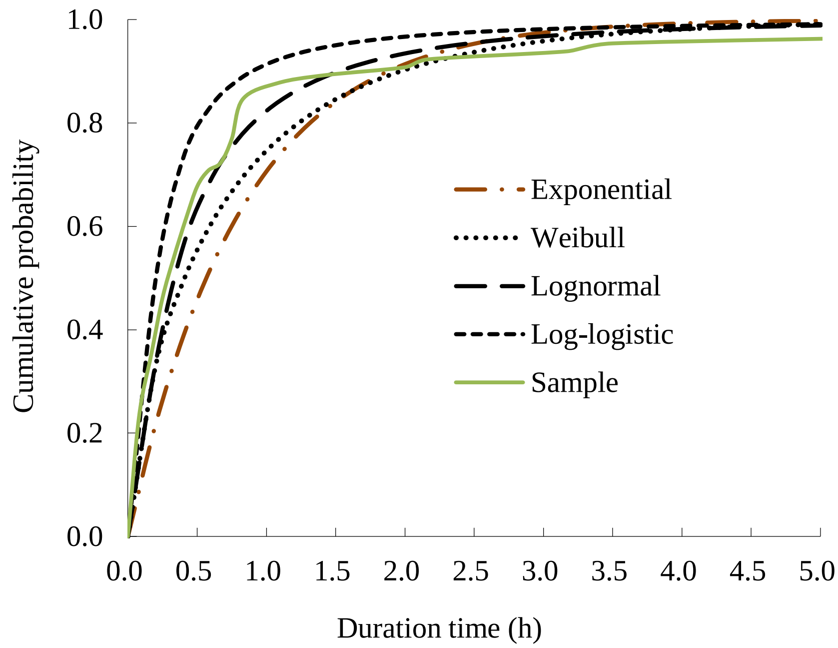

Figure 7.2 Cumulative distribution of fog duration time without covariates

Estimated results with covariates

(1) Correlation analysis of potential variables

Before a statistical calculation is done, the data have to be examined carefully. If some of the variables are significantly correlated, one of the correlated variables is likely to be a predictor as good as all of them. Correlation coefficients between variables can be computed to detect significantly correlated variables.

The correlation analysis is presented in Table 7.2. The correlation is high between "air_temp", "dew_point", and "board_temp". There is positive correlation between each other for these three variables. As some of the variables are significantly correlated, only one of the correlated variables was selected to the fog duration model. Finally, seven variables were selected to study the fog duration, which are listed in the first column in Table 7.3.

Table 7.2 Correlations between potential influential variables

Variable	2	3	4	5	6	7	8	9	Mean
1.visibility	0.01	0.27	0.08	-0.05	-0.34	0.14	-0.08	-0.02	767.40
2.air_temp		-0.16	-0.52	0.56	0.04	**0.83**	**0.95**	0.14	59.56
3.humidity			0.21	-0.40	-0.54	0.42	-0.34	0.19	93.84
4. barometric_pressure				-0.28	-0.27	-0.37	-0.56	0.07	30.00
5. wind_speed					-0.11	0.28	0.55	0.31	2.99
6.solar_radiation						-0.22	0.28	-0.30	102.34
7.dew_point							**0.69**	0.24	57.34
8.board_temp								0.07	65.30
9.subsurface_moisture									0.30

（2）Parameter estimated results

To identify important influenced factors using a parametric approach, one needs to select the most appropriate parametric model and identify the most significant subset of covariates. In this study, hazard-based duration model was used to identify influenced factors of fog duration. Four parametric distribution models were fitted to the data for 65 fog duration events to determine the variables related to fog duration time. The possible influencing variables considered were visibility, air_temp, humidity, barometric_pressure, wind_speed, solar_radiation, and subsurface _moisture.

We firstly applied the stepwise selection procedure ($p<0.10$) to select the best subset of covariates separately for the exponential, Weibull, lognormal, and Log-logistic models. The results of covariates' selections are presented in Table 7.3. Three covariates (wind_speed, solar_radiation and subsurface_moisture) are selected as the most significant covariates in the exponential model. The same two covariates (wind_speed and solar_radiation) are selected as the most significant covariates in the Weibull and lognormal models. Meanwhile, two different covariates (humidity and barometric_pressure) are selected as the most significant covariates in the log-logistic model.

Then, we applied the information criterion (AIC and BIC) procedures to select the best parametric model with covariates. Table 7.3 shows the values of BIC and AIC for different parametric models with the selected covariates. Based on these values, the log-logistic model with two covariates was selected as the final model for the data since its AIC or BIC value is the smallest among all the models. However, it is not known if the log-logistic model is significantly better than the other models.

Table 7.3 Parametric estimated results with the selection of model and covariates simultaneously

Variable	Exponential	Weibull	Lognormal	Log-logistic
visibility	–[a]	–	–	–
air_temp	–	–	–	–
humidity	–	–	–	0.022
barometric_pressure	–	–	–	2.737
wind_speed	-0.287	-0.246	-0.183	–
solar_radiation	-0.001	-0.001	-0.001	–
subsurface_moisture	4.440	–	–	–
CONS	-0.804	0.386	-0.409	-85.302
$\gamma(\sigma)$	*None*[b]	0.857	1.088	0.607
LL	-106.746	-107.018	-97.736	-97.507
BIC	230.189	230.734	212.170	**211.712**
AIC	221.491	222.036	203.472	**203.014**

[a] –, the variable is insignificant (p>0.10).

[b] *None*, this parameter does not exist in this model

（3）Analysis of the covariates' effects

The results of parametric estimation are presented in Table 7.3. Five variables- humidity, barometric_pressure, wind_speed, solar_radiation and subsurface_moisture -were selected for use in the models, all related significantly (p<0.10) to fog duration time. The positive sign of the regression coefficient indicates that the increase of this variable has a positive effect on fog disappearance. It also means that the fog duration time decreases with the increase of the variable. Therefore, the increase of "wind_speed" or "solar_radiation" would decrease the fog duration time. On the contrary, the negative sign of the regression coefficient indicates that the increase of this variable has a negative effect on fog disappearance and a longer time of fog duration. Therefore, the increase of "humidity", "barometric_pressure" or "subsurface_moisture" would increase the fog duration time.

（4）the goodness of the fitted models

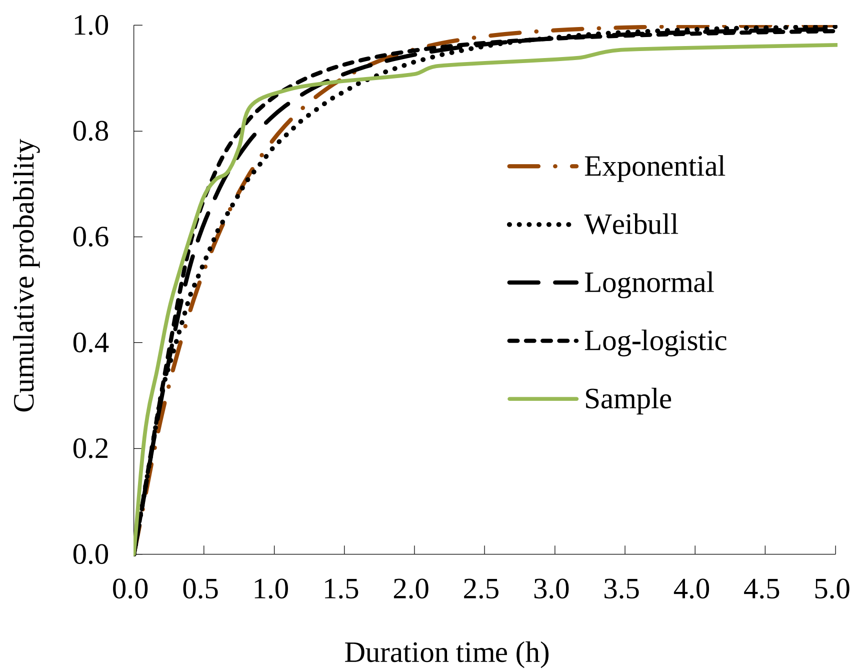

Figure 7.3 Cumulative distribution of fog duration time with covariates

Once a specified parametric model and a subset of covariates are selected, the goodness of fit of this model should be assessed. Figure 7.3 gives the comparisons of the cumulative distributions of the sample and four parametric models. We can see that the Log-logistic distribution model gives the best description of fog duration with the significant covariates. It is noted that the sample cumulative probability indicates the specific condition for individual sample, while the estimated results of parametric models indicate the average condition that is related with different influential factors and all samples.

In addition, the graphical method of Cox-Snell residual procedure with covariates can be used to assess the goodness of fit of the parametric regression model. The graph should be closed to a straight line with unit slope and zero intercept if the fitted model for the duration time T is correct. Figure 7.4 shows the Cox-Snell residuals plots from fitting the exponential, Weibull, lognormal, and log-logistic models, respectively with the significant covariates to the fog duration data. The four graphs look similar, and all are close to a straight line with unit slope and zero intercept. No significant differences are observed in these graphs. The results obtained are similar to those from Figure 7.3. The differences among the four distributions are small. The log-logistic distribution is slightly better than the others when the values of the Cox-Snell residuals are less than two (it represents 86.15% of all samples).

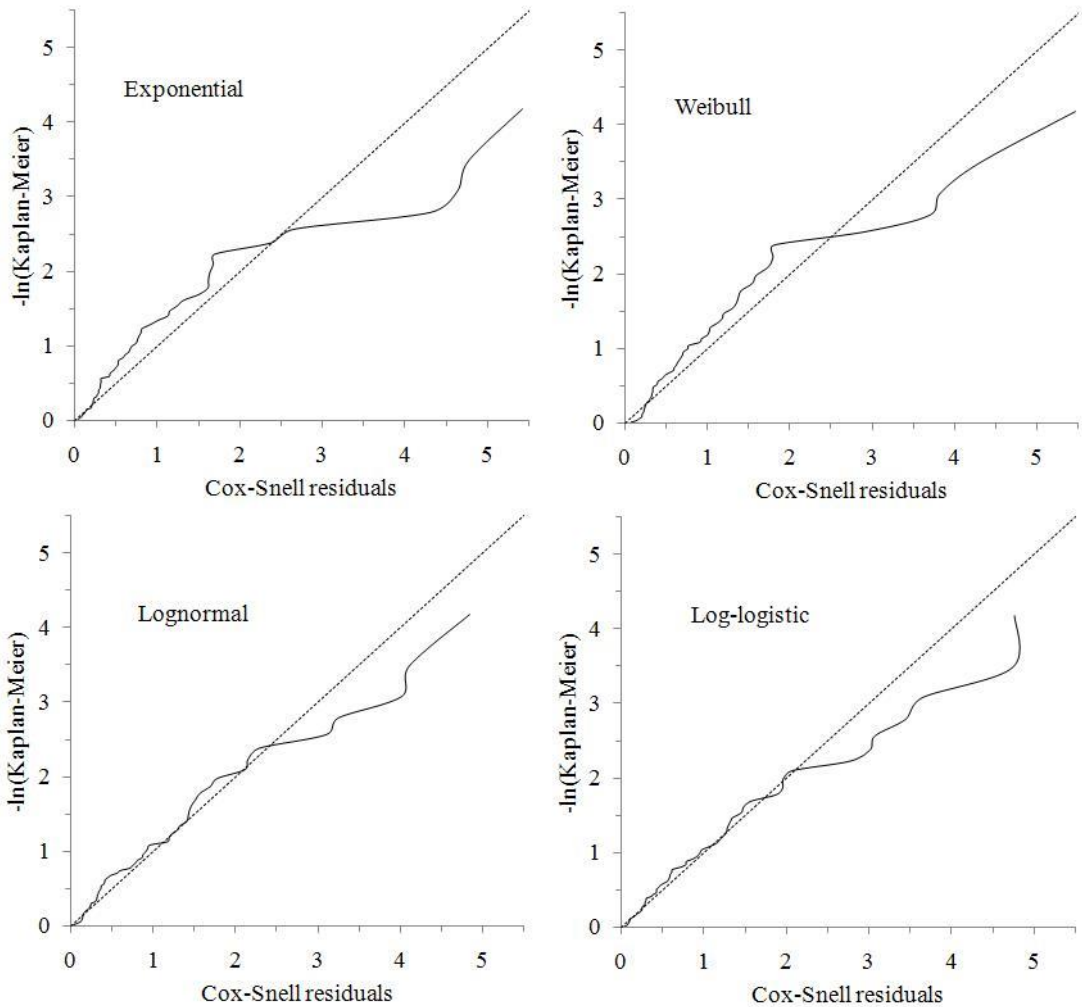

Figure 7.4 Cox-Snell residuals plots from the fitted the exponential, Weibull, lognormal, and log-logistic models on fog duration data

7.4 Chapter Summary

In summary, we used hazard-based duration model to investigate fog duration time and its influencing factors. The following several conclusions were made:

(1) In our samples, half of all low-visibility events last 20 minutes or less. 67.7% of all samples last no more than 30 minutes. 84.6% of all samples last no more than 60 minutes.

(2) Hazard-based duration model is appropriate to model fog duration time and its

influenced factors. The lognormal distribution model gives the best description of fog duration without covariates. The log-logistic model gives the best description of fog duration with covariates.

(3) The increase of “humidity”, “barometric_pressure” and “subsurface_moisture” would increase the fog duration time. Meanwhile, the increase of “wind_speed” and “solar_radiation” would decrease the fog duration time.

8. EVALUATION OF THE PERFORMANCE OF THE FOG DETECTION ALGORITHM

As has been introduced in chapter 3, the PraxSoft developed the fog prediction algorithm based on the weather datasets they collected which includes measurements of temperature and relative humidity from the Fog Measurement Station (FMS) at different elevations above the ground, along with soil moisture, wind speed and rainfall measurements. These measurements provided an objective micro-level assessment of the current state of the thermodynamic profile near the ground surface along with soil conditions to determine if a visibility constraint (fog) exists or is likely forming.

In addition to micro-level sensor data and traditional site location metadata parameters, for this project we also store a land cover/land use classification code that best describes the nature of the land cover at and around the weather observation and FMS sites. The United States Geological Survey (USGS) NLCD 1992 2-digit land cover classification codes is being used. A means has been developed to enter these metadata values. Each USGS NLCD code will also have an assigned "Land Impact" value that is utilized in the Fog Index calculation.

In this section, our research team at UCF conducted an evaluation of the performance of the fog prediction algorithm developed by Praxsoft.

8.1 Evaluation of the Performance of the Initial Fog Detection Algorithm

The performance of the initial fog detection algorithm completed around April 11 was first evaluated in general by using the Table 8.1 for classification. The major purpose of this evaluation is to figure out whether the fog detection algorithm can be used to predict the reduced visibility by showing high or moderate fog index.

The following four measures were used as performance criteria to evaluate the relative performances of the fog detection algorithm (Miranda-Moreno, 2006):

False Discovery Rate (FDR): the ratio of false positives (Type I errors) among all detected fog events by a model. Smaller values are better.

$$\text{FDR}=\frac{V}{D} \tag{8.1}$$

False Negative Rate (FNR): the ratio of false negatives (Type II errors) among all detected non-fog events by a model. Smaller values are better.

$$\text{FNR}=\frac{R}{X} \tag{8.2}$$

Sensitivity (SENS): the ratio of correctly detected fog events. Larger values are better.

$$\text{SENS}=\frac{S}{n_1} \tag{8.3}$$

Specificity (SPEC): the ratio of correctly detected non-fog events. Larger values are better.

$$\text{SPEC}=\frac{U}{n_0} \tag{8.4}$$

n_{0}: number of “true” good visibility
n_1: number of “true” reduced visibility

Table 8.1 Possible Outcomes of Classification

	Number of observation "detected" as high fog index	Number of observation "detected" as moderate fog index	Number of observation "detected" as low fog index
Number of reduced visibility	U		V
Number of good visibility	R		S
	X		D

U: number of observations of reduced visibility correctly identified as high fog index
V: number of Type I errors
R: number of Type II errors
S: number of observations of good visibility correctly identified as low fog index
D: number of observations of visibility identified as low fog index
X: number of observations of visibility identified as high fog index

Table 8.2 Results of all the observations

	Number of observation "detected" as high fog index	Number of observation "detected" as moderate fog index	Number of observation "detected" as low fog index
Number of reduced visibility(<2000)	425	6	6
Number of good visibility(>=2000)	6997	3182	1544
	12160		1550

The performance of the algorithm was first evaluated in general by using the above tables of classification and criteria. The total number of observations is 12160. It can be seen from Table 8.2 that the number of Type II error that the observation of good visibility was detected as high fog index in the prediction algorithm was 6997. In addition, the observation of good visibility was detected as moderate fog index was also 3182. The number of Type I error that the reduced visibility was detected as low fog index was 6. The result of four performance criteria measurements was shown in Table 8.3. It then can be concluded from the results that this algorithm can be used to detect the fog days but it is very easy to make a false alarm when the day is actually clear.

Table 8.3 Results of four performance criteria measurements

Criteria	Value
FDR (smaller is better)	**0. 4%**
FNR (smaller is better)	**57.5%**
SENS (larger is better)	**13.2%**
SPEC (larger is better)	**97.2%**

Next, In order to further validate the predictions of the fog index in the cases with reduced visibility, the visibility in the days with reduced visibility are matched by the prediction of the fog index in the same days. Fourteen cases with reduced visibility were studied. The starting date and time and ending date and time for the 14 cases are summarized in Table 8.4.

Table 8.4 The starting date and time and ending date and time for the 14 fog cases

Case	Limits	Fog Index (High)		Reduced Visibility	
		Date	Time	Date	Time
1	Starting	01/28/2014	20:30:48	02/01/2014	0:08:44
	Ending	02/01/2014	15:03:54	02/01/2014	08:39:15
2	Starting	02/01/2014	16:15:28	02/02/2014	01:38:44
	Ending	02/02/2014	10:38:36	02/02/2014	09:23:42
3	Starting	02/02/2014	22:13:43	02/03/2014	08:15:40
	Ending	02/03/2014	10:17:52	02/03/2014	08:49:20
4	Starting	02/03/2014	19:18:26	02/04/2014	01:03:58
	Ending	02/04/2014	09:49:16	02/04/2014	09:02:02
5	Starting	02/06/2014	19:17:29	02/08/2014	22:06:16
	Ending	02/09/2014	09:50:36	02/08/2014	23:54:21
6	Starting	02/06/2014	19:17:29	02/09/2014	0:54:56

	Ending	02/09/2014	09:50:36	02/09/2014	01:35:20
7	Starting	02/11/2014	21:01:19	02/12/2014	03:21:30
	Ending	02/13/2014	04:01:13	02/12/2014	20:27:59
8	Starting	02/19/2014	19:15:05	02/20/2014	05:14:08
	Ending	02/20/2014	08:36:08	02/20/2014	06:08:00
9	Starting	02/21/2014	19:29:13	02/22/2014	02:45:28
	Ending	02/22/2014	20:24:49	02/22/2014	18:46:20
10	Starting	02/25/2014	20:41:15	02/26/2014	04:58:59
	Ending	02/27/2014	16:30:00	02/26/2014	16:41:05
11	Starting	03/03/2014	20:45:02	03/04/2014	05:54:31
	Ending	03/04/2014	10:48:00	03/04/2014	07:50:05
12	Starting	03/04/2014	19:46:19	03/05/2014	06:21:28
	Ending	03/05/2014	10:54:56	03/05/2014	09:16:43
13	Starting	03/08/2014	19:14:15	03/09/2014	0:31:55
	Ending	03/09/2014	09:29:10	03/09/2014	4:52:00
14	Starting	03/10/2014	09:43:11	03/11/2014	09:32:24
	Ending	03/11/2014	11:58:25	03/11/2014	09:59:20

From the summary of starting date and time and ending date and time for the 14 cases are in Table 8.4, we can conclude that when there is a reduced visibility the fog index is showing high fog in 100% of the cases. However, the problem is that the fog index starts to predict high fog before the visibility drops by a period of time in the range of 5 hours to 3 days and it keep showing high fog after the visibility is normal by a period of time in the range of 45 minutes to 23 hours, which means a lot of time was falsely detected as fog period.

8.2 Evaluation of the Performance of the Modified Fog Detection Algorithm

The fog detection algorithm was modified recently by PraxSoft after we identified the above problem. Therefore, the performance of the modified algorithm was evaluated again by using the same method and criteria. The total number of observations is 10493 which include the analysis period from 1/2/2014 to 04/01/2014 in the new dataset. It can be seen from Table 8.5 that the number of Type II error that the observation of good visibility was detected as high or moderate fog index in the prediction algorithm was 2058 and 2778 separately. The number of the reduced visibility detected as low fog index or none fog index was only 12 in total. The result of four performance criteria measurements was shown in Table 8.6. It then can be concluded from the results that this updated algorithm is still efficient to detect the fog days but it is still easy to make a false alarm when the day is actually clear. The total number of the observations of good visibility detected as high or moderate fog index was 4836 which consists 46.1% of all the observations. Overall, it can be seen from the Table 8.6 that the performance of the updated algorithm was much better compared to the original one.

Table 8.5 Results of observations of the updated Algorithm

	Number of observation “detected” as high fog index	**Number of observation “detected” as moderate fog index**	**Number of observation “detected” as low fog index**	**Number of observation “detected” as none fog index**
Number of reduced visibility(<2000)	132	177	3	9
Number of good visibility(>=2000)	2058	2778	2546	2790
	2190	2955	2549	2799

Table8.6 comparison of four performance criteria measurements for two algorithm

Criteria	Original algorithm	Modified algorithm
FDR (smaller is better)	**0. 4%**	**0. 32%**
FNR (smaller is better)	**57.5%**	**19.6%**
SENS (larger is better)	**13.2%**	**52.4%**
SPEC (larger is better)	**97.2%**	**96.2%**

Next, in order to further validate the predictions of the fog index in the cases with reduced visibility, the visibility in the days with reduced visibility are matched by the prediction of the fog index in the same days. Fifteen cases with reduced visibility were studied. The starting date and time and ending date and time for the 15 cases are summarized in Table 8.7.

Table 8.7 The starting date and time and ending date and time for the 15 fog cases

Case	Limits	Fog Index (High or moderate)		Reduced Visibility	
		Date	Time	Date	Time
1	Starting	01/28/2014	20:30:48	02/01/2014	0:08:44
	Ending	02/01/2014	12:40:48	02/01/2014	08:39:15
2	Starting	02/01/2014	17:21:00	02/02/2014	01:38:44
	Ending	02/02/2014	10:58:36	02/02/2014	09:23:42
3	Starting	02/02/2014	22:13:43	02/03/2014	08:15:40
	Ending	02/03/2014	9:30:14	02/03/2014	08:49:20
4	Starting	02/03/2014	19:28:22	02/04/2014	01:03:58
	Ending	02/04/2014	09:31:25	02/04/2014	09:02:02
5	Starting	02/06/2014	19:29:21	02/08/2014	22:06:16
	Ending	02/09/2014	08:45:19	02/08/2014	23:54:21
6	Starting	02/06/2014	19:19:21	02/09/2014	0:54:56
	Ending	02/09/2014	08:45:19	02/09/2014	01:35:20

7	Starting	02/11/2014	21:01:19	02/12/2014	03:21:30
	Ending	02/12/2014	09:40:38	02/12/2014	09:18:55
8	Starting	02/19/2014	19:21:02	02/20/2014	05:14:08
	Ending	02/20/2014	08:00:29	02/20/2014	06:08:00
9	Starting	02/21/2014	21:40:12	02/22/2014	02:45:28
	Ending	02/22/2014	20:24:49	02/22/2014	18:46:20
10	Starting	02/25/2014	22:45:52	02/26/2014	04:58:59
	Ending	02/26/2014	09:08:42	02/26/2014	08:00:47
11	Starting	03/03/2014	22:43:53	03/04/2014	05:54:31
	Ending	03/04/2014	09:13:12	03/04/2014	07:50:05
12	Starting	03/04/2014	20:33:54	03/05/2014	06:21:28
	Ending	03/05/2014	10:07:19	03/05/2014	09:16:43
13	Starting	03/08/2014	19:26:42	03/09/2014	0:31:55
	Ending	03/09/2014	08:53:32	03/09/2014	4:52:00
14	Starting	03/10/2014	23:25:12	03/11/2014	09:32:24
	Ending	03/11/2014	09:52:28	03/11/2014	09:59:20
15	Starting	03/18/2014	20:19:12	03/19/2014	03:57:24
	Ending	03/19/2014	09:03:28	03/19/2014	07:49:20

From the summary of starting date and time and ending date and time for the 15 cases are in Table 8.7, we can conclude that when there was a reduced visibility the fog index showed high fog or at least moderate index in 100% of the cases before the fog began. In most cases, the fog index starts to predict high or moderate fog before the visibility drops by a period of several hours and it keeps showing high or moderate fog index for several hours after the visibility is back to normal. There are only three cases that the fog index starts to predict high or moderate fog before the visibility drops by a period of three days, which is not so accurate for the prediction. Overall, it also can be seen from the analysis of these detailed fog cases that the performance of modified algorithm is much better compared to the original one, but still need much adjustment and validation.

8.3 Chapter Summary

The chapter mainly evaluated the performance of the fog detection algorithm developed by PraxSoft. Four measures: False Discovery Rate, False Negative Rate, Sensitivity and Specificity were used as performance criteria to evaluate the relative performances of the fog detection algorithm. A comparison of original and modified fog detection algorithm was presented in the chapter and it can be seen that the performance of modified algorithm is much better compared to the original one. The modified algorithm is efficient to detect the fog days but the percentage of making a false alarm when the day is actually clear is still a little bit high.

9. FURTHER EXPLORATION OF THE RELATIONSHIP BETWEEN TRAFFIC PARAMETERS AND REDUCED VISIBILITY

The matched case control logistic regression models were used in this section to further explore the relationship between reduced visibility and traffic flow characteristics. The results may help in monitoring the reduced visibility in real time and reducing the negative effects of reduced visibility accordingly by sending warning messages to the motorists. The main objective of this study is to quantify the relationship between traffic flow characteristics and visibility and therefore we may be able to determine the change of visibility levels only by using traffic flow parameters. The advantage of using this conditional logistic regression models is to better explore the relationship between traffic flow variables and visibility while controlling the effect of other confounding variables such as location, time and the geometric design elements of highway sections (i.e., horizontal and vertical alignments).

9.1 Data Preparation of Polk County

Similar to the datasets used for the aforementioned analysis of impact of reduced visibility on traffic flow characteristics, the combined dataset was composed of two components which include the traffic data and weather data for the whole Polk County.

9.1.1 Weather Data

There are two airports in Polk County. One is Bartow Municipal airport and the other is Lakeland Linder Regional airport. The location of two airports was identified and we draw two buffer circles based on the center of these two airports. The weather condition in one circle was considered as the same and the weather information was obtained from the weather reports for these two airports. The radius of the circle is 5 miles. Figure 9.1

shows the location of these two airports and Figures 9.2 and 9.3 show the sample of weather data in these two airports. There are twenty variables in total for the weather report which includes visibility, wind speed and some other important weather related variables.

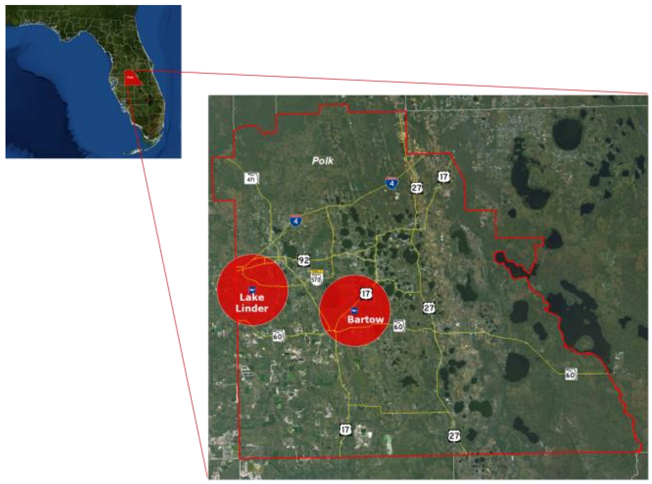

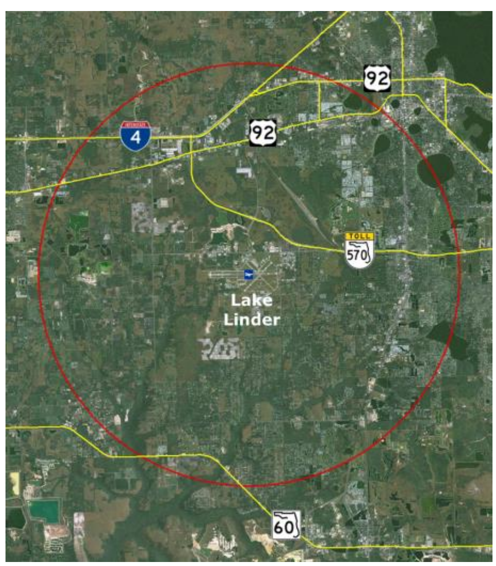

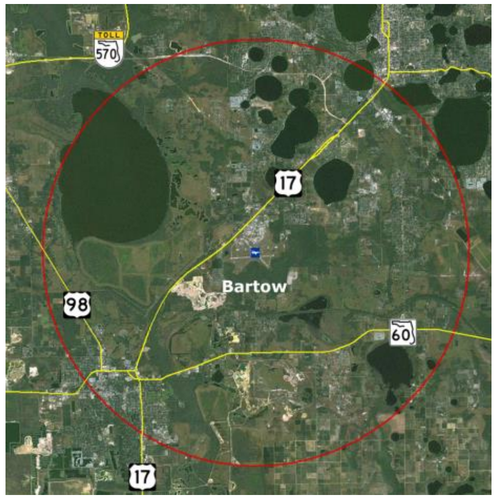

Figure 9.1 Location of two airports in Polk County

U.S. Department of Commerce
National Oceanic & Atmospheric Administration

QUALITY CONTROLLED LOCAL CLIMATOLOGICAL DATA
(final)
HOURLY OBSERVATIONS TABLE
BARTOW MUNICIPAL AIRPORT (12809)
BARTOW, FL
(01/2014)

National Climatic Data Center
Federal Building
151 Patton Avenue
Asheville, North Carolina 28801

Elevation: 125 ft. above sea level
Latitude: 27.95
Longitude: -81.783
Data Version: VER2

Date	Time (LST)	Station Type	Sky Conditions	Visibility (SM)	Weather Type	Dry Bulb Temp (F)	Dry Bulb Temp (C)	Wet Bulb Temp (F)	Wet Bulb Temp (C)	Dew Point Temp (F)	Dew Point Temp (C)	Rel Humd %	Wind Speed (MPH)	Wind Dir	Wind Gusts (MPH)	Station Pressure (in. hg)	Press Tend	Net 3-hr Chg (mb)	Sea Level Pressure (in. hg)	Report Type	Precip. Total (in)	Alti-meter (in. hg)
1	2	3	4	5	6	7	8	9	10	11	12	13	14	15	16	17	18	19	20	21	22	23
01	0015	0	SCT100	10.00		61	16.0	55	12.8	50	10.0	67	5	030		30.12			M	AA		30.26
01	0035	0	BKN100	10.00		61	16.0	55	12.8	50	10.0	67	8	020		30.14			M	AA		30.27
01	0055	0	SCT100	10.00		61	16.0	56	13.3	52	11.0	72	7	040		30.12			M	AA		30.26
01	0115	0	SCT090	10.00		61	16.0	56	13.3	52	11.0	72	8	020		30.12			M	AA		30.26
01	0135	0	OVC090	10.00		61	16.0	56	13.3	52	11.0	72	6	040		30.11			M	AA		30.25
01	0155	0	FEW070 OVC090	10.00		61	16.0	56	13.3	52	11.0	72	7	010		30.11			M	AA		30.25
01	0215	0	BKN070 BKN090	10.00		59	15.0	55	12.8	52	11.0	78	8	030		30.10			M	AA		30.24
01	0235	0	FEW047 SCT070 BKN090	10.00	-RA	59	15.0	56	13.4	54	12.0	84	7	020		30.10			M	AA		30.24
01	0255	0	BKN090	10.00		59	15.0	56	13.4	54	12.0	84	9	030		30.10			M	AA		30.24
01	0315	0	BKN090	10.00		59	15.0	56	13.4	54	12.0	84	6	020		30.11			M	AA		30.25
01	0335	0	FEW070 BKN090	10.00		59	15.0	56	13.4	54	12.0	84	8	030		30.10			M	AA		30.24
01	0355	0	FEW070 BKN090	10.00		59	15.0	57	13.7	55	13.0	87	8	030		30.10			M	AA		30.24
01	0415	0	FEW031 BKN070 OVC090	10.00		59	15.0	57	13.7	55	13.0	87	9	020		30.10			M	AA		30.24
01	0435	0	OVC070	10.00		57	14.0	55	12.9	54	12.0	90	7	020		30.10			M	AA		30.24
01	0455	0	SCT070 BKN085	10.00		57	14.0	56	13.2	55	13.0	93	9	020		30.09			M	AA		30.23
01	0515	0	BKN085	10.00		57	14.0	55	12.9	54	12.0	90	10	030	16	30.09			M	AA		30.23
01	0535	0	BKN070 BKN085	10.00		57	14.0	55	12.9	54	12.0	90	11	020		30.09			M	AA		30.23
01	0555	0	OVC070	10.00	-DZ	57	14.0	55	12.9	54	12.0	90	13	020	18	30.10			M	AA		30.24
01	0615	0	SCT033 OVC070	10.00		57	14.0	56	13.2	55	13.0	93	10	030		30.10			M	AA		30.24
01	0750	0	SCT020 OVC060	5.00	-RA	57	14.0	56	13.2	55	13.0	93	8	040		30.11			M	AA		30.25
01	0850	0	SCT017 OVC023	3.00	-RA	57	14.0	57	13.8	57	14.0	100	8	030		30.11			M	AA		30.25
01	0955	0	SCT013 OVC025	10.00		59	15.0	59	15.0	59	15.0	100	8	030		30.12			M	AA		30.26
01	1050	0	SCT013 OVC023	10.00		61	16.0	61	16.1	61	16.0	100	7	020		30.12			M	AA		30.26
01	1247	0	BKN006 OVC023	8.00		63	17.0	M	M	M	M	M	8	040		30.06			M	AA		30.20
01	1350	0	OVC006	10.00		63	17.0	63	17.2	63	17.0	100	5	040		30.02			M	AA		30.16
01	1435	0	OVC005	10.00		64	18.0	64	17.7	64	18.0	100	8	030		30.01			M	AA		30.15
01	1450	0	CLR005	10.00		63	17.0	M	M	63	17.0	M	6	010		M			M	AA		30.15
01	1455	0	OVC005	10.00		63	17.0	63	17.2	63	17.0	100	5	020		30.01			M	AA		30.15

Figure 9.2 Weather data at Bartow Airport

U.S. Department of Commerce
National Oceanic & Atmospheric Administration

QUALITY CONTROLLED LOCAL
CLIMATOLOGICAL DATA
(final)
HOURLY OBSERVATIONS TABLE
LAKELAND LINDER REGIONAL AIRPORT (12883)
LAKELAND, FL
(01/2014)

National Climatic Data Center
Federal Building
151 Patton Avenue
Asheville, North Carolina 28801

Elevation: 142 ft. above sea level
Latitude: 28
Longitude: -82.05
Data Version: VER2

Date	Time (LST)	Station Type	Sky Conditions	Visibility (SM)	Weather Type	Dry Bulb Temp (F)	Dry Bulb Temp (C)	Wet Bulb Temp (F)	Wet Bulb Temp (C)	Dew Point Temp (F)	Dew Point Temp (C)	Rel Humd %	Wind Speed (MPH)	Wind Dir	Wind Gusts (MPH)	Station Pressure (in. hg)	Press Tend	Net 3-hr Chg (mb)	Sea Level Pressure (in. hg)	Report Type	Precip. Total (in)	Alti-meter (in. hg)
1	2	3	4	5	6	7	8	9	10	11	12	13	14	15	16	17	18	19	20	21	22	23
01	0015	0	OVC100	10.00		59	15.0	53	11.7	48	9.0	67	8	040		30.12			M	AA		30.27
01	0035	0	OVC100	10.00		59	15.0	53	11.7	48	9.0	67	7	020		30.11			M	AA		30.26
01	0055	0	SCT070 OVC100	10.00		59	15.0	54	12.3	50	10.0	72	8	030		30.11			M	AA		30.26
01	0115	0	OVC090	10.00		59	15.0	54	12.3	50	10.0	72	7	040		30.11			M	AA		30.26
01	0135	0	OVC090	10.00		59	15.0	54	12.3	50	10.0	72	6	030		30.10			M	AA		30.25
01	0155	0	OVC090	10.00	-RA	59	15.0	55	12.8	52	11.0	78	6	020		30.10			M	AA		30.25
01	0215	0	OVC090	10.00		59	15.0	55	12.8	52	11.0	78	7	030		30.09			M	AA		30.24
01	0235	0	OVC090	10.00		59	15.0	55	12.8	52	11.0	78	7	040		30.09			M	AA		30.24
01	0255	0	SCT070 OVC090	10.00		57	14.0	54	12.3	52	11.0	83	9	030		30.09			M	AA		30.24
01	0315	0	SCT070 OVC090	10.00		59	15.0	55	12.8	52	11.0	78	8	030		30.09			M	AA		30.24
01	0335	0	SCT070 OVC090	10.00		59	15.0	55	12.8	52	11.0	78	9	030		30.09			M	AA		30.24
01	0355	0	OVC090	10.00		59	15.0	55	12.8	52	11.0	78	9	020		30.09			M	AA		30.24
01	0415	0	BKN080 OVC090	10.00		59	15.0	55	12.8	52	11.0	78	7	020		30.09			M	AA		30.24
01	0435	0	OVC080	10.00		59	15.0	55	12.8	52	11.0	78	10	030		30.09			M	AA		30.24
01	0455	0	SCT070 OVC080	10.00		59	15.0	56	13.4	54	12.0	84	9	030		30.08			M	AA		30.23
01	0515	0	OVC080	10.00	-DZ	57	14.0	55	12.9	54	12.0	90	9	020		30.09			M	AA		30.24
01	0535	0	BKN075 OVC085	10.00		57	14.0	54	12.3	52	11.0	83	11	030		30.08			M	AA		30.23
01	0555	0	BKN075 OVC085	10.00	-RA	57	14.0	55	12.9	54	12.0	90	10	030		30.09			M	AA		30.24
01	0645	0	BKN038 OVC075	10.00	-RA	57	14.0	55	12.9	54	12.0	90	10	030		30.09			M	AA		30.24
01	0755	0	SCT035 OVC065	10.00	DZ	59	15.0	57	13.7	55	13.0	87	8	040		30.10			M	AA		30.25
01	0845	0	SCT015 BKN037 OVC046	5.00	DZ	59	15.0	57	13.7	55	13.0	87	7	060		30.11			M	AA		30.26
01	0950	0	SCT007 OVC028	5.00	DZ	59	15.0	59	15.0	59	15.0	100	8	030		30.11			M	AA		30.26
01	1050	0	BKN007 OVC020	4.00	DZ	61	16.0	61	16.1	61	16.0	100	10	030		30.10			M	AA		30.25
01	1150	0	OVC005	4.00	-RA	61	16.0	61	16.1	61	16.0	100	9	030		30.08			M	AA		30.23
01	1255	0	OVC005	5.00	BR	63	17.0	63	17.2	63	17.0	100	10	030		30.03			M	AA		30.18
01	1354	0	OVC005	6.00	BR	63	17.0	63	17.2	63	17.0	100	5	020		30.01			M	AA		30.16
01	1454	0	OVC007	6.00	BR	63	17.0	63	17.2	63	17.0	100	8	040		30.00			M	AA		30.15
01	1550	0	OVC007	7.00		64	18.0	63	17.4	63	17.0	97	9	050		29.98			M	AA		30.13
01	1650	0	OVC007	7.00		64	18.0	63	17.4	63	17.0	97	9	030		29.98			M	AA		30.13
01	1750	0	OVC003	4.00	BR	63	17.0	63	17.2	63	17.0	100	10	030		29.98			M	AA		30.13

Figure 9.3 Weather data at Lakeland Airport

9.1.2 Traffic Data

Traffic flow data used in this study were collected from the RITIS system which is shown in Figure 9.4. There are over 10000 loop detectors for the whole Florida State and we collected traffic data information from the 60 detectors which are located in Polk County and also within those circles of two airports close to the Polk County. In this way the extracted traffic data can be merged with weather data mentioned above to create the combined dataset. There are fifteen detectors of them within the buffer circle of Barton airport and forty-five detectors of them within the circle of Lakeland airport.

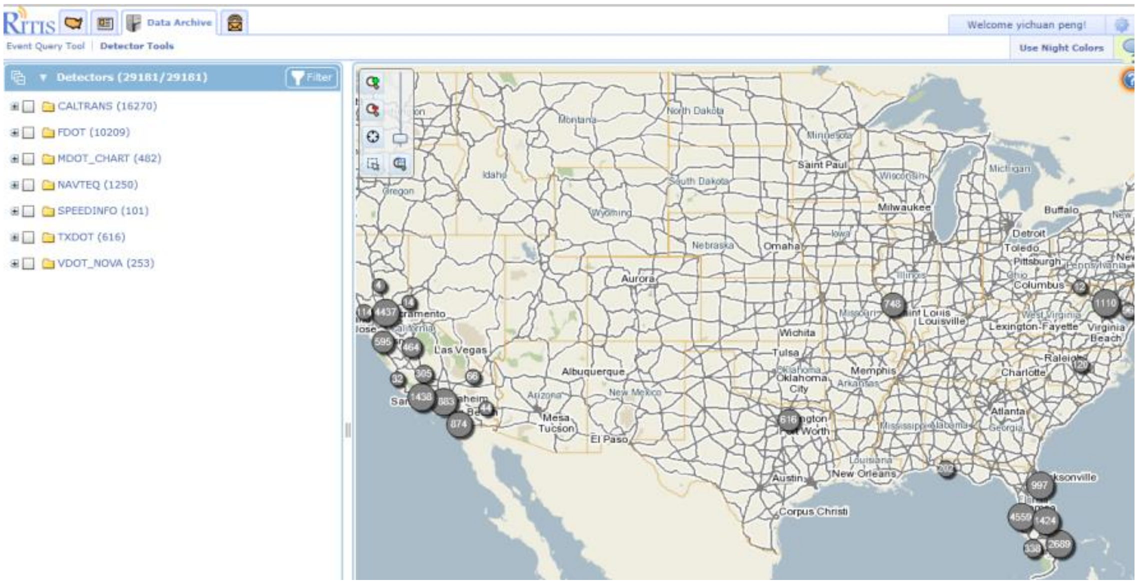

Figure 9.4 Data of All detectors in RITIS

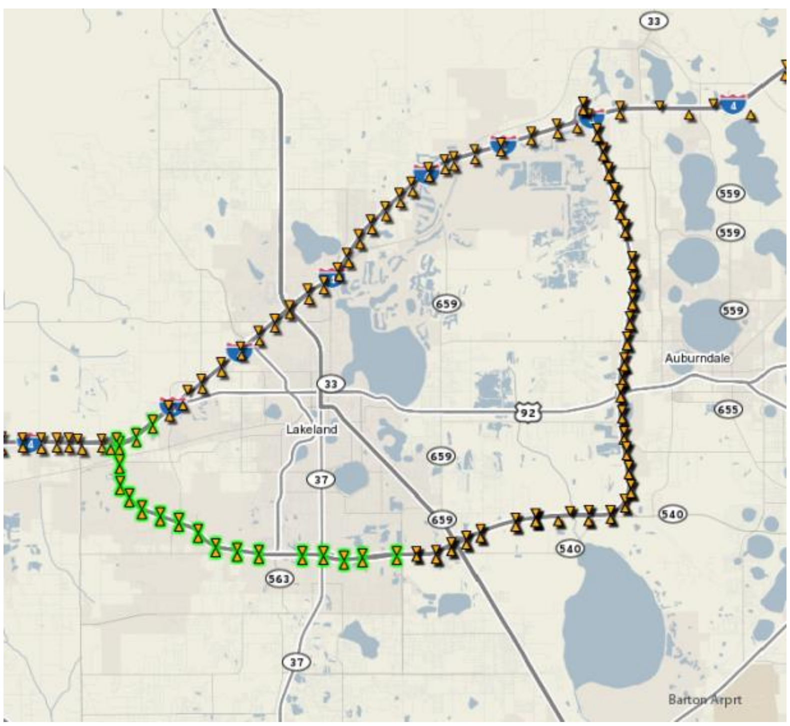

Figure 9.5 (a) 45 detectors within five miles of Lakeland airport in Polk County

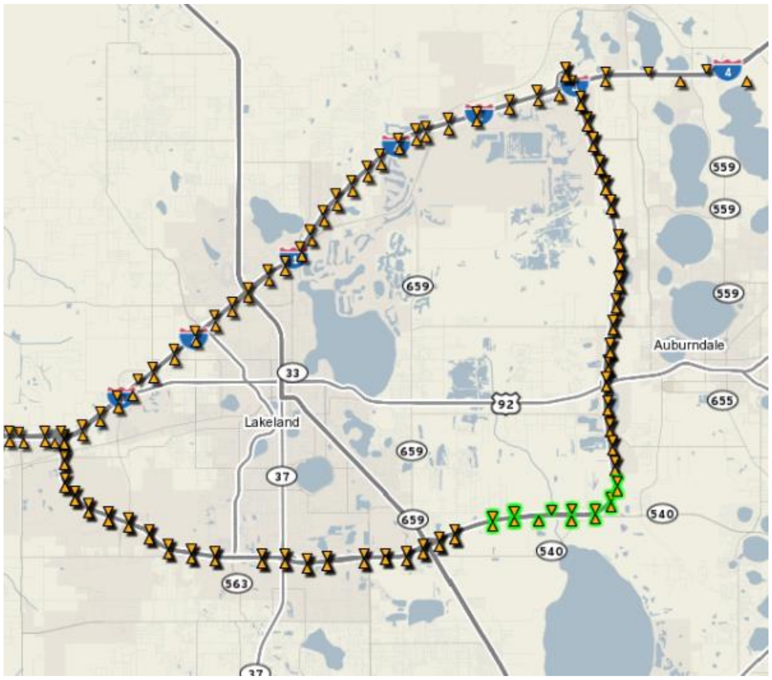

(b) 15 detectors within five miles of Bartow airport in Polk County

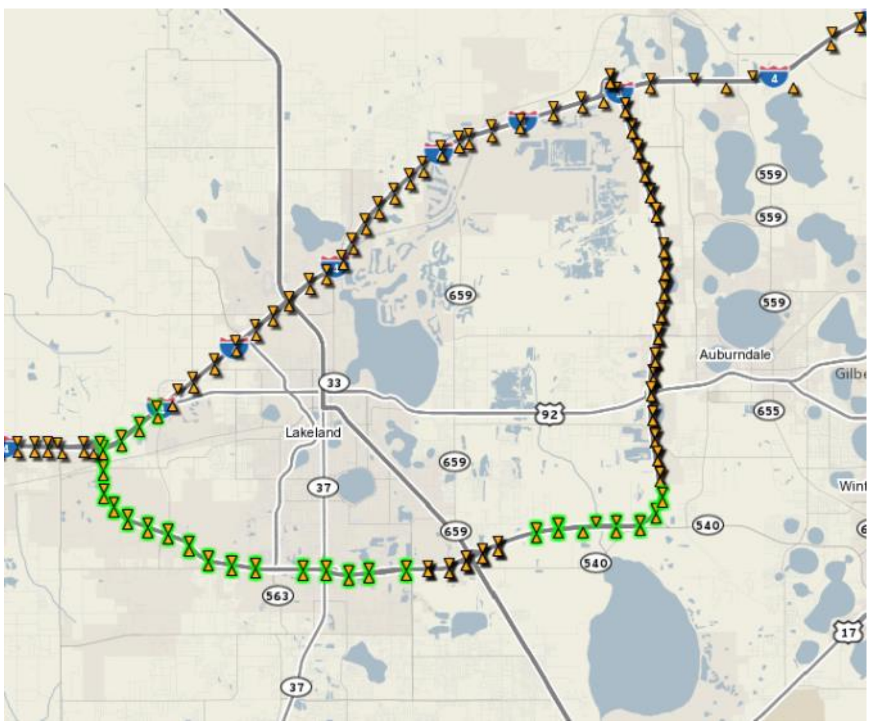

Figure 9.6 60 detectors within five miles of two airports in Polk County

Figure 9.7 shows the original raw traffic dataset which contains the following traffic flow variables: every 1 minute for each lane in each direction: 1) average speed 2) volume and 3) lane occupancy (percentage of time interval, 1 minute, the loop detector was occupied).

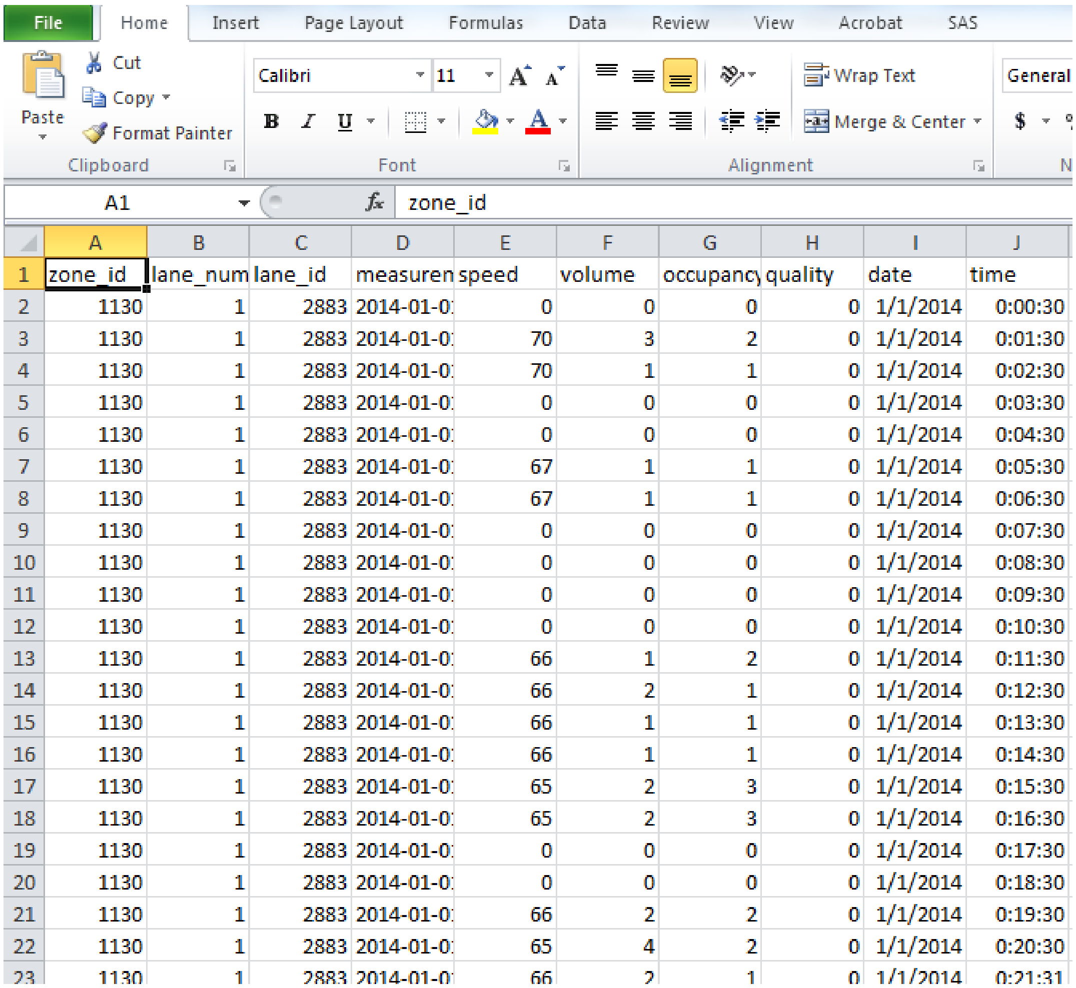

	A	B	C	D	E	F	G	H	I	J
1	zone_id	lane_num	lane_id	measuren	speed	volume	occupancy	quality	date	time
2	1130	1	2883	2014-01-0	0	0	0	0	1/1/2014	0:00:30
3	1130	1	2883	2014-01-0	70	3	2	0	1/1/2014	0:01:30
4	1130	1	2883	2014-01-0	70	1	1	0	1/1/2014	0:02:30
5	1130	1	2883	2014-01-0	0	0	0	0	1/1/2014	0:03:30
6	1130	1	2883	2014-01-0	0	0	0	0	1/1/2014	0:04:30
7	1130	1	2883	2014-01-0	67	1	1	0	1/1/2014	0:05:30
8	1130	1	2883	2014-01-0	67	1	1	0	1/1/2014	0:06:30
9	1130	1	2883	2014-01-0	0	0	0	0	1/1/2014	0:07:30
10	1130	1	2883	2014-01-0	0	0	0	0	1/1/2014	0:08:30
11	1130	1	2883	2014-01-0	0	0	0	0	1/1/2014	0:09:30
12	1130	1	2883	2014-01-0	0	0	0	0	1/1/2014	0:10:30
13	1130	1	2883	2014-01-0	66	1	2	0	1/1/2014	0:11:30
14	1130	1	2883	2014-01-0	66	2	1	0	1/1/2014	0:12:30
15	1130	1	2883	2014-01-0	66	1	1	0	1/1/2014	0:13:30
16	1130	1	2883	2014-01-0	66	1	1	0	1/1/2014	0:14:30
17	1130	1	2883	2014-01-0	65	2	3	0	1/1/2014	0:15:30
18	1130	1	2883	2014-01-0	65	2	3	0	1/1/2014	0:16:30
19	1130	1	2883	2014-01-0	0	0	0	0	1/1/2014	0:17:30
20	1130	1	2883	2014-01-0	0	0	0	0	1/1/2014	0:18:30
21	1130	1	2883	2014-01-0	66	2	2	0	1/1/2014	0:19:30
22	1130	1	2883	2014-01-0	65	4	2	0	1/1/2014	0:20:30
23	1130	1	2883	2014-01-0	66	2	1	0	1/1/2014	0:21:31

Figure 9.7 Sample of traffic data for the Polk County

Finally, a merged dataset consisting of both traffic data and visibility data was created to be applied into matched case control logistic regression models. Since the one minute raw traffic data was noticed to have random noise and are difficult to work with in a modeling framework (Abdel-Aty et al. 2008), therefore, the raw data were aggregate into 5-

minutes levels to obtain averages and standard deviations for speed, volume, and occupancy.

9.2 Methodology

As already mentioned at the beginning of this chapter, the matched case control logistic regression model was applied in this study to further explore the relationship between visibility and traffic flow characteristics. In this study, observations with reduced visibility are selected first. Then, for each selected observation, some non-traffic flow variables associated with each fog are selected as matching factors. In this study the variables used to match cases and controls are: location, day of the week and time of reduced visibility. Using these matching factors, a total of non-fog cases are then selected randomly from each subpopulation of non-fog cases.

Matched case-control logistic regression has been adopted in epidemiological studies. In addition, it was used in few transportation related studies such as Abdel-Aty et al. (2004). The detailed description of the modeling can be seen in Abdel-Aty et al. (2004). The data of all corresponding reduced visibility were extracted from the combined dataset and a total of three times of observations with good visibility were randomly selected from the combined dataset. The final created datasets were then applied with matched case logistic regression models. In this study, SAS package (procedure PHREG) was used to fit the proposed stratified conditional logistic regression model, widely known as matched case-control analysis in epidemiological studies (the reader is referred to SAS Institute Inc, 2008).

9.3 Modeling Results

The following five traffic flow variables: mean speed and headway, variance of speed and headway and average occupancy in five minutes were used as input in the model. It is noted that the headway data was calculated based on the volume in one minute. The visibility was divided into two levels: the visibility level was considered as 0 for the good visibility (>=1Statue Mile(SM)) and the visibility level was classified as 1 for the reduced visibility(<1(SM)). The modeling result was show in the Table 9.1.

Table 9.1: Modeling results for two visibility levels

Analysis of Maximum Likelihood Estimates						
Parameter	**DF**	**Parameter Estimate**	**Standard Error**	**Chi-Square**	**Pr > ChiSq**	**Hazard Ratio**
speed	1	-0.03708	0.00993	13.9293	0.0002	0.964
Speed standard deviation	1	0.01618	0.00533	9.2011	0.0024	1.016
headway	1	0.02940	0.00486	36.6278	<.0001	1.030
Headway standard deviation	1	0.22346	0.06713	11.0810	0.0009	1.250
Average Occupancy	1	0.00716	0.00357	4.0209	0.0449	1.007

The results indicated that higher mean of headway, variance of speed and headway and higher occupancy were related to the increase of the likelihood of a reduced visibility while lower mean speed was related to the increase of the likelihood of a reduced visibility.

After that, the visibility was further divided into three levels to further investigate the relationship between traffic flow characteristics and visibility. The visibility level was considered as 0 for the good visibility (>=1(SM)) and the visibility level was classified as 1 for the moderate visibility (0.25(SM)<=visibility<1 (SM)) and the visibility level was classified as 2 for the low visibility (visibility<0.25).The modeling result was shown in the Table 9.2:

Table 9.2 Modeling results for three visibility levels

Parameter	DF	Parameter Estimate	Standard Error	Chi-Square	Pr > ChiSq	Hazard Ratio
speed	1	-0.03857	0.01075	12.8625	0.0003	0.962
Speed standard deviation	1	0.02152	0.00602	12.7908	0.0003	1.021
headway	1	0.03039	0.00497	37.4117	<.0001	1.031
Headway standard deviation	1	0.30653	0.07281	17.7224	<.0001	1.359
Average Occupancy	1	0.00594	0.00374	2.5189	0.1125	1.006

Similar results indicated that higher mean of headway, variance of speed and headway were related to the increase of the likelihood of a reduced visibility while lower mean speed was related to the increase of the likelihood of a reduced visibility. The relationship between average occupancy and visibility was not significant in this result.

9.4 Chapter Summary

This chapter applied matched case control logistic regression models to the combined traffic and weather datasets for the Polk County. The variables used to match cases and controls are: location, day of the week and time of reduced visibility. The results indicated that higher mean of headway, variance of speed and headway were related to the increase of the likelihood of a reduced visibility while lower mean speed was related to the increase of the likelihood of a reduced visibility.

10. CONCLUSIONS

In summary, there are several major conclusions based on the analyses above:

1. An array of low-cost environmental sensors, arranged at varying levels above the ground surface, could effectively detect the onset of fog and meet or exceed existing performance of traditional and much more expensive technologies. A combination of sensors and software algorithms were developed to detect and provide the basis to predict the onset of fog.

2. Several most important weather parameters were analyzed and it is concluded that fog is most likely to form when the values of humidity and subsurface moisture are higher. It is also more likely to form fog when the wind speed is lower and the air temperature is more close to the dew point.

3. The mean headway and headway variation are significantly higher while the mean speed and volume are significantly lower in fog case compared to clear case based on the analysis of one fog case in the morning. There isn't significant difference in speed variation in both cases.

4. It is shown from scatter plot analysis that the relationship between speed and headway as well as the relationship between speed and volume is different in fog case compared to the pattern in clear case. It is meaningful to conduct more scatter plot analysis in further to figure out the relationship of this traffic flow characteristics under fog situations.

5. The impact of reduced visibility on passenger cars is more significant compared to trucks. The mean headway, variation of headway and speed are significantly higher while the mean speed is significantly lower in the fog case compared to the clear case for the cars. In comparison, there isn't significant difference in the mean headway for the trucks and there isn't significant difference in the standard deviation of speed and headway lower in the fog case compared to the clear case for the trucks.

6. It also can be concluded that the differences of mean of headway, speed and standard deviation of headway and are all significant under different visibility levels. The mean of headway will increase when the visibility drops. The mean speed will decrease when the visibility drops. The mean of standard deviation of headway will increase when the visibility drops.

7. The distribution of traffic flow characteristics is very similar in both directions and the effect of reduced visibility on both directions is also similar. The effects of reduced visibility on different lanes are different. For the outer lane, the mean speeds under good visibility level and moderate visibility level are both significantly higher than mean speed under low visibility level. The difference of mean speed under good visibility level and moderate visibility level is not significant the mean headway under good visibility level are significantly higher than both mean headways under low visibility level and moderate visibility level. The difference of mean headway under low visibility level and moderate visibility level is not significant. For the middle lane, the mean speeds will increase as the visibility increases. The mean headway increases as the visibility drops and the mean

headway under good visibility level are significantly higher than both mean headways under low visibility level and moderate visibility level. The difference of mean headway under low visibility level and moderate visibility level is not significant. For the inner lane, the mean speeds under good visibility level and moderate visibility level are both significantly higher than mean speed under low visibility level. The difference of mean speed under good visibility level and moderate visibility level is not significant. The mean headway will decrease as the visibility increases.

8. Hazard-based duration model is appropriate to model fog duration time and its influenced factors. The lognormal distribution model gives the best description of fog duration without covariates. The log-logistic model gives the best description of fog duration with covariates. The increase of "humidity", "barometric_pressure" and "subsurface_moisture" would increase the fog duration time. Meanwhile, the increase of "wind_speed" and "solar_radiation" would decrease the fog duration time.

9. As for the evaluation of the fog detection algorithm, the updated algorithm is efficient to detect the fog days but it is still likely to make a false alarm when the day is actually clear. Overall, the performance of the updated algorithm was much better compared to the original one and it can be used to detect almost all the fog cases.

10. The matched case control logistic regression model was used to further explore the relationship between traffic flow characteristics and different visibility levels. The results indicated that higher mean of headway, variance of speed and headway and higher

occupancy were related to the increase of the likelihood of a reduced visibility while lower mean speed was related to the increase of the likelihood of a reduced visibility.

The following are some directions for future research:

It is important to further modify the fog detection algorithm to develop a more accurate model to describe the relationship between weather parameters and visibility and to predict the fog formation.

In addition, there may be some other statistical methods such as time-series modellings can be applied to further explore the relationship between reduced visibility and traffic flow characteristics. It is also meaningful to compare the effect of fog with other weather types such as rain or smog on traffic flow characteristics.

Moreover, it is important to investigate the effect of reduced visibility on traffic crashes.

After that, the similar analysis can also be expanded to the whole state to get a more comprehensive and generalized results which can be applied to the whole state for different kinds of road segments and traffic flow conditions since both weather data and traffic data for the whole state were collected by our research team.

REFERENCES

Abdel-Aty, M., Uddin, N., Abdalla, F., Pande, A., and Hsia, L. (2004). Predicting freeway crashes based on loop detector data using matched case–control logistic regression.*Transportation Research Record*, 1897, 88–95.

Abdel-Aty, M., Ahmed, M., Lee, J., Shi, Q., and Abuzwidah, M. (2012a) Synthesis of Visibility Detection Systems. (FDOT Report BDK 78 977-11) University of Central Florida.

Abdel-Aty, M., Hassan, H., Ahmed, M., and Al-Ghamdi, A.S. (2012b) Real-time prediction of visibility related crashes. *Transportation Research Part C*: Emerging Technologies, 24, 288-298.

Alfelor, R., Billot, R., El Faouzi, N., and Pisano, P. (2013) Approaches and Gaps in Weather-Responsive Traffic Management: US and European Perspectives. Transportation Research Board 92nd Annual Meeting.

Akin, D., Sisiopiku, V., and Skabardonis, A. (2011). Impacts of weather on traffic flow characteristics of urban freeways in Istanbul. *Procedia-Social and Behavioral Sciences*, 16, 89-99.

Ali, O., Al-Harthei, H., and Garib, A. (2013) Real-Time Fog Warning System for the Abu Dhabi Emirate (UAE). *Journal of Traffic and Logistics Engineering*, 1, 213-217.

Babari, R., Hautière, N., Dumont, É., Paparoditis, N., and Misener, J. (2012) Visibility monitoring using conventional roadside cameras–Emerging applications. *Transportation Research Part C*: Emerging Technologies, 22, 17-28.

Berg, P., Arentze T., Timmermans H. A latent class accelerated hazard model of social activity duration. *Transportation Research Part A*, 2012, 46(1): 12-21.

Bhat, C. A generalized multiple durations proportional hazard model with an application to activity behavior during the evening work-to-home commute. *Transportation Research Part B*, 1996, 30(6): 465-480.

Bhat, C., Frusti, T., Zhao, H., Schonfelder S, Axhausen K W. Intershopping duration: an analysis using multiweek data. *Transportation Research Part B*, 2004, 38(1): 39-60.

Billot, R., El Faouzi, N., Sau, J., and De Vuyst, F. (2010) Integrating the Impact of Rain into Traffic Management. Transportation Research Record: *Journal of the Transportation Research Board*, 2169, 141-149.

Chang, H., Yeh, T. Exploratory analysis of motorcycle holding time heterogeneity using a split-population duration model. *Transportation Research Part A*, 2007, 41(6): 587-596.

Chen, C., Niemeier, D. A mass point vehicle scrappage model. *Transportation Research Part B*, 2005, 39(5): 401-415.

Chung, Y. Development of an accident duration prediction model on the Korean Freeway Systems. *Accident Analysis and Prevention*, 2010, 42(1): 282-289.

Chan, P. (2013) Short-term climatology and performance of lidar-based visibility map at the Hong Kong International Airport. *International Journal of Remote Sensing*, 34, 956-967.

Guo, H., Gao, Z., Yang, X., Zhao, X. and Wang, W. Modeling travel time under influence of on-street parking, *Journal of Transportation Engineering*, 2012, 138(2): 229-235.

Hassan, H. and Abdel-Aty, M. (2013) Predicting reduced visibility related crashes on freeways using real-time traffic flow data. *Journal of Safety Research*, 45, 29-36.

Hassan H., Abdel-Aty M. and Oloufa, A. (2011a). The effect of warning messages and variable speeds in different visibility conditions. Transportation Research Board,90th Annual Meeting Compendium of Papers, paper no. 11-0354

Hassan, H. and Abdel-Aty, M. (2011b) Analysis of drivers' behavior under reduced visibility conditions using a Structural Equation Modeling approach. *Transportation Research Part F*: Traffic Psychology and Behaviour, 14, 614-625.

Hou, T., Mahmassani, H.S., Alfelor, R., Kim, J. and Saberi, M. (2013) Calibration of Traffic Flow Models under Adverse Weather and Application in Mesoscopic Network Simulation Procedures. Transportation Research Board 92nd Annual Meeting, .

Jomaa, D., Yella, S., and Dougherty, M. (2013) Review of the effectiveness of vehicle activated signs. *Journal of Transportation Technologies*, 3, 123-130.

Knupp, K. "Chapter 7: Common Thermodynamic Processes in the Atmosphere". *University of Alabama National Space Science and Technology Center. n.d.* Web. 19 March 2014

Lee, B. and Timmermans, H. A latent class accelerated hazard model of activity episode durations, *Transportation Research Part B*, 2007, 41(4): 426-447.

Lee, E., Wang, J. *Statistical Methods for Survival Data Analysis*, John Wiley & Sons, Inc., New York, 2003.

Leviäkangas, P., Öörni, R., Hautala, R., Rossa, A., Zardini, F., and Domenichini, F. (2010) Fog warning system in Venice region. Proceedings of the 17th World Congress on ITS, 25-29.

Lindqvist, H., Kiuru, J., Parikka, J., Vilkman, A., Jankó, D., Zardini, F., Dubbert, J., FMI, M.H., FMI, I.J., and Luoto, M. (2009) D6. 1 Pilot Specifications, ROADIDEA 215455 Deliverable.

Miranda-Moreno, L., 2006. Statistical models and methods for the identification of hazardous locations for safety improvements. Ph.D. Dissertation, Department of Civil Engineering, University of Waterloo, Canada.

Maze, T., Agarwai, M. and Burchett, G. (2006) Whether weather matters to traffic demand, traffic safety, and traffic operations and flow. *Transportation Research Record*, 1948, 170-176.

Mueller, A., Trick, L. (2012) Driving in fog: The effects of driving experience and visibility on speed compensation and hazard avoidance. *Accident Analysis & Prevention*, 48, 472-479.

Murphy, R., Swick, R., Hamilton, B., and Guevara, G. (2012) Best Practices for Road Weather Management, FHWA-HOP-12-046, Washington DC.

Ni, R., Nguyen, B. and Zhuo, Y. (2013) Age-related difference in steering control under reduced visibility conditions. *Displays*, 34, 120-124.

Nam, D. and Mannering F. An exploratory hazard-based analysis of highway incident. *Transportation Research Part A*, 2000, 34(2): 85-102.

Paselk, T. and Mannering F. Use of duration models for predicting vehicular delay at US/Canadian border crossing. *Transportation*, 1994, 21: 249-270.

Royston, P. Explained variation for survival models. *Stata Journal*, 2006, 6(1): 83–96.

Radiation Fog". Cambridge School of Navigation: *Competent Skipper Notebook. S. J. Starkie*. December 2013. Web. 19 March 2014

"Radiation Fog Formation". *Experimental Aircraft Info*. 2014. Web. 19 March 2014.

Shahabi, M., Hlaing, A., Martinelli, D. and Unnikrishnan, A. (2012) Fog Detection for Interstate and State Highways. (Report WVU-2010-01) West Virginia University.

Yamamoto, T., Madre, J. and Kitamura, R. An analysis of the effects of French vehicle inspection program and grant for scrappage on household vehicle transaction. *Transportation Research Part B*, 2004, 38(10): 905-926.

Yang, X., Gao, Z., Guo, H. and Huan, M. Survival analysis of car travel time near a bus stop in developing countries. *Science in China Series E*, 2012, 55(8): 2355-2361.